Cortical Control of Intraspinal Microstimulation to Restore Motor Function After Paralysis

Cortical Control of Intraspinal Microstimulation to Restore Motor Function After Paralysis

Jonas B. Zimmermann

Thesis Submitted for the Degree of
Doctor of Philosophy

Institute of Neuroscience
Faculty of Medical Sciences
Newcastle University
Newcastle Upon Tyne, UK

Advisors:
Dr Andrew Jackson
Prof Stuart N. Baker

September 2012

Newcastle University

Meinen geliebten Großeltern.

Abstract

Spinal cord injury (SCI) is a devastating condition affecting the quality of life of many otherwise healthy patients. To date, no cure or therapy is known to restore functional movements of the arm and hand, and despite considerable effort, stem cell based therapies have not been proven effective. As an alternative, nerves or muscles below the injury could be stimulated electrically. While there have been successful demonstrations of restoration of functional movement using muscle stimulation both in humans and non-human primates, intraspinal microstimulation (ISMS) could bear benefits over peripheral stimulation. An extensive body of research on spinal stimulation has been accumulated – however, almost exclusively in non-primate species. Importantly, the primate motor system has evolved to be quite different from the frog's or the cat's – two commonly studied species –, reflecting and enabling changes in how primates use their hands. Because of these functional and anatomical differences, it is fair to assume that also spinal cord stimulation will have different effects in primates. This question – what are the movements elicited by ISMS in the macaque – will be addressed in chapters 2 and 3.

Chronic intraspinal electrode implants so far have been difficult to realise. In chapter 4 we describe a novel use of floating microelectrode arrays (FMAs) as chronic implants in the spinal cord. Compared to implanted microwires or other arrays, these FMAs have the benefit of a high electrode density combined with different lengths of electrodes. We were able to maintain these arrays in the cord for months and could elicit movements at low thresholds throughout.

If we could build a neural prosthesis stimulating the spinal cord, how would it be controlled? Remarkable progress has been recently achieved in the field of brain-machine interfaces (BMIs), for example enabling patients to control robotic arms with neural signals recorded from chronically implanted electrodes. Chapter 5 of this thesis examines an approach that combines ISMS with cortical control in a macaque model for upper limb paralysis for the first time and shows that there is a behavioural improvement. We have devised an experiment in which a monkey trained to perform a grasp-and-pull task receives a temporary cortically induced paralysis of the hand reducing task performance. At the same time, cortical recordings from a different area allow us to control ISMS at sites evoking hand

movements – thus partially restoring function.

Finally, in appendix A we describe a system we developed in order to introduce automated positive reinforcement training (aPRT) both at the breeding facility and in our animal houses. This system potentially reduces time spent on training animals, adds enrichment to the monkeys' home environment, and allows for suitability screening of monkeys for behavioural neuroscience experiments.

Acknowledgments

The work described in this thesis could not have done without the generous help and advice of many people.

In chapter 2 I use data collected by Vasileios Glykos. Saša Koželj kindly let me use her animal for some experiments. Some data presented in chapter 3 were collected by Andrew Jackson and Kazuhiko Seki. I am grateful to Marc Schieber and Hansjörg Scherberger for sharing their experiences with the FMAs whose implantation into the spinal cord is described in chapter 4. The animals used for experiments described in chapters 4 and 5 were trained by Jennifer Tulip. Shurong Li and Jennifer Tulip did most of the histological processing. Norman Charlton showed me how to use the CNC machine and other great tools in his workshop, helped me build manipulanda and devices used for my experiments, and built them when I lacked the skills. Paul Flecknell, Aurelié Thomas, Silke Corbach-Soehle, Caroline Fox and Denise Reed provided excellent veterinary support during surgeries and beyond.

I shared the office space with Kianoush Nazarpour, Thomas Hall and Claire Schofield, who shared their thoughts on work, life, and MATLAB. The senior scientists of our group – Stuart Baker, Andrew Jackson and Mark Baker – provided a great work atmosphere, encouraging independent thought and experiment – and stimulating (scientific) exchange through our Cheese & Wine lab meetings. I would like to thank Mark Cunningham and Alexander Thiele for serving on my progress review panel and giving independent advice throughout my project. Kazuhiko Seki was very kind to host me for a month at his lab in Tokyo. For their assistance with the positive reinforcement training project, I would like to thank David Farningham and Mellissa Nixon (CfM), and Henrik Johansen and Søren Ellegaard (MBRose).

On many occasions, I relied on help, advice or a piece of kit from friends and colleagues working at the Institute of Neuroscience. An attempt to list all of them will have to be unsuccessful, I try it anyway. May those forgotten excuse me. In alphabetical order: Felipe De Carvalho, Lauren Dean, Cyril Eleftheriou, Karen Fisher, Ferran Galán, Emma Gilmore, Sabine Gretenkord, Bonne Habekost, Terri Jackson, Stephan Jaiser, Karen Parkin, Tobias Pistohl, Lee Reed, Barbara-Anne Robertson, Evelyne Sernagor, Harbaljit Sohal, Demetris

Soteropoulos, Edina Tozser, Ashley Waddle, Laura Watson, Liz Williams, Claire Witham, Boubker Zaaimi.

Andrew Jackson has been tremendously supportive advisor. I hope I learned much from him; his lateral thinking, quick-wittedness, and mastery in creative Sleek Tape use amaze me.

I could not have stemmed this project without support and encouragement from my family and friends, who in the last months have seen very little of me. Last, my greatest thanks go to Kari, for her boundless love.

Jonas B. Zimmermann

Publications

Some ideas and figures have been published previously:
Peer-reviewed articles:

Jackson, Andrew and Jonas B. Zimmermann (2012). 'Neural interfaces for the brain and spinal cord – restoring motor function'. In: *Nature Reviews Neurology*.

Zimmermann, Jonas B., Kazuhiko Seki and Andrew Jackson (2011b). 'Reanimating the arm and hand with intraspinal microstimulation'. In: *Journal of Neural Engineering* 8.5.

Conference abstracts:

Zimmermann, Jonas B., Stuart N. Baker and Andrew Jackson (2009). 'Functional upper limb movements generated by cervical intraspinal microstimulation in the monkey'. In: *39th Society for Neuroscience Annual Meeting*. 370.22/EE40. Society for Neuroscience. Chicago, IL.

Zimmermann, Jonas B. and Andrew Jackson (2010). 'Investigating microstimulation of the macaque cervical spinal cord to elicit functional upper limb movements'. In: *BCI Meeting 2010*. Monterey, CA.

— (2011a). 'Closed-loop cortical control of intraspinal microstimulation restores hand function in the macaque monkey'. In: *41st Society for Neuroscience Annual Meeting*. 142.80/E23. Society for Neuroscience. Washington, DC.

— (2012). 'Nonlinear summation of evoked forces and EMG using intraspinal microstimulation trains in the macaque monkey'. In: *Neural Control of Movement 22nd Annual Meeting*. 2-D-83. Venice, Italy.

Contents

List of Figures

List of Tables

Acronyms

1DI · first dorsal interosseus. 29, 65, 70, 74, 77, 82–84, 91

ADM · abductor digiti minimi. 17, 56

AIP · anterior interparietal area. 3

APB · abductor pollicis brevis. 14, 27, 29, 48, 65, 74, 82, 83

APL · abductor pollicis longus. 29

aPRT · automated positive reinforcement training. iv, 100–102, 104, 110–112

aPRTD · automated positive reinforcement training device. 101, 103, 104, 107, 109, 110, 112

AS · arcuate sulcus. 67

BMI · brain-machine interface. iii, 1, 2, 5, 20–22, 61, 62, 91, 94, 95, 98

CBC · Comparative Biology Centre. 103, 106, 107

CfM · Centre for Macaques. 103, 106, 107

cISMS · cervical intraspinal microstimulation. 9, 11, 12, 21, 24, 34, 42, 62, 70, 88, 90, 92, 94–96

CM · corticomotoneuronal. 2, 3, 9, 41

CNS · central nervous system. 1, 41

CS · central sulcus. 67

DAB · diaminobenzidine. 51

ECR · extensor carpi radialis. 65, 74, 81, 82

ECU · extensor carpi ulnaris. 29

EEG · electroencephalogram. 5

EMG · electromyogram. 5, 13, 16–18, 20, 21, 23–29, 32, 37–41, 48, 50, 51, 53, 55, 56, 62, 64–66, 68, 70, 74, 76–78, 80–86, 93, 95

FCR · flexor carpi radialis. 14

FCU · flexor carpi ulnaris. 29, 65, 74, 82

FDP · flexor digitorum profundus. 29, 56, 65, 74, 82

FDS · flexor digitorum superficialis. 14, 56, 65, 74, 82

FES · functional electrical stimulation. 1, 6–8, 11, 12, 61, 62, 94, 97, 98

FMA · floating microelectrode array. iii, v, 24, 45–48, 50, 52–60, 66, 92, 95, 96, 111, 112

GABA · γ-Aminobutyric acid. 5, 63, 90

GFAP · glial fibrillary acidic protein. 51, 56–58

ICMS · intracortical microstimulation. 5, 22, 67, 75, 90

ISMS · intraspinal microstimulation. iii, 2, 6–12, 14, 18, 20–24, 40, 42, 44–46, 52, 59, 61, 62, 67, 72, 75, 81, 85, 86, 89, 90, 92, 94–97, 99, 115

ISpI · inter-spike interval. 88, 89, 93, 94

ISpIH · inter-spike interval histogram. 68

IStI · inter-stimulus interval. 24, 41

LED · light emitting diode. 102, 103, 107, 109

LFP · local field potentials. 68

M1 · primary motor cortex. 2–5, 22, 62, 63, 65–67, 72, 74, 90, 94

MEA · microelectrode array. 45

MFa · *Macaca fascicularis*. 111

MFu · *Macaca fuscata*. 111

MIP · medial interparietal area. 4

MMu · *Macaca mulatta*. 111, 112

MRI · magnetic resonance imaging. 64

MUAP · motor unit action potential. 70, 83, 91

NHP · non-human primate. 101, 103

PBS · phosphate-buffered saline. 51

PC · personal computer. 68

PETH · peri-event time histogram. 71

PMd · dorsal premotor cortex. 2–5, 66

PMv · ventral premotor cortex. 2–5, 62, 65, 66, 73, 88, 91, 94

PRT · positive reinforcement training. v, 100, 101, 104, 109

PStTH · peri-stimulus time histogram. 82, 83

PT · pyramidal tract. 22

RFID · radio frequency identification. 50, 100–104, 106–110

SCEP · spinal cord evoked potential. 24, 25, 29, 30, 32–37, 51–53, 55, 56, 70, 75, 78, 79, 82, 90

SCI · spinal cord injury. iii, 1, 2, 6, 8, 62, 91, 94, 96

SEM · standard error of the mean. 53, 73, 76, 77, 81, 84, 85

streptavidin-HRP · streptavidin conjugated horseradish peroxidase. 51

StTA · stimulus-triggered average. 25, 29, 70

UEA · 'Utah' electrode array. 45

Note: Throughout this thesis, thresholds for statistical significance (Type-I error) are referred to by α. Probabilities determined by statistical tests are designated by p.

1 Introduction and Background

In this chapter I will give a motivation for and discuss the scientific foundations of the work presented in this thesis. This work builds on the vast body of research on the motor system amassed mainly in the last century, combines several experimental techniques, and connects different parts of the central nervous system.

1.1 Introduction

More than 1000 people in the United Kingdom fall victim to spinal cord injury (SCI) every year, and about one third of them become quadriplegic (Wyndaele et al. 2006). To date, there is no effective therapy that goes beyond aiding natural recovery of function, leaving many patients permanently paralysed. Regeneration of neural tissue using stem cells is certainly a very interesting approach, however this technique is still in its infancy and may never be available to patients. Recently the field of brain-machine interfaces (BMIs) has received much attention for several demonstrations how brain activity can be recorded and used to control muscle stimulation in monkeys (Ethier et al. 2012) and the movement of robotic arms in human patients (Hochberg et al. 2012).

While robotic arms are a first step to some independence, patients usually still have their own healthy – but forceless – arms, whose reanimation would be much more beneficial. Functional electrical stimulation (FES) of muscles is way to reanimate paralysed limbs, but this technique comes with several problems as we will see below. Although SCI disables the motor pathways connecting the cortex with the motoneurons innervating the muscles, the spinal circuits below the injury do not degenerate completely; they may even by more active than usual leading to awkward spasticity.

Could the spinal cord be stimulated electrically in order to restore movement? Several groups have explored this approach, predominantly with the aim of restoring walking, using rodents or cats as the model organism. Reaching, grasping, and complex object manipulations are movements that have evolved in primates, which makes investigation of techniques to restore these upper-limb movements difficult or impossible in other species. Relatively

few laboratories have the capacities to perform experiments using primates, and therefore the exploration of spinal stimulation for neuroprostheses has received comparatively little attention.

In this thesis I aim to further the field by investigating properties of intraspinal microstimulation (ISMS) in the macaque cervical spinal cord, and I demonstrate online brain-control of ISMS in a model for upper-limb paralysis in order to restore functional movements. First, however, I introduce the necessary concepts of motor control and BMIs.

1.2 Background and Context

First, I will give an overview of the neural control of hand and arm movements in normal healthy subjects.[1] Specifically, I will focus on how planned or executed movements can be inferred or 'decoded' from cortical activity, and on the role of spinal cord circuits in movement execution. I will then examine recent advances in BMIs, which use neural activity to control devices, including computer cursors or robotic arms. Finally, I will review therapeutical strategies for SCI and stroke,[2] including current spinal cord stimulation systems.

1.2.1 Primary and Premotor Cortices

Anatomical Organisation Many cortical areas are known to play a role in planning and execution of reaching and grasping movements (Kalaska et al. 1997). Most prominent is primary motor cortex (M1) spanning the precentral gyrus and the anterior bank of the central sulcus, historically identified by electrical surface stimulation as evoking movements at minimal thresholds (Grünbaum et al. 1901, Penfield et al. 1937). This area provides the main cortical output towards the spinal cord, accounting for half the corticospinal neurons terminating in the cervical cord (Dum et al. 1991, Lemon 1993). In macaques and other primates, a large number of these corticospinal cells are corticomotoneuronal (CM) cells, i.e. neurons whose axons project monosynaptically to motoneurons in the ventral horn of the spinal cord (Lemon 2008). Premotor areas such as ventral premotor cortex (PMv) and dorsal premotor cortex (PMd) anterior to M1 have reciprocal connections with M1 and between each other (Dum et al. 2002, 2005). These premotor areas also project to the spinal cord, accounting for 4–10 % of corticospinal neurons terminating in the cervical cord (Dum et al. 1991, He et al. 1993), however no CM cells have been found there (Rathelot et al. 2006).

[1] It is worth noting that how we think about human motor control is greatly influenced by experiments conducted on animals, especially macaque monkeys.

[2] Here and in the remainder of this thesis, I focus on treating motor deficits when talking about SCI or stroke.

On the other hand, both PMv and PMd receive input from visual areas in the parietal cortex in two distinct pathways, PMv from the anterior interparietal area (AIP) and PMd from area V6A (Grafton 2010).

Function of M1 Function of the motor areas was first explored using electrical surface stimulation in the late 19th century (e.g.Fritsch et al. 1870, Ferrier 1874, Grünbaum et al. 1901). Different parts of the body were caused to move depending on where the stimulation took place. Systematic mapping led to the motor maps of Penfield and Woolsey for humans and monkeys, respectively (Penfield et al. 1937, Woolsey et al. 1952). However (as these researchers were well aware), the cortex lacks the sharp borders between areas and the continuous motor representation these maps may suggest.

While M1 is essential in control of coordinated movements as shown by lesion studies (e.g.Travis 1955), the exact role of M1 in motor control has been widely debated. One line of evidence suggested that M1 acts essentially as a muscle controller, determining the level of muscle activation required to perform a given movement (Evarts 1968). The existence of CM connections suggests M1 has a direct connection to muscles. However, a given CM cell can synapse onto several motoneurons innervating different muscles (Fetz et al. 1976), suggesting that the cortical contribution is more complicated than a simple representation of muscle activity.

A different experimental approach – the experimenters had monkeys perform centre-out reaching movements – found that many M1 neurons show cosine tuning to a preferred movement direction, and that the actual direction of the hand movement could be decoded in two or three dimensions from the population activity of M1 cells (Georgopoulos et al. 1982, 1983, 1986, Schwartz et al. 1988, Georgopoulos et al. 1988). Centre-out movements performed in these tasks involve multi-joint and proximal movements as opposed to the single-joint wrist movements of Evarts's (1968) experiment.

How can these different results be reconciled? One hypothesis is that circuitry in M1 transforms information about movements from an extrinsic, object-related space to an intrinsic, muscle-related space. In an experiment dissociating muscle activation from movement direction in a wrist flexion task, Kakei et al. (1999) found both neurons tuned to movement direction and neurons tuned to muscle activation, suggesting that some part of this transformation does indeed take place in M1. A potential physiological basis for this was described by Rathelot et al. (2009): They describe two distinct subareas in M1, 'old' and 'new' M1. The 'old' area, in the rostral part of M1, does not contain CM cells, but rather controls movement through indirect connections to muscles. The 'new', caudal area, which developed in old world monkeys, contains CM cells projecting onto hand and arm motor

units and allows direct control of muscles. Neurons in the 'old' area could the be expected to show behaviour as described by Georgopoulos and colleagues: connecting indirectly to proximal muscles, they provide a movement direction pattern. Neurons in the 'new' area on the other hand, projecting directly to motoneurons of distal muscles, would be expected to fit Evarts's descriptions better.

Reach and Grasp in PMv and PMd In contrast to M1, neurons in premotor areas anterior to M1 (PMv and PMd) have been found to correlate mostly with abstract task parameters. It was therefore suggested that these premotor areas subserve visuomotor transformations, translating object position in a visual reference frame into motor plans to perform reach and grasp movements (Jeannerod et al. 1995, Wise et al. 1997). Studies investigating reaching and grasping movements have used a variety of task manipulations – for example different grasp types, positions of object, cue periods, object and hand orientations, and known or unknown object – in order to determine individual contributions of the premotor areas. Neurons in PMv have been found consistently to be selective for direction of hand movement independent of posture (Kakei et al. 2001), the kind of object presented (Raos et al. 2006), and the grasp required for the task (Rizzolatti et al. 1988, Fluet et al. 2010), and populations of PMv neurons can be used to decode these task parameters (Townsend et al. 2011). So called 'mirror' neurons, which not only respond to certain grasp types when planning or performing an action but also when another subject performs a similar action, were also found in PMv (Gallese et al. 1996, Rizzolatti et al. 1996), suggesting a more abstract role of PMv neurons in the representation of goal-directed movements.

In contrast to PMv, cells in PMd are more related to hand direction or target of movement. For example, Kurata (1993) found neurons whose activity was tuned to instructed direction and intensity of movement during a preparatory period. The role of PMd in transformations from visual to motor spaces is exemplified by the following experiment: Pesaran et al. (2006) recorded the activity of PMd and medial interparietal area (MIP) neurons while monkeys were performing a reaching task designed to dissociate between eye, hand, and target positions. Most PMd neurons were tuned to relative positions of hand, eye, and target in a joint fashion which did not allow separation of a single one of these variables. In comparison, MIP neurons mostly represented target position in an eye-centred coordinate frame, meaning that initial hand position did not influence firing rates.

Together, while being part of different streams of information, both PMv and PMd subserve preparation of actions by integrating different aspects of context and feed this information to M1 for movement execution.

Interaction of M1 and PMv PMv and M1 are strongly and reciprocally connected (Muakkassa et al. 1979, Godschalk et al. 1984), both areas have corticospinal projections (He et al. 1993), and intracortical microstimulation (ICMS) of both areas evokes hand and arm movements. This opens the possibility of two pathways through which PMv could influence movement execution: directly via spinal projections and mediated through M1. Schmidlin and coworkers addressed this question by deactivating M1 of macaques using the GABA-agonist muscimol, thus blocking one potential pathway (Schmidlin et al. 2008). PMv and hand area of M1 were electrically stimulated with microelectrodes before and after muscimol injection, and electromyogram (EMG) responses to stimulation were strongly reduced. These results suggest that PMv affects grasping mostly through its connections with M1.

The effect of muscimol injection into M1 on neural activity in PMv during task performance has not been tested so far. While activity in PMv could be altered due to lack of feedback from M1, it is also possible that the strong input from parietal areas into PMv (Davare et al. 2011) does not change the modulation patterns of grasp-related activity in PMv.

Using Cortical Signals to Control BMIs Brain-machine interfaces are devices that use neural signals to control actuators such as computer cursors, robotic arms, or stimulating implants. Various brain signals recorded with different techniques have been used to control BMIs. For experiments with human subjects, signals such as electroencephalograms (EEGs) can be recorded non-invasively and have been used to control BMIs, such as spelling devices or other computer input (Birbaumer et al. 1999). Because the skull and scalp act as a lowpass spatial filter for neural signals, the information content of EEG signals is limited. Combined activity of individual neurons instead can be used to control BMIs that require faster feedback or more degrees of freedom. Using recordings from M1, it is possible to decode the trajectory of a whole arm and many of its degrees of freedom (Vargas-Irwin et al. 2010). But even when subjects do not move their own limbs decoding of action is possible: For instance, monkeys could control position of a robot arm and aperture of its gripper to feed themselves in real time, using the spiking activity of many M1 neurons (Velliste et al. 2008). This technique has already been transferred to humans: Hochberg et al. (2012) have employed a similar setup to allow quadriplegic human patients to control a robotic arm.

Control of BMIs does not have to rely on complicated decoding algorithms, however. Single neurons in PMv or PMd are found to contain information about the onset of a grasping or reaching movement, and these signals are reliable even on a trial by trial basis (Rizzolatti et al. 1988). There is also ample evidence that monkeys can learn to regulate single neuron activity: As early as 1969 Fetz demonstrated that providing monkeys feedback about a single neuron's firing rate enabled them to control the firing rate in order to receive juice

rewards (Fetz 1969). This paradigm was extended by using the neuron's firing rate to control stimulation of muscles to either flex or extend the wrist (Moritz et al. 2008). However, it is unknown whether several dimensions can be controlled volitionally and independently in this manner.

1.2.2 Repair Strategies After Spinal Cord Injury or Stroke

In this section I will briefly introduce various options available to restore motor function after SCI or stroke. Axonal regrowth and cell replacement to bridge damaged areas is seen by many as the most elegant way to repair traumatic injuries. Despite considerable efforts put into development of stem cell based therapies, only little progress has been made to date (Nandoe Tewarie et al. 2009, Boulenguez et al. 2009, Sahni et al. 2010). Other techniques to restore function are FES (of muscles or peripheral nerves) and ISMS (Barbeau et al. 1999, Giszter 2008), and both methods are also seen as having the potential for aiding rehabilitation by providing means of shaping residual neural activity (Jackson et al. 2012).

Functional Electrical Stimulation The advances in brain control of computers and robots are certainly very impressive and offer patients left with few means to interact with the outside world a step towards more independence. However, it seems patients would gain much more if they were able to use their own arms and hands again. In order to reanimate paralysed limbs, muscles can be stimulated electrically, attempting to recreate normal activation patterns.

Several approaches exist for FES systems: stimulating electrodes can be implanted to stimulate the peripheral nerve (Grill et al. 2009) or muscle (Peckham et al. 2002) or they can act transcutaneously (Nathan 1997). Available FES systems use myoelectric control signals from proximal, unaffected muscles or other signals such as from a sip/puff sensor to operate the prosthesis (Kilgore et al. 2008).

In experiments with macaques, FES has already been controlled by brain activity, in simple wrist flexion/extension tasks (Moritz et al. 2008, Pohlmeyer et al. 2009) as well as a task requiring a monkey to grasp a ball (Ethier et al. 2012). One major issue of FES systems remains, however: the complicated biophysical configuration of the hand is difficult to control by muscle stimulation. There are 35 muscles acting on the hand alone, and every skilled movement involves an orchestrated activation of several muscles. Current systems are limited in number of muscles stimulated, and have only a few pre-programmed grasp patterns (Kilgore et al. 2008). Decoding of muscle activation patterns for a different movements is possible (Johnson et al. 2009, Nazarpour et al. 2012), although computationally expensive.

Conversely, FES lacks selectivity of stimulation, especially when using transcutaneous electrodes and when stimulating intrinsic hand muscles (Westerveld et al. 2012). Although co-activation of synergistic muscles might be beneficial, adjacent muscles are often functionally independent, and in these cases, co-stimulation is unwanted. In order to control coordinated hand movements normally involving several muscles and joints with FES applied to few muscles, tendon transfers have been used (Keith et al. 1996), but this again makes the required surgery more invasive and less reversible.

Furthermore, FES prostheses suffer from the fact that electrical stimulation recruits muscle fibres in reverse order: fast fatiguing large muscle fibres are activated first, before the slow and fatigue resistant fibres (Prochazka 1993). This rapid fatiguing can be to some degree remedied by week-long muscle stimulation training (Rupp et al. 2007). Additionally, current systems stagger stimulation pulses delivered to different electrodes along one muscle (Popović et al. 2009) or synergistically acting muscles (Decker et al. 2010), however, this comes at the cost of requiring multiple electrode implants per muscle, more stimulation channels, and more computational power.

Another issue of FES systems is the reliability of electrodes. Mechanical stress acting on the electrode during movement may lead to breaking of electrodes or leads, or movement of electrodes relative to muscles (Aoyagi et al. 2004). Also, electrodes could get encapsulated in scar tissue, decreasing efficacy of stimulation, and percutaneous electrodes might additionally suffer from infection contracted along the wires. In a study covering over 60 subjects with upper limb percutaneous electrode implants, Knutson et al. (2002) found that after three years, the electrode survival rate was less than 70 %.

Basic Properties of ISMS As an alternative to muscle stimulation, ISMS has been suggested as a method to activate surviving spinal circuitry (Mushahwar et al. 1997, Barbeau et al. 1999, Mushahwar et al. 2000c, Giszter et al. 2000a, Grill 2000). So far, most experiments investigating the effects of ISMS have been conducted in the lumbar cord of frogs and cats. One important result from stimulation of the frog motoneuron pools in the lumbar enlargement was the observation of converging force fields (Bizzi et al. 1991, Giszter et al. 1993). With a hindlimb held by a force transducer at different positions, ISMS causes forces to be exerted pointing towards an equilibrium point. The forces produced and the equilibrium point were different for various stimulation sites. One conclusion from this work is that ISMS activates muscle synergies dependent on the state of the limb, giving the spinal cord a bigger role in motor control than thought previously. Subsequently, convergent force fields were also reported for rat (Tresch et al. 1999) and cat (Lemay et al. 1999) lumbar cord stimulation.

For potential neuroprosthetic applications it might be beneficial to combine stimulation of several sites in order to increase behavioural repertoire. Again investigating the frog lumbar cord, Mussa-Ivaldi et al. (1994) reported that concurrent stimulation of two sites yields the same force fields that would be expected from linear summation of the fields obtained by single site stimulation alone. While linear summation of force fields was also reported in the rat (Tresch et al. 1999), Grill and Lemay found a 'winner-take-all' pattern in which force fields obtained by co-stimulation match the response of stimulation of one site alone to be predominant in the cat (Grill et al. 2002, Lemay et al. 2009). The latter results have to be interpreted with care, however, because all but two stimulation electrode pairs comprised electrodes in the ipsi- and contralateral cord relative to the measured limb, whereas in the studies cited above stimulation electrodes were always in the ipsilateral cord. These results are important as they have been used as evidence to argue for a proposed modular organisation of the spinal cord (Bizzi et al. 1995, 2000, d'Avella et al. 2003, Bizzi et al. 2008). Individual modules are thought to produce synergistic activation of muscles, and complex movements are executed by activating individual modules in a temporal order. Whether this suggested relative independence of spinal modules also holds for primates has to be seen, and in chapter 3 I present some evidence against it.

ISMS to Restore Hindlimb Movements Several groups have investigated the potential of ISMS to restore motor function for patients suffering from SCI or stroke. The lumbar cord has been the main target of stimulation experiments, presumably because walking is not as complex a movement as skilled grasping and because it can be studied in animal models other than primates. There are also more potentially benefitting patients – not only because any lesion rostral to the lumbar enlargement can lead to paraplegia, but also because an injury leading to upper limb paralysis is likely to damage the cervical enlargement as well, making it difficult to use healthy structures as target for ISMS.

In intact (Mushahwar et al. 2000c, 2002, Tai et al. 2003), decerebrate (Lemay et al. 2004) or spinal (Saigal et al. 2004, Barthélemy et al. 2006, Guevremont et al. 2006) cats, ISMS readily evokes leg movements, including bilateral stepping and weight-bearing knee extension. In chronically implanted cats, stimulation effects were found to be stable over months (Mushahwar et al. 2000c).

A benefit of ISMS over FES could be that since ISMS electrodes would only have to be implanted at one location, the implant surgery would only require access to one site, aiding healing and reducing risk of infection. Furthermore, ISMS in preferentially activates fatigue resistant muscle fibres in contrast to FES (Bamford et al. 2005), and functional relevant muscle groups tend to be gradually and selectively activated (Mushahwar et al. 1998,

2000b).

These results suggest that ISMS is a technique worth developing further in order to build novel neural prostheses. However, care must be taken when results from frog, rat, or cat experiments are to be transferred to humans: because old-world primates developed remarkable skills in using their hands, and their motor systems changed to have a greater dependence on direct CM cells as opposed to the indirect connections found in rodents, cats, and other mammals (Lemon 2008). Due to the difference in anatomy it is likely that ISMS has different effects on the human or macaque cervical cord. However, previous results can still be used to guide investigation and to form hypotheses.

ISMS in Macaque Monkeys Despite the progress in ISMS in other species, ISMS in macaques has only recently been subject of a study. However, stimulation of the cervical spinal cord in macaque monkeys may be the best approach to study feasibility for human implants. Motoneurons in the macaque cervical spinal cord are organised in distinct but partly overlapping columns of cells innervating different hand and arm muscles (Jenny et al. 1983). One might then expect to find a similar organisation of movement responses to ISMS reflecting the locations of activated motoneurons. However, this is not the case: in a pioneering experiment, Moritz et al. showed that stimulating the ventral horn produces arm and hand movements, including many grasp-like movements, but these effects lack the clear organisation of motoneuron columns (Moritz et al. 2007). Whether cervical intraspinal microstimulation (cISMS) in the macaque lends itself to neuroprosthetic applications through restoration of functional movements is hitherto unknown. In this thesis I aim to fill in some of the gaps.

Spinal Cord Stimulation in Humans While ISMS has not been tried on human patients yet, epidural stimulation to control neuropathic pain (Simpson 1997, Compton et al. 2012, Epstein et al. 2012) or micturition (Maher et al. 2007) is used clinically. Epidural stimulation has also been found to elicit stepping patterns (Dimitrijevic et al. 1998), and after some training, epidural stimulation enabled one patient to stand and even exert some voluntary control of movement (Harkema et al. 2011).

1.3 Overview of This Thesis

In chapter 2 I give an account of experiments we conducted to further characterise the motor responses to cISMS in anaesthetised macaques and to demonstrate that functional movements can be elicited by cISMS (cf. also Zimmermann et al. 2011b).

A spinal prosthesis would need several stimulation channels to achieve multiple degrees of freedom. Experiments in frogs and rats suggest that no interactions occur between concurrently stimulated electrodes, however, in chapter 3 I provide evidence for non-linear interactions between stimulation sites in the macaque spinal cord.

A major hurdle for the advancement of ISMS both in animal models and humans is the availability of stable and safe spinal implants. In a patient, an implant should last for decades, being able to stimulate the tissue. Furthermore, it is highly desirable that an implant does not induce further damage to the cord, given the flexibility of the vertebral column and the large movements of the cord relative to the surrounding spinal canal. We therefore also investigated the suitability of an electrode array for chronic spinal stimulation. In chapter 4 I describe the implant technique we developed and show results from long-term stimulation.

At this point, I can collect the previous results, add cortical recording, a model lesion, and a behavioural task and ask whether chronic ISMS can be used to restore function in the awake macaque. In chapter 5 I demonstrate how we used brain activity from premotor cortex to control ISMS in real time while the monkey's hand was temporarily paralysed.

Finally, in appendix A I introduce an automated training system for macaques, which I designed to facilitate selection of suitable monkeys for behavioural experiments.

2 Properties of Single Channel ISMS in the Macaque Monkey

Little is known about cervical intraspinal microstimulation in macaque monkeys. In this chapter, we will lay the experimental basis for intraspinal microstimulation experiments. We will investigate how the spinal cord responds to microstimulation, and we will demonstrate that functional movements can be obtained.

Data from monkeys Am and Ha were collected as part of master's projects by myself and Vasileios Glykos, respectively. The model for muscle activation was developed and data from monkey Am was initially analysed as part of my master's project (Zimmermann 2009). Surgical preparations of animals Sa, Th, and O were performed jointly by Andrew Jackson and myself. All experimental and analysis scripts were written and all other experiments conducted by myself. This chapter is based on Zimmermann et al. (2011b), and parts were also presented in Zimmermann et al. (2010).

2.1 Introduction

While FES systems targeting muscles and peripheral nerves can generate simple arm and hand movements (Keith 2001, Popovic et al. 2002), restoring normal function to the paralysed upper-limb remains a formidable challenge. Up to 35 muscles act synergistically on the fingers and thumb alone to produce an enormous repertoire of manipulative ability. Many of these muscles are small and inaccessible via surface stimulation, and even extensive subcutaneous implants are problematic since neighbouring muscles act differently on the hand. Furthermore, stimulation of motor nerves produces an inverted recruitment order whereby large fibres are preferentially activated (Prochazka 1993), leading to noisy force production and rapid fatigue.

Pioneering work in the lumbar cord of species including frogs (Bizzi et al. 1995, Giszter et al. 2000b), rodents (Tresch et al. 1999) and cats (Mushahwar et al. 2000c, Grill et al. 2002) has

suggested that ISMS may provide a means of artificially eliciting movements which avoids many disadvantages of conventional FES. Microampere current delivered to individual sites in the grey matter activates spinal circuitry (Schouenborg 2008) that recruits co-ordinated patterns of muscle contractions. For example, stimulation of intermediate laminae in the frog spinal cord elicits convergent force fields that act to bring the leg to a particular point in space (Mussa-Ivaldi et al. 1994). Since motoneurons are activated transsynaptically, recruitment order is likely to be normalised and fatigue reduced (Bamford et al. 2005).

We are investigating whether ISMS in cervical segments of the primate spinal cord can generate functional movements of the upper-limb. Although the relative spinal and supraspinal contributions to upper-limb control in the primate remain unclear (Lemon 2008), segmental premotor interneurons with divergent projections to motoneurons are modulated with upper-limb movements such as wrist flexion/extension (S. I. Perlmutter et al. 1998). Short trains of microstimulation in the cervical cord at near-threshold current often elicits responses in multiple muscles, with co-activation of fingers and thumb flexion being particularly common (Moritz et al. 2007). These results suggest that cISMS may provide a means to activate co-ordinated muscle patterns that form the building blocks for functional movements such as reaching and grasping.

Here we report a series of experiments in anaesthetised monkeys to test whether longer trains of stimuli delivered to a small number of implanted cervical spinal electrodes can generate functional movements of the upper limb. We first analyse muscle responses to trains of stimuli at fixed frequency, and identify a non-linear frequency-dependence that presumably reflects spinal mechanisms. We show that these results are described by a simple recurrent model, which can be inverted to generate stimulus trains for arbitrary, graded motor output. We conclude with a discussion of some advantages and disadvantages of cISMS in the context of developing closed-loop Brain-Machine Interfaces to restore volitional control of the upper-limb to paralysed patients.

2.2 Materials and Methods

2.2.1 Animals and Surgical Procedures

Experiments were performed on six female rhesus macaque monkeys (monkeys Am, Sa, Th, Ha, O and Ma; see table B.1). We include data on responses to muscle and peripheral nerve stimulation under ketamine/dormitor sedation from monkey Ma. The other monkeys were terminally anaesthetised (induced with ketamine, maintained with isoflourane during surgical dissection, and then switched to an IV infusion of propofol at 0.5 $mg\,kg^{-1}\,min^{-1}$

and alfentanil at 0.2 µg kg^{-1} min^{-1} to maintain spinal excitability during stimulation experiments). Respiration was supported by artificial ventilation through a tracheotomy and body temperature, blood pressure, blood oxygenation, and end-tidal CO_2 were monitored throughout.

EMG signals from arm and hand muscles were amplified (1000×), high-pass filtered at 30 Hz (Neurolog NL824, Digitimer) and sampled at 1 kHz (Power 1401, Cambridge Electronic Design). In three monkeys (Am, Sa, and Th) we recorded from 16 muscles, in monkey Ha from 5, in monkey O from 2, and in monkey Ma from one muscle.

Motor responses were recorded either as grip force in the hand or as isometric forces and torques at the wrist. To record grip force, a Foley catheter was inflated with air and connected to a pressure sensor. For isometric force recording, the hand of the monkey was fixed into a padded clamshell mounted to a six-axis force/torque transducer.

2.2.2 Spinal Cord Stimulation

Access to the cervical spinal cord was gained through a laminectomy of vertebrae C4–T1, and the dura mater was removed. Teflon-insulated tungsten microwires (50 µm diameter, ~100 kΩ impedance) were inserted 3–6 mm into the cervical spinal cord (on average 10 per animal) targeting the motoneuron pools of the ventral horn. In one animal, a 16-channel Michigan Probe was used for stimulation. Since we did not expect to find a significant somatotopicity of stimulation effects (Moritz et al. 2007), we covered the extent of the cervical enlargement between C6 and T1 at lateralities between 1 and 3 mm. Penetration depth was determined by making a sharp bend in the microwire at the appropriate length.

2.2.3 Stimulation Protocols

Stimuli (biphasic, cathodic phase first, 200 µs per phase) were delivered using Model 2100 and Model 2200 isolated stimulators (AM Systems). The data we report here were collected using the following stimulation protocols:

Intensity series Single stimuli were delivered in pseudo-random order with intensities between 5 and 50 µA in 5 µA increments (10 individual stimuli per intensity; interstimulus interval 500 ms). If no EMG responses were seen, a second series used intensities between 20 and 200 µA in 20 µA increments. Motor threshold was defined as the lowest current required to evoke an EMG response in one muscle with at least 50 % probability. For subsequent stimulation protocols, stimulus currents were increased to achieve consistent visible muscle contractions (typically 1.5–10× motor threshold).

Frequency series To investigate the motor response to different stimulation frequencies, we delivered a pseudo-randomised sequence of stimulus trains (15 pulses each) at frequencies from 10 to 100 Hz (in 10 Hz steps) and with a 2 s interval between trains. Each frequency was repeated 20 times in one session.

Regular and Long/Short Interval Stimulation To explore the effect of varying the temporal structure within a stimulus train, we constructed stimulus trains containing 20 stimuli at 6 average frequencies (20, 22, 25, 29, 33 and 36 Hz) using two methods. In the 'regular' condition, successive stimuli in a train were separated by a uniform inter-stimulus interval. In the 'long/short interval' conditions, alternate intervals were fixed at 50 ms (in order to maintain a fused contraction), or shortened so as to preserve the same overall duration as in the regular condition (and thus the same average frequency). Note that since the inter-stimulus interval at 20 Hz is 50 ms, there is no difference between regular and long/short interval stimulus trains at this frequency. One stimulation session contained 5 trials per condition delivered in pseudo-randomised order.

We compared the effects of ISMS with muscle and nerve stimulation using this stimulation paradigm. In one monkey, we performed three stimulation experiments using needle electrodes in hand and forearm muscles (APB, FCR, FDS). In the same monkey, we performed the same experiment using surface electrode median nerve stimulation. Finally, we used another monkey's median and ulnar nerve cuff implants to deliver these stimulus trains. Thresholds for muscle and nerve stimulation were determined visually, and subsequent stimuli were delivered 20 % above threshold.

2.2.4 Muscle Response Model

Force responses elicited by single motor unit action potentials have been previously approximated by critically damped second order systems (Milner-Brown et al. 1973). Here, following our observations, we assume that this model is a sufficient approximation for intraspinal stimuli as well. Accordingly, we assumed a normalised twitch force response to a single stimulus occurring at time zero to have a time course as given by

$$f(t) = \begin{cases} \frac{t}{\tau} \exp\left(1 - \frac{t}{\tau}\right) & t \geq 0 \\ 0 & \text{otherwise,} \end{cases} \tag{2.1}$$

where τ is the time of the maximum and here assumed to be 50 ms, as this time course was suggested by our initial stimulation experiments. We further assumed that the twitch re-

sponse amplitude depends on the times of previous stimuli. We then constructed a simple recurrent modulation model with only four parameters consisting of two decaying exponentials:

$$r(t_n) = 1 + \sum_{i=1}^{n-1} \left(p_1 \exp\left(-\frac{t_i}{p_2}\right) + p_3 \exp\left(-\frac{t_i}{p_4}\right)\right). \tag{2.2}$$

The two exponential terms were introduced in order to capture facilitation and suppression we observed in response to stimulation at different frequencies.

The frequency series data for muscles that were consistently activated by a given stimulation site were normalised to the first response in a train. We then performed least squares minimisation to fit the model parameters for each stimulation site–muscle pair. Two thirds of the trials were used to fit the data, allowing the model fit to be tested on the remaining data. R^2-values were computed for the testing subset. It is worth noting that, since the model in eq. (2.2) does not necessarily allow a constant solution equal to the mean of the training data, R^2-values can be negative.

In order to predict the motor response for a stimulus train given by its times $t_{1\ldots n}$, we convolved these stimulus times with the twitch force response from eq. (2.1) multiplied by the respective amplitude $r(t_i)$ and sum these scaled responses:

$$F(t) = \sum_{i=1}^{n} r(t_i) \cdot f(t - t_i). \tag{2.3}$$

Single twitches and their summation are shown in fig. 2.2 B. To construct a stimulus train for evoking a given target motor response, we progressively compared the current force prediction with the target function in time steps of 1 ms. Whenever the predicted motor response fell below the target function, a stimulus was delivered and the force prediction updated accordingly. Stimulation rates were limited by imposing a minimum inter-stimulus interval of 7 ms.

Although here this method was used to control open-loop stimulation with pre-constructed stimulus trains, it could easily be adapted for closed-loop stimulation since only information about past stimuli and the current target force are used to generate new stimuli (see section 5.2.6 for an application). Furthermore, once appropriate parameters have been determined, this algorithm requires minimal computational resources and can be executed in real time.

2.3 Results

2.3.1 Dataset

We report data on spinal cord stimulation from six animals, using 46 microwire electrodes and one Michigan probe (Monkey Am: 14 microwires, monkey Ha: 2, monkey Sa: 9, monkey Th: 21, and one Michigan probe in monkey O). We determined motor threshold for 40 microwires, with an average threshold of 63 µA (SD 55 µA). On average, stimulation evoked EMG responses in 2.5 (SD 1.6) muscles at threshold. The remaining 6 microwires did not show stimulation effects up to 200 µA.

We then performed stimulation experiments using the protocols described above. Frequency response data was acquired from 24 stimulation electrodes, yielding 346 site-muscle combinations for analysis. Of these sites, 17 elicited reliable EMG responses in at least one muscle throughout the recording (90 site-muscle combinations). For long/short interval stimulation, data was collected from 9 spinal sites of monkeys Am, Ha, O, and Sa, 3 peripheral nerves (median and ulnar nerves of monkey O, median nerve of monkey Ma), and 3 muscles of monkey Ma.

2.3.2 Frequency-dependence of muscle responses evoked by ISMS trains

Rectified EMG responses for trains of 15 intraspinal stimuli at different frequencies are shown in fig. 2.1. Of those stimulation site-muscle combinations with a consistent EMG response (90), about half showed rapid overall suppression after only a few stimuli (averaged data shown in fig. 2.1 D). Another 18/90 pairs showed facilitation for the first few high frequency stimuli and then suppression (fig. 2.1 C). The third large group showed strong facilitation for high frequency stimulation that lasted for the entire duration of the stimulation trains (15/90 pairs; cf. fig. 2.1 B). The remaining stimulation site-muscle combinations (17) showed more complex response patterns that were not easily classified. In many cases, a single stimulation electrode contributed to more than one class of response in combination with different muscles.

We then fitted the parameters for the muscle response model (eq. (2.2)) for every stimulation site-muscle combination that fell in one of these categories. The best fit for a site-muscle combination typically consisted of a sum of positive and negative decaying exponentials. The time constants of these decaying exponentials (p_2 and p_4 in eq. (2.2)) were in the range of 50–200 ms. For the groups showing high frequency facilitation, the time constant for the negative exponential was usually larger than the one for the positive, yielding recurrent modulation functions schematically shown in fig. 2.2 A.

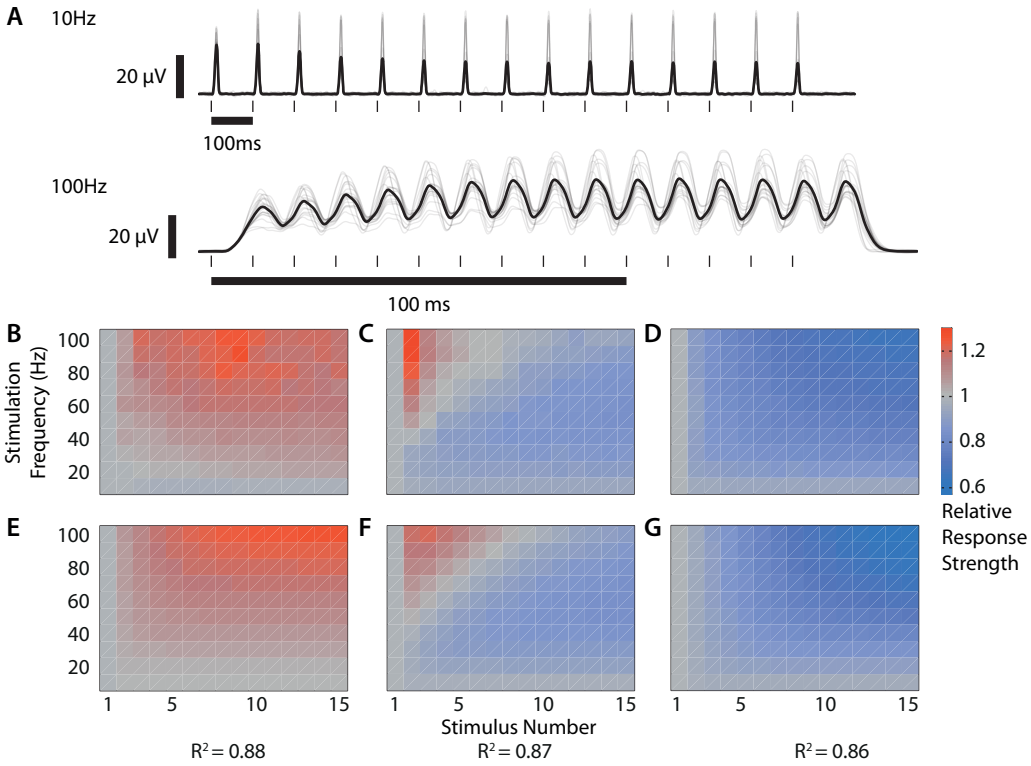

Figure 2.1: Muscle responses to intraspinal microstimulation. *(A)* Example rectified EMG responses from muscle ADM to trains of 15 stimuli delivered at 10 Hz *(top)* and 100 Hz *(bottom)*. Individual traces shown in grey, average in black. Stimuli indicated by marks. *(B–D)* Three common types of frequency response pattern. Rectified EMG was normalised by the response to the first stimulus before averaging across trials and stimulation site-muscle combinations. Response to the nth stimulus is shown along the x-axis, stimulation frequency along the y-axis. *(B)* Response increases for higher frequencies and remains constant for low rates (15/90 stimulation site-muscle pairs), *(C)* initial facilitation for high frequencies, then suppression (18/90), *(D)* general suppression for frequencies over 10 Hz (40/90). *(E–G)* Predicted responses using the model given in eq. (2.2) with parameters fit to data shown in panels B–D. R^2 values for the fits are 0.88, 0.87, and 0.86, respectively.

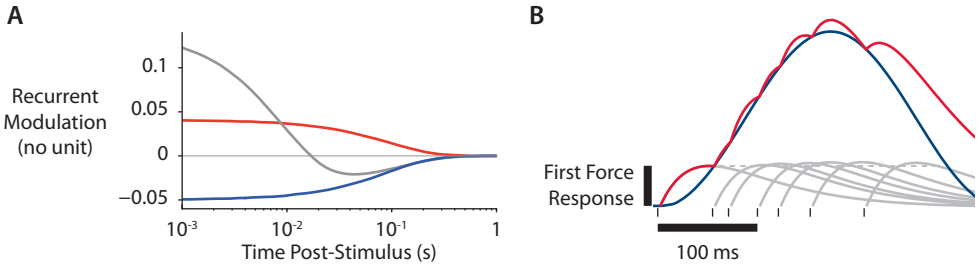

Figure 2.2: *(A)* Dual exponential model of recurrent facilitation/suppression with parameters from example fits shown in fig. 2.1; *red:* high frequency facilitation, (cf. fig. 2.1 B), *grey:* mixed facilitation/suppression, (cf. fig. 2.1 C) *blue:* overall suppression (cf. fig. 2.1 D). *(B)* Illustration of the stimulus train construction process. Whenever the force prediction *(red)* falls below the target *(blue),* a stimulus (black mark) is delivered and the prediction updated. The amplitude of a twitch response is modulated by prior stimuli according to (2.2). Individual twitch responses are shown in *grey*, the dashed line represents the amplitude of the first response as a reference.

The mean R^2-value for these fits was 0.37 (SD 0.29). We also used the average data from each response group to fit the recurrent modulation function. The respective model predictions are shown in fig. 2.1 E–G, and the group R^2 values were 0.88, 0.87, and 0.86, respectively.

2.3.3 Long/short interval stimulation of the spinal cord elicits stronger muscle contractions than regular stimulation

From the observation that many stimulation sites showed facilitated EMG responses to high frequency stimulation, we speculated that stimulation trains containing high frequency components might prove to be a more efficient method to generate force compared to regular trains of the same average frequency. By limiting the maximum inter-stimulus interval in the long/short trains (to 50 ms), a fused contraction can be maintained while the shorter interval can evoke temporal facilitation. To determine the locus of facilitation, we also delivered equivalent stimulus trains directly to muscles and peripheral nerves. We compared motor responses measured either as grip pressure or as isometric forces of the wrist resulting from regular and long/short interval stimulation trains of increasing average frequency. Stimulus amplitudes were on average 144 µA for ISMS, 3.3 mA for nerve stimulation, and 1.4 mA for muscle stimulation. Absolute force values recorded varied within stimulation site groups by as much as an order of magnitude, but on average were comparable across groups. This variation can be partially accounted for by the effectiveness with which different muscles activated by stimulation contributed to forces we could measure at the wrist or hand. In fig. 2.3 A, sample responses to a 20 Hz stimulus train, and for regular and long/

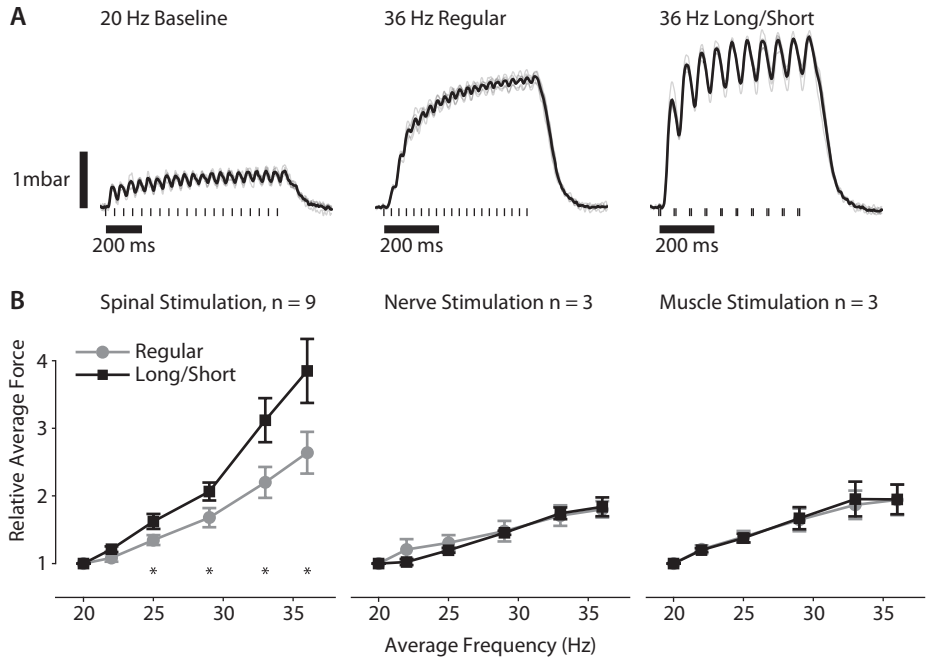

Figure 2.3: Motor response to regular and long/short interval stimulation trains delivered to the spinal cord, peripheral nerve, or muscle. Conditions were either regular trains of 20 stimuli delivered at 20, 22, 25, 29, 33, or 36 Hz, or trains of the same duration and number of stimuli, with alternate inter-stimulus interval fixed at 50 ms or shortened to preserve average frequency (long/short interval condition). *(a)* sample force trajectories for the 20 Hz baseline (*left,* stimuli are identical in regular and long/short conditions), 36 Hz regular *(centre)* and long/short *(right)* conditions. Individual trials shown in grey and average across trials in black. Stimuli were delivered at marks. *(b)* Average forces generated during stimulation of the spinal cord *(left),* peripheral nerve *(centre),* and muscles *(right).* Average forces were normalised by the response to 20 Hz stimulation. Asterisks mark conditions for which long/short stimulation trains caused significantly stronger forces than regular trains $(p < 0.05)$. Error bars: SEM

short 36 Hz conditions are shown. Measured motor responses were averaged across trials and normalised by the response to 20 Hz stimulation.

Panel B compiles these results for spinal cord, peripheral nerve, and muscle stimulation experiments across animals and stimulation sites. For spinal cord, nerve, and muscle stimulation, average force increased with frequency. However, the slope of this increase is stronger in the spinal cord compared with other stimulation targets. Furthermore, only in the spinal cord was there a significant difference between regular and long/short stimulus trains ($p < 0.05$). This shows that by varying the temporal pattern of spinal stimulation it is possible to increase the amount of force generated by a given number of stimuli, whilst preserving a fused contraction of the muscles. Therefore, temporal facilitation within the spinal cord provides opportunities for efficient activation of muscles with a minimal number of stimuli.

2.4 Discussion

This is the first study to investigate the upper-limb muscle activity and movements elicited by long trains of microstimulation in the cervical spinal cord of primates. We find that stimulation through a small number of electrodes can produce functional movements including reaching and grasping that involve co-ordination of multiple muscles. EMG responses show a mixed pattern of temporal facilitation and suppression that can be reasonably approximated by a simple dual exponential model. The advantage of this model is that it can be inverted to construct on-line stimulus trains that produce arbitrary, graded force profiles. Such an approach is in principle applicable in BMI paradigms where the desired force profile would be decoded in real-time from cortical activity. Therefore a relatively simple connection from cortex to spinal cord may provide a means to restore volitional movements of the paralysed limb. Such a connection could be implemented by an autonomous electronic device equipped with simple recording and stimulation capabilities (Jackson et al. 2006b).

In the present study we have not addressed the neural mechanisms by which movements are produced. Stimulation could act directly by depolarising motoneuron cell bodies and initial segments, as well as indirectly via afferent fibres, descending pathways and local intraspinal circuits. We see a non-linear frequency dependence of the muscle response to ISMS, in contrast to direct stimulation of the motor nerves and although we cannot rule out a contribution from intrinsic mechanisms such as persistent inward currents or slow afterhyperpolarisation (Eken et al. 1989), it is likely that non-linear synaptic interactions within the spinal cord are involved and include both excitatory and inhibitory influences. Previous studies have suggested that fibres may have lower stimulation thresholds than cell bodies

(Gustafsson et al. 1976, Histed et al. 2009) and that afferent fibres are activated at lower intensities than efferent fibres (Gaunt et al. 2006). However, with trains of supra-threshold stimulation it is likely that all of these components contribute to the movements we observe. Nevertheless, the functional organisation of descending projections, reflex pathways and segmental inputs to motoneurons may explain the naturalistic movements involving multiple muscles that we observe from stimulation at a single site. Exploiting these transsynaptic pathways to motoneurons has the additional advantage that a more natural recruitment order may be obtained (Mushahwar et al. 2000a, Bamford et al. 2005).

An important caveat is that these experiments were performed under general anaesthesia which is difficult to compare directly with an injured spinal cord. Aoyagi et al. (2004) have found ISMS responses can vary between the anaesthetised and decerebrate state. We deliberately chose an anaesthetic regime with minimal effect on spinal cord excitability, nevertheless further experiments using chronic implants will be required to extend these results to the awake animal. The situation after spinal cord injury is further complicated by plastic changes leading to hyperreflexia and spasticity. Nevertheless, it is possible that artificially restoring naturalistic patterns of activity to spinal circuits through ISMS may help to reduce the detrimental plasticity that results from depriving motoneurons of descending input.

2.5 Conclusion

In this experiment we have investigated single channel stimulation of the macaque cervical spinal cord. Response properties of EMG and force vary between stimulation sites and muscles, however a simple model can capture these responses well. Using this model may improve BMIs using cISMS by optimising stimulation trains designed to evoke a certain force response.

3 Intraspinal Microstimulation: Interactions Between Stimulation Sites

After having investigated single channel intraspinal microstimulation, we now turn our attention to interactions between stimulation channels. The occurrence of non-linear summation and suppression of responses to ISMS in the macaque is interesting because it has not been found in other species before and can have major implications for the design of brain-machine interfaces using ISMS.

Data from monkeys C and R were collected and analysed by Andrew Jackson. All other experiments were conducted jointly by AJ and myself, and data were analysed by myself. Parts of this chapter were presented in Zimmermann et al. (2012).

3.1 Introduction

In the previous chapter I have reported on the results of experiments using single channel ISMS. However, neural prostheses employing ISMS to control complex hand and arm movements will have to stimulate several channels concurrently. In section 1.2.2 on page 7 we discussed experiments in frogs, rats, and cats showing that in these species concurrent stimulation of microelectrodes in the lumbar cord produces linear summation of evoked forces.

Similar results have been found for cortical stimulation: in cat M1, Ethier and colleagues found that movements elicited by ICMS add linearly when two sites are stimulated simultaneously (Ethier et al. 2006). Baker et al. (1998) have addressed the question of cortical interactions in the macaque M1 using paired ICMS delivered to one or two sites and comparing the results to ICMS paired with pyramidal tract (PT) stimulation. For pulses delivered at several delays to pairs of electrodes, they found most responses to be according to the linear prediction, and comparing ICMS delivered to two sites with ICMS paired with PT stimulation suggested that modulations of responses were due to interactions on the spinal

level. If this modulation of responses indeed occurs at the spinal level, then it might also be possible to observe it using ISMS.

In the experiments described in this chapter we investigate whether paired stimulation of the macaque cervical spinal cord can evoke EMG responses that cannot be explained by the linear sum of responses to stimulation of a single channel. We show that both supra- and sub-linear interactions appear frequently and over various inter-stimulus delays and electrode distances. Furthermore, we show that non-linear interactions of EMG can also be obtained for longer trains of stimulation, and that this is also expressed in non-linear summation of isometric forces measured at the wrist. Finally, we conclude with the discussion of implications of these non-linearities for the use of animal models and therapeutic devices using ISMS.

3.2 Methods

3.2.1 Experimental protocol

Six purpose-bred female macaques were used for this study: monkeys C, R, Sa, Th, Ti and X (see appendix B). All procedures followed the National Institutes of Health Guideline for the Care and Use of Laboratory Animals and the UK Animals (Scientific Procedures) Act 1986, and were approved by local ethics committees at Newcastle University and Okazaki National Institutes.

Experiments were performed under terminal anaesthesia maintained initially with inhalation agents. A tracheotomy and artificial ventilation were used to support respiration while body temperature, blood pressure, blood oxygenation and end-tidal CO_2 were monitored throughout. Pairs of braided stainless steel wires were inserted into fore-arm muscles for EMG recording (monkey C: 14 muscles on the right side; monkey R: 16 muscles on the left side; see Table 1). Correct placement was verified by observing movements evoked by stimulation. EMG was high-pass filtered at 30 Hz, amplified with a gain of 1000 and sampled at 5 kHz. In monkeys Sa, Th, Ti, and X, the left hand was held in a 6-axis force and torque transducer distal to the wrist, with the hand in a pronate position and shoulder abducted ~70°, elbow at an angle of ~90°. Forces were sampled at 1 kHz. A laminectomy extending from C4 to T1 vertebrae was opened and the dura mater was resected. At this point the anaesthetic regime was gradually transferred to a continuous IV infusion of propofol (0.5 $mg\,kg^{-1}\,min^{-1}$) and opioid (monkey C: alfentanil 0.2 $\mu g\,kg^{-1}\,min^{-1}$; monkey R: remifentanil 1 $\mu g\,kg^{-1}\,min^{-1}$) in order to provide stable anaesthesia for the duration of the experiment without depressing spinal excitability.

Multiple cISMS electrodes made from Teflon-insulated tungsten micro-wire (diameter 50 µm, tip impedance ~0.2 MΩ at 1 kHz) were inserted into the spinal cord to depths of 3–5 mm ipsilateral to the EMG electrodes. A return electrode was sutured to the back muscles close to the laminectomy. Additionally, a floating microelectrode array (FMA; MicroProbes, Gaithersburg, MD, USA) – consisting of 18 platinum/iridium electrodes, impedance ~50 kΩ, array size 1.8 × 4.2 mm², electrode length 3–5 mm, diameter 50 µm – was implanted into the cords of monkeys Ti and X (cf. section 4.2.2). ISMS was delivered according to three stimulation sequences:

Intensity Series First, the threshold for eliciting a spinal cord evoked potential (SCEP) in the EMG responses to single stimulus pulses delivered to each spinal electrode was determined. Biphasic, constant-current stimuli (0.2 ms per phase) were delivered at a rate of 2 stimuli/s. A sequence of intensities in 5 µA steps up to a maximum of 50 µA were delivered in pseudorandom order (20 stimuli per intensity). If no response in any muscle was elicited at 50 µA, a second series consisting of 20 µA steps up to 200 µA was used. If no response was elicited at 200 µA the spinal electrode was repositioned or ignored.

Paired Pulse Series (Experiment 1) Once the SCEPs from individual stimulation had been characterised, stimuli were delivered to pairs of electrodes with 13 inter-stimulus intervals (IStIs) in the range −30 to +30 ms. The pseudorandom stimulation sequence consisted of 20 repetitions of each interval interspersed with an equal number of stimuli delivered to each electrode alone, with an overall stimulation rate of 2 Hz per channel. Intensities for each electrode were chosen to be slightly above the motor threshold and typically activated 1 to 5 muscles when delivered individually.

Interleaved Train Series (Experiment 2) To establish whether evoked movements depended on interactions between stimulation sites, a pseudo-randomised series of trains (50 Hz, 0.5 s duration) was delivered to pairs of electrodes having an inter-train interval of 2 s. Trains were delivered at various time shifts between both sites (time shifts used were 0, ±2.5, ±5 and +10 ms; in one animal, time shifts were −9 to +10 ms in 1 ms steps, those were analysed with their closest multiple of 2.5 ms), and trains were delivered to each electrode alone as control.

At the end of the experiment, electrolytic lesions were made by passing DC current through several spinal electrodes and the animals were perfused with formaldehyde. The cervical spinal cord was removed for histological treatment.

3.2.2 Analysis

Intensity Series Stimulus-triggered averages (StTAs) of rectified EMG in each muscle from 30 ms pre- to 30 ms post-stimulus were compiled for each intensity. To determine the latency of SCEP onset, the 99th percentile of the distribution of background EMG level in each StTA was calculated from the pre-stimulus period; latency was defined as the earliest point at which the StTA exceeded this level in the post-stimulus period. The latency of SCEPs varied across muscles, but was less affected by stimulus intensity or site. Therefore, for each muscle we chose a fixed 10 ms time-window beginning slightly before the earliest response latency (but after any stimulus artefact) and used the integrated rectified EMG over this range for subsequent analysis. For each intensity, the presence of a statistically significance SCEP was assessed by comparing this 10 ms time-window after each stimulus with an equivalent pre-stimulus range using a paired t-test. The motor threshold for each muscle was defined as the minimum stimulus intensity that elicited a significant SCEP at the $\alpha = 0.01$ level.

Paired Pulse Series Care must be taken when analysing the summation of EMG averages due to the non-linearity introduced by rectification (Baker et al. 1995). To overcome this problem we used the method of Baker et al. (1998) to compare the SCEP following paired stimuli with a prediction generated under the null hypothesis of linear summation of unrectified EMG responses from each spinal electrode individually. Briefly, a series of predicted sweeps were calculated by summing the unrectified responses to single stimuli delivered to each electrode alone, U_i^1 and U_i^2, time-shifted by the appropriate inter-stimulus interval, τ. These were then rectified and averaged to give a predicted StTA response at time t following the second of the pair of stimuli:

$$C(\tau, t) = \frac{1}{N} \sum_{i=1}^{N} \left| U_i^1(t + \tau) + U_i^2(t) \right| \tag{3.1}$$

However, this overestimates the background EMG level (since two backgrounds are combined in the sum). Therefore an equivalent background must be added to the real response to paired stimulation before rectification to allow unbiased comparison; this was taken from the pre-stimulus period of single electrode stimulation:

$$T(\tau, t) = \frac{1}{N} \sum_{i=1}^{N} \left| U_i^{12}(t) + U_i^1(t - 30\,\text{ms}) \right| \tag{3.2}$$

where U_i^{12} is the i^{th} response to paired stimulation. We only tested for significant non-linearity in the EMG response to the second stimulus because the response to the first stim-

ulus may be corrupted by the second stimulus artefact, and in any case should be not be causally effected by subsequent events. Comparisons were made over the same 10 ms time-window as used for the intensity series, delayed relative to the second stimulus as appropriate for each muscle. A paired t-test (across individual rectified sweeps) compared the integrated signal in this window for actual versus predicted responses. Two spinal electrodes were considered to be interacting if there was a significant difference for at least one muscle for one inter-stimulus interval at the $\alpha = 0.01$ level, Bonferroni-corrected for multiple comparisons across muscles and intervals. Depending on all the significant non-linearities over different muscles and intervals, the interaction between a pair of electrodes was classed as super-linear, sub-linear or mixed.

Interval Train Series EMG responses were extracted in sweeps including a period before stimulation onset. Responses to single electrode stimulation were first combined according to (3.1) and then rectified and integrated over the whole stimulation period (500 ms + 20 ms, to account for response latency) yielding values $\hat{C}(\tau)$ for each stimulation electrode pair – muscle combination. EMG responses from interleaved stimulation trains were corrected for background noise according to (3.2) and then processed as single electrode responses above and yielded integrated combined stimulation effects $\hat{T}(\tau)$. For each electrode pair and muscle, the differences of interleaved stimulation EMG responses and their linear prediction across stimulation conditions (time shifts) were tested against the null hypothesis that there was no difference between conditions using ANOVA ($\alpha = 0.05$). Only pair-muscle combinations for which the null hypothesis had to be rejected were analysed further. We then tested linear predictions and measured EMG in each condition for equality using a two-sample t-test ($\alpha = 0.05$, Bonferroni-corrected for multiple comparisons).

Raw force/torque transducer recordings were transformed into 3D-force data, smoothed with a 50 ms boxcar kernel, and divided into sweeps. From each sweep the average pre-stimulation (350 ms window) force was subtracted. We then built linear summation prediction sweeps similar to (3.1). Sweeps were then averaged during the latter half of the stimulation period (250 ms) to give measured and predicted force vectors $\vec{T}(\tau, j)$ and $\vec{C}(\tau, j)$, where τ denotes the condition (time shift) and j the trial number. We then analysed direction and magnitude of force responses independently. As magnitude, we used the usual Cartesian length $\|\cdot\|$ of vectors $\vec{T}(\tau, j)$ and $\vec{C}(\tau, j)$. We performed an ANOVA on the $\left\|\vec{T}(\tau, j)\right\| - \left\|\vec{C}(\tau, j)\right\|$ across stimulation conditions for each stimulation pair ($\alpha = 0.05$). We then tested for each stimulation electrode pair and condition whether the $\left\|\vec{T}(\tau, j)\right\|$ and $\left\|\vec{C}(\tau, j)\right\|$ had to be assumed different using a two-sample t-test ($\alpha = 0.05$, Bonferroni-corrected for multiple comparisons). For those that were significantly different, we calcu-

monkey	C	R	Sa	Th	Ti	X	*sum*
paired-pulse interactions							
stimulation electrodes	11	10					21
pairs	48	27					75
train interactions							
stimulation electrodes			10	14	5	7	36
pairs			24	19	4	21	68

Table 3.1: Numbers of electrodes and combinations tested in paired-pulse and train interaction experiments.

lated the mean ratios $R(\tau) = \sum_{j=1}^{N} \left(\left\| \vec{T}(\tau, j) \right\| \right) / \sum_{j=1}^{N} \left(\left\| \vec{C}(\tau, j) \right\| \right)$, where N is the number of trials per condition. In order to analyse effects of stimulation conditions on force direction, we transformed the measured force vectors into spherical coordinates on the unit sphere:

$$\tilde{T}(\tau, j) = \begin{pmatrix} \operatorname{atan2}\left(\vec{T}_2(\tau, j), \vec{T}_1(\tau, j) \right) \\ \arccos\left(\vec{T}_3(\tau, j) / \left\| \vec{T}(\tau, j) \right\| \right) \end{pmatrix}, \tag{3.3}$$

and proceeded accordingly with the predicted force vectors $\vec{C}(\tau, j)$. We then tested the $\tilde{T}(\tau, j)$ for common mean direction ($\alpha = 0.05$; Fisher et al. (1987)). If the null-hypothesis of a common mean direction had to be rejected for a pair of electrodes, we tested whether the measured force direction $\tilde{T}(\tau, j)$ differed from the linear prediction $\tilde{C}(\tau, j)$ for each condition ($\alpha = 0.05$; Bonferroni-corrected for multiple comparisons). Where there was a significant difference in direction, we calculated the angular deviation $\delta(\tau) = \arccos \frac{\vec{T}(\tau) \cdot \vec{C}(\tau)}{\left\| \vec{T}(\tau) \right\| \left\| \vec{C}(\tau) \right\|}$, where $\vec{T}(\tau)$ and $\vec{C}(\tau)$ are the averaged measured and predicted force directions, respectively.

3.3 Results

3.3.1 Dataset

The analysis presented here is based on data collected from six animals. For experiment 1 (paired pulse stimulation), 21 electrodes were stimulated in 75 combinations, for experiment 2 (interleaved train stimulation), 36 electrodes were used in 68 combinations (see table 3.1).

Figure 3.1 A shows individual, unrectified EMG sweeps recorded from APB following single stimuli delivered to an electrode in the C7 segment of the cervical cord. At the

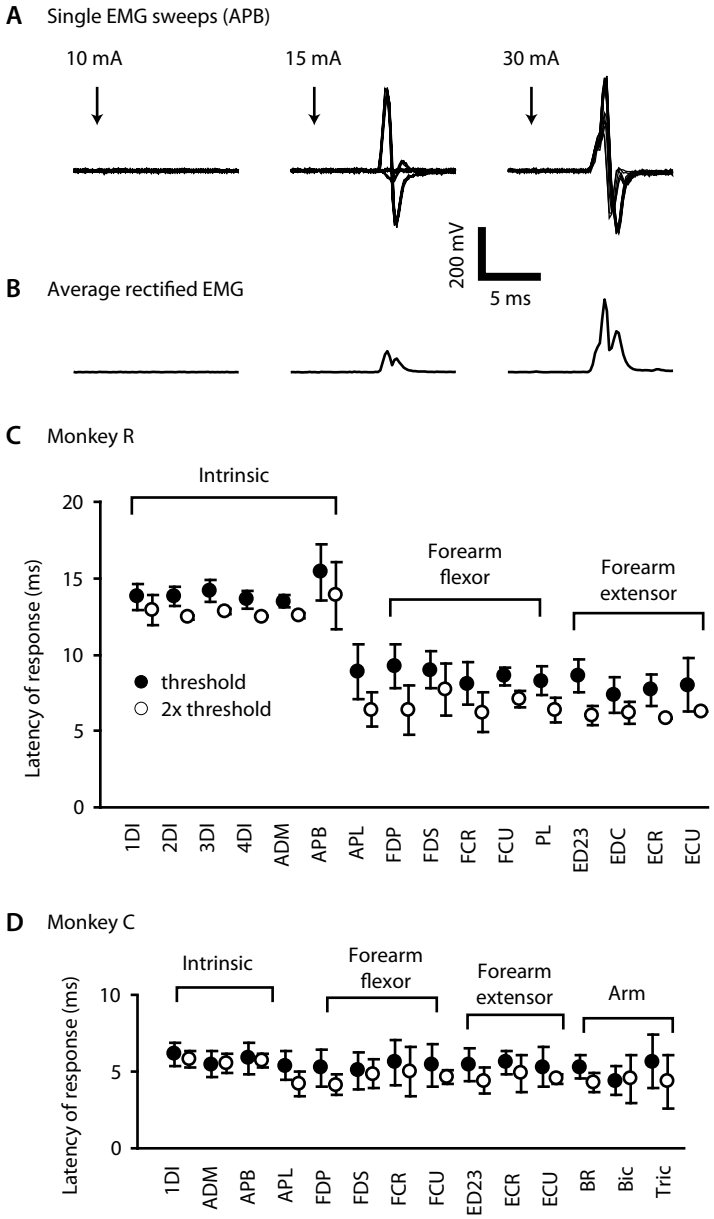

Figure 3.1: Effects of single pulse intraspinal microstimulation. *(A)* Single EMG sweeps (APB) at different stimulus intensities. Threshold was at 15 mA, with an evoked potential occurring in approximately 50 % of trials. *(B)* Averages of these sweeps, rectified. *(C,D)* Latencies of responses for different muscles at threshold and 2× threshold, monkeys R and C, respectively.

threshold intensity of 15 μA, an SCEP was seen in approximately half of sweeps. These all-or-nothing potentials likely represent single motor units firing in response to stimulation. The response timing was very consistent with jitter was less than the sampling resolution (200 μs), comparable to measures of jitter in monosynaptic reflexes (Fetz et al. 1983, Jabre et al. 1995) and suggesting a relatively direct excitation of motoneurons or their first-order inputs. At twice threshold (30 μA), the stimulus reliably elicited an SCEP in every sweep, but the latency was not greatly reduced. Figure 3.1 B shows StTAs of rectified EMG for these data.

Average latencies of significant SCEPs (fig. 3.1 C, D) exhibited a proximal-distal gradient consistent with increased peripheral conduction distance. The latency of SCEPs differed substantially between the two animals. Response onset in monkey R was approximately twice that for monkey C in comparable muscles. Several factors may have contributed to this discrepancy including size, age and subspecies differences between the monkeys. However since the absolute latency increase was also reflected in a greater proximal-distal gradient in monkey R, it is likely that the discrepancy reflects differences in proximal conduction times rather than a different mechanism of spinal excitation.

3.3.2 Intensity series

Figure 3.2 shows StTAs for all recorded muscles at different intensities of stimulation. For this stimulation electrode (C7 segment), the lowest threshold SCEP was observed in finger muscles (1DI and FDP) and ulnar wrist muscles (FCU and ECU). As stimulation intensity increased, SCEPs were also observed in thumb muscles (APB and APL). This broad activation pattern where supra-threshold stimuli activated a range of muscle groups was typical of most spinal electrodes. The minimum intensity at which a significant SCEP was seen in at least one muscle ranged from 5–120 μA, with a mean (SD) of 26(34) μA for monkey C and 57(30) μA for monkey R. Following stimulation at twice this minimum threshold, significant SCEPs were seen in up to 12 muscles (mean: 6, SD: 4).

In agreement with Moritz et al. (2007), grasping movements of the fingers and thumb were commonly seen following supra-threshold stimulation at many sites, as well as a range of wrist, elbow and shoulder movements. To characterise supra-threshold activation patterns, we determined the presence or absence of a significant SCEP at the lowest current which activated at least four muscles (or the highest stimulation intensity tested in cases where this activated fewer than four). These patterns for all electrodes in both monkeys are shown in fig. 3.3. For each animal, the electrodes have been grouped into three categories according to a distal-proximal gradient of activation, although within each category a variety of different

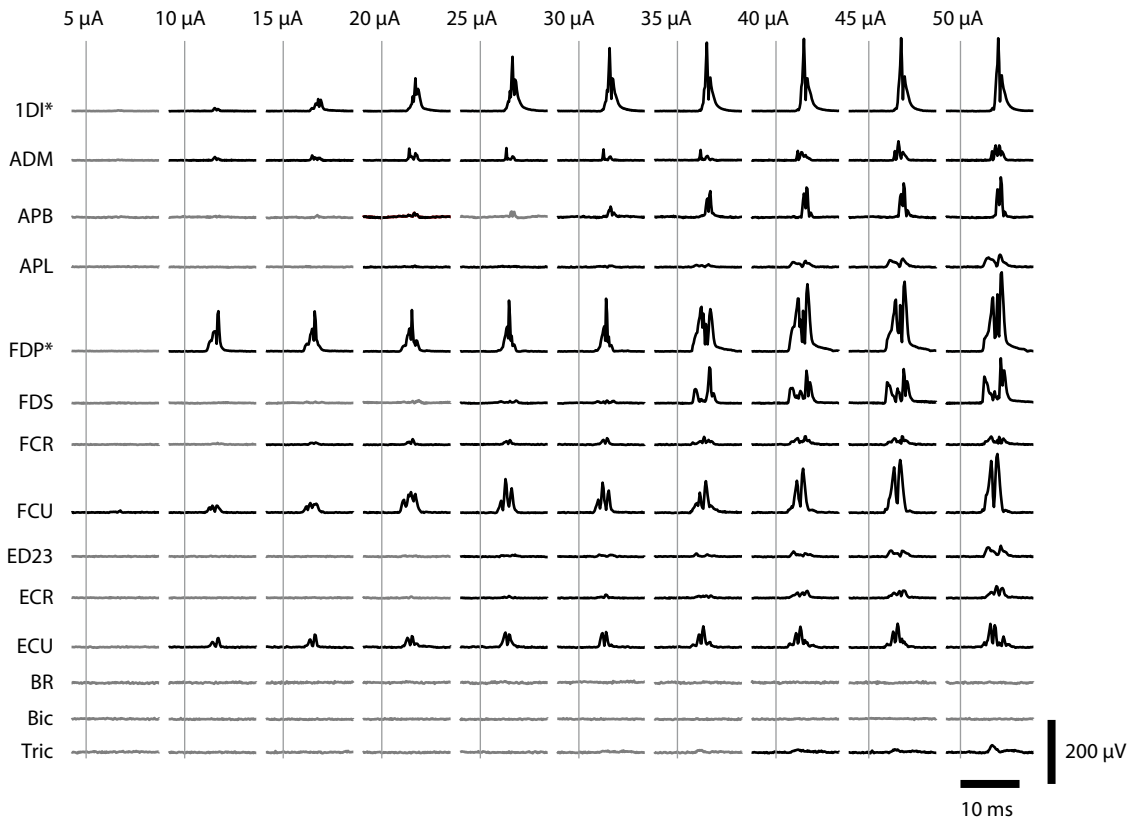

Figure 3.2: SCEPs for all recorded muscles at different stimulation intensities. Vertical lines mark times of stimulus pulses. Monkey C, wire 10.

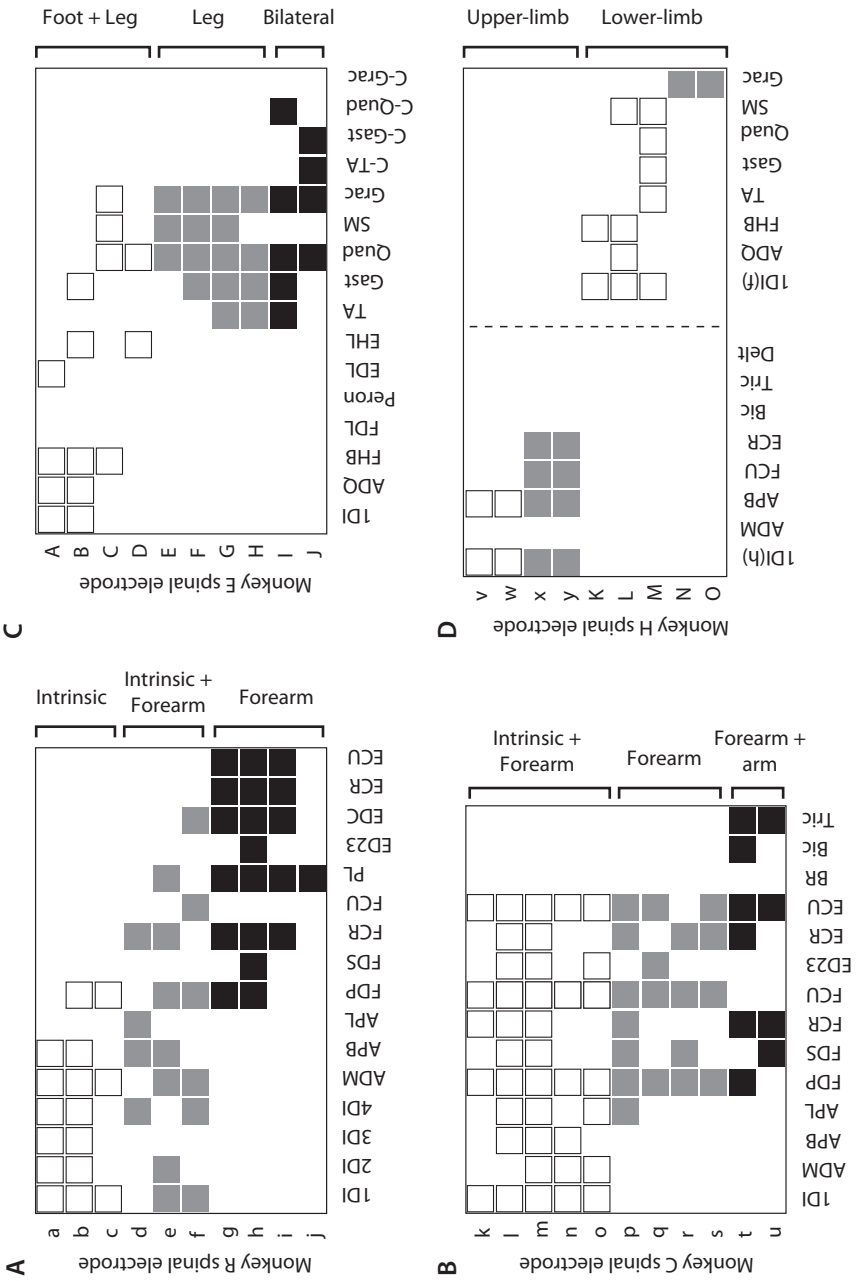

Figure 3.3: Muscle groups activated by supra-threshold stimulation pulses.

patterns can be observed.

3.3.3 Experiment 1: Paired Pulse Series

Non-linearities in the Response to Paired Stimulation Pairs of single stimuli were delivered at two sites with inter-stimulus intervals up to 30 ms. For each interval, we looked for sub- or supra-linear summation in the response to paired stimulation by comparing against the SCEP that would be predicted by linear summation of unrectified EMG (see methods). For

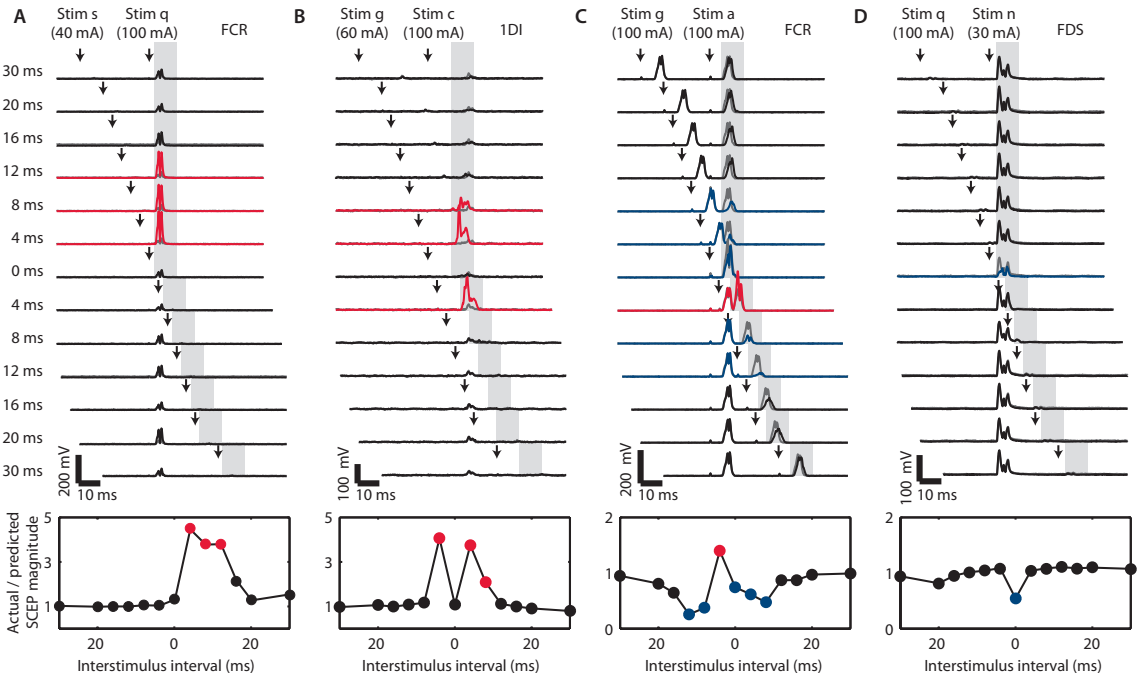

Figure 3.4: Rectified and averaged spinal cord evoked potentials resulting from paired stimulation of two electrodes, four sample cases. Every row represents a different delay between the stimulation pulses. Panels at bottom show the ratio of actual and expected SCEPs as a function of the delays. *(A)* Facilitation of response to stimulation on one electrode by preceding stimulation on another electrode. No difference in response was found for the opposite order of stimulation. *(B)* Facilitation occurs at short delays irrespective of stimulus order. *(C)* Significant facilitation is found at one interval, while suppression occurs at neighbouring latencies. *(D)* Suppression of response is found for concurrent stimulation.

most pairs of electrodes, the majority of muscles exhibited linear summation. However, we also found a wide variety of non-linear interactions, of which examples are shown in fig. 3.4. The most common non-linear interaction was a facilitation of the SCEP (fig. 3.4 A), which often had an asymmetric dependence on inter-stimulus interval peaking at 4 or 8 ms. Interactions of this type were seen both with stimuli that were below and above threshold for eliciting an SCEP when delivered alone. Less common was the symmetric pattern shown

in fig. 3.4 B in which two near-threshold stimuli evoked a large response when delivered together with an interval of +4 or −4 ms.

As well as supra-linear interactions, we found instances where the response to paired stimulation was smaller than that predicted by linear summation. Figure 3.4 C shows an example in which responses to the second stimulus is suppressed by prior stimulation of a different site. In this case, both stimuli are above the threshold for eliciting an SCEP. Therefore a possible explanation is that the individual SCEPs comprise overlapping populations of same motor units, which are unable to respond to both stimuli in quick succession. However, this cannot explain the example shown by fig. 3.4 D, in which a sub-threshold stimulus suppresses the SCEP from a second site. Sub-linear interactions of this type were seen most often with an inter-stimulus interval of zero. While it is conceivable that simultaneous stimuli may not excite the tissue with comparable efficacy due to shunting of current between electrodes, this seems unlikely since SCEPs elicited by these stimuli in other muscles exhibited linear summation over all intervals (data not shown). Therefore these sub-linear interactions in specific muscles may arise from activation of inhibitory pathways although further experiments are needed to confirm this.

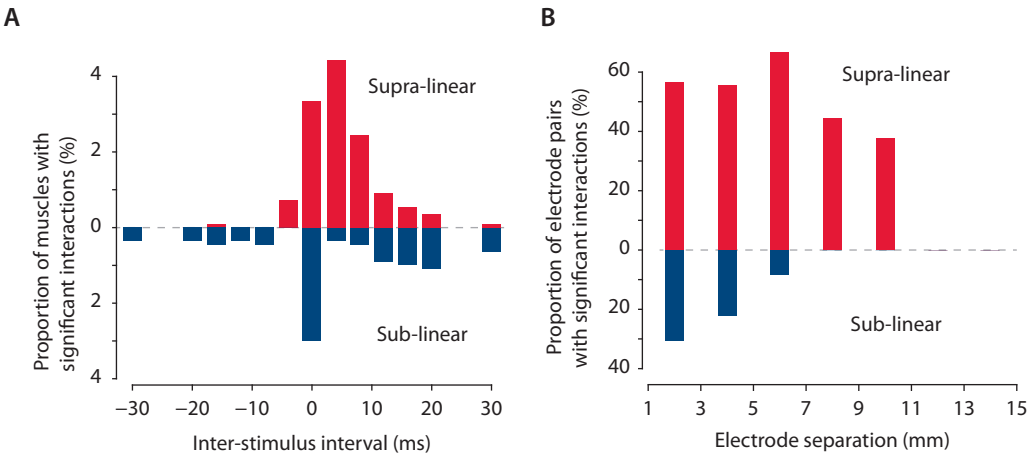

Figure 3.5: *(A)* Proportion of muscles with significant interactions at different inter-stimulus intervals. Supra-linear interactions are more abundant and more prevalent at short latencies than sub-linear interactions. *(B)* Proportion of electrode pairs with at least one muscle with significant interactions as function of electrode separation. Supra-linear interactions are found over larger distances than sub-linear interactions.

Temporal Pattern of Non-linear Interactions Overall, 38 out of 75 tested pairs of stimulation electrodes (51 %) exhibited a significant supra-linear interaction in at least one muscle for at least one inter-stimulus interval. The red bars in fig. 3.5 A show the percentage of muscles

that exhibited significant supra-linearity for each interval, averaged across all pairs of stimulation electrodes. In compiling this average, there is an ambiguity as to whether intervals should be plotted to the left or right of time zero (i.e. which of the pair of stimuli to measure the interval relative to). We resolved this by orienting the time axis for each pair of electrodes such that the majority of significant interactions between that pair were to the right of time zero. This highlights the asymmetric time-dependence of supra-linear interactions (cf. fig. 3.4 A) which peak at around 4 % of muscles for inter-stimulus intervals of 4 ms. The width of this distribution indicates that some interactions extended out to inter-stimulus intervals of 20 ms.

16 out of 75 electrode pairs (21 %) exhibited significant sub-linear summation in at least one muscle. The blue bars in fig. 3.5 A show the percentage of muscles exhibiting sub-linear effects for each interval across all pairs of stimulation electrodes. Again, the time axis has been oriented for each pair of electrodes such that the majority of significant interactions were to the right of time zero. The distribution of sub-linear interactions showed greater symmetry around time zero, with suppression for intervals between 8–20 ms in either direction seen for many electrode pairs (cf. fig. 3.4 C). For other pairs, sub-linear interactions were seen only with an interval of zero (cf. fig. 3.4 D).

Spatial Pattern of Non-linear Interactions Figure 3.6 shows the approximate medio-lateral and rostro-caudal locations of electrodes based on photographs taken during the experiment and post-mortem histology. In agreement with Moritz et al. (2007) we found no clear somatotopy to the motor effects elicited by cISMS, although there was a slight tendency for SCEPs in distal muscles to be elicited from more caudal sites. Overlaid on this map are coloured lines indicating supra-linear, sub-linear or mixed interactions between electrodes. Significant interactions were widespread throughout the cervical enlargement, often extending across multiple segments. Figure 3.5 B shows how the number of electrode pairs exhibiting supra- or sub-linear interaction (as a proportion of the number of electrode pairs tested) varies with electrode separation. Supra-linear interactions were seen with electrode separations up to 10 mm with a mean ±SD of 4.6 ± 2.4 mm. Sub-linear interactions had a shorter range up to separations of 5 mm with a mean ±SD of 2.9 ± 0.9 mm. This difference was significant ($p < 0.001$, unpaired t-test), consistent with the idea that many sub-linear interactions may have resulted from stimuli that directly activated overlapping populations of motor units.

Non-linear summation of responses occurred between stimulation electrodes with both similar and different motor outputs according to the distal-proximal categories defined in fig. 3.3.Of 20 tested pairs in which both electrodes were grouped in the same category 13

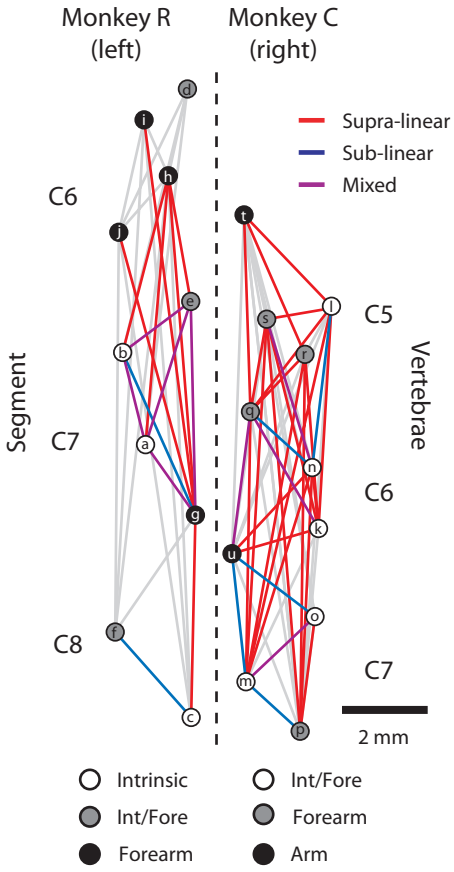

Figure 3.6: Map of electrode locations. Shades of circles represent location of muscles with SCEPs evoked from this site. Lines connecting circles indicate that this pair of electrodes was tested for interactinos. Colour of lines indicates whether and what kinds of interactions were found.

(65 %) exhibited a supra-linear interaction compared with 25 out of 55 pairs that spanned different categories (45 %), but this difference was not significant (p = 0.13, χ^2-test). 3 electrode pairs in the same category (15 %) versus 13 of the pairs in different categories (24 %) exhibited sub-linear interaction and again this was not significant (p = 0.42, χ^2-test).

Supra-linear Interactions are Most Pronounced in Intrinsic Hand Muscles Although interactions were distributed between electrodes in each distal-proximal category, we found that supra-linear summation was more common in distal muscles, particularly in the intrinsic muscles of the hand. For example in monkey C, 19 out of the 63 supra-linear interactions (30 %) counted across different muscles occurred in intrinsic hand muscles, even though these accounted for only 3 of the 14 recorded muscles. This discrepancy could be explained if intrinsic hand muscles are over-represented in the distribution of stimulation effects from each site. However, at these intensities, only 18 % of significant SCEPs evoked by individual stimulation were seen in intrinsic hand muscles. These percentages and equivalent data

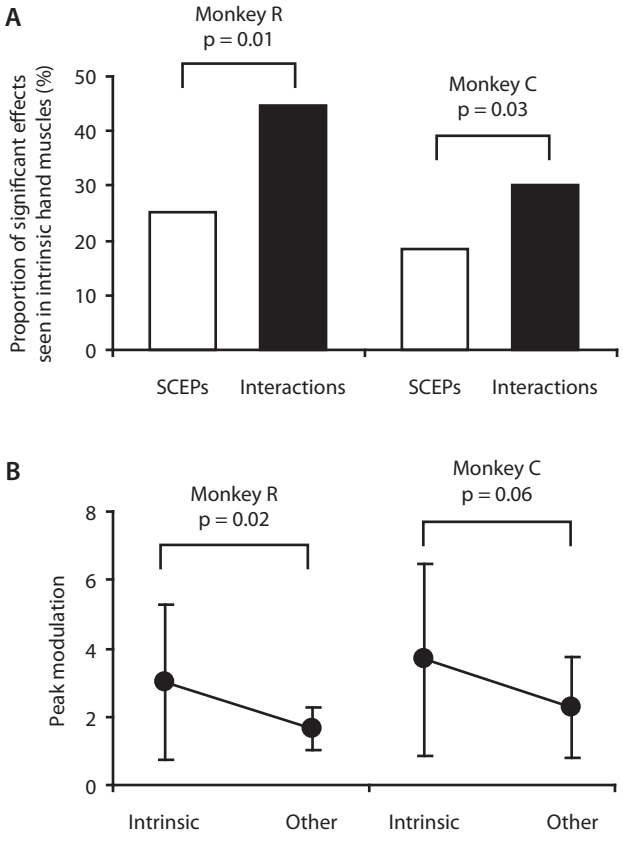

Figure 3.7: *(A)* Proportion of significant effects in intrinsic hand muscles. See text for explanation. *(B)* Supra-linear interactions are more pronounced in intrinsic hand muscles compared to other muscles.

for Monkey R are shown in fig. 3.7 A. The difference between the intrinsic/non-intrinsic distribution of SCEPs versus supra-linear summation effects was significantly different in both animals (χ^2-test, Monkey R: $p = 0.01$; Monkey C: $p = 0.03$). As a further test, we normalised the response to paired stimulation by the response predicted from linear summation, and averaged these values separately across intrinsic hand and other muscles in which there was a significant supra-linear interaction. Where multiple inter-stimulus intervals for a pair of stimulation sites yielded significant supra-linear summation in a given muscle, the maximum normalised response was used. The data summarised in fig. 3.7 B show that the average magnitude of supra-linear interactions was greater in intrinsic hand muscles than other muscles for both monkeys (Monkey R mean (SD): 3.0 (2.3) vs. 1.7 (0.6), $p = 0.02$ unpaired t-test; Monkey C: 3.7 (2.8) vs. 2.3 (1.5), $p = 0.06$).

3.3.4 Experiment 2: Interleaved Trains Stimulation

To test whether the non-linearities observed in paired pulse stimulation as described in Experiment 1 are relevant for longer stimulation protocols, we delivered interleaved trains of stimuli (50 Hz per channel, 0.5 s duration, several time shifts, see methods) to pairs of electrodes. We first identified for each pair of stimulation electrodes muscles that showed a significant effect of the time shift between trains on the difference between measured integrated EMG and its linear prediction using an ANOVA (see methods). For those identified muscles, we then performed a two-sample t-test between linear prediction and measured EMG to determine the conditions for which non-linear interactions occurred (Bonferroni-corrected for multiple comparisons) and determined whether the interaction was sub- or supra-linear. We then counted the number of muscles that showed sub- or supra-linear interactions in at least one condition for each pair. Figure 3.8 A shows this distribution. Crucially, we found that for 60 % of the tested pairs there was at least one muscle amongst the ones we recorded EMG from with supra-linear interactions. Sub-linear interactions occurred less frequently, in 53 % of tested pairs. Also, 75 % of pairs with sub-linearly interacting muscles had only 4 or fewer muscles showing this effect. This is in contrast to pairs with supra-linear interactions, where the average number of muscles showing an effect is higher.

Next, we asked whether different time shifts between stimulation trains would affect the occurrence of interactions (fig. 3.8 B). For each pair of electrodes and time shift we counted the number of muscles showing significant supra- or sub-linear interactions. The same ambiguity as to which electrode is to be counted first arises as discussed for the paired pulses experiment. We resolved this ambiguity again by aligning the data so that a majority of the

interactions are to the right of zero. Supra-linear effects again concentrated around short positive time shifts, whereas sub-linear effects were distributed more evenly.

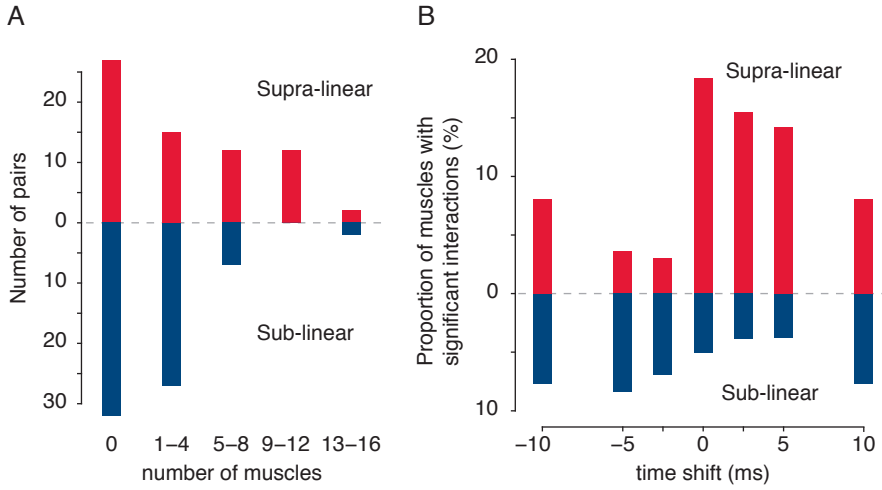

Figure 3.8: *(A)* Numbers of electrode pairs that had x numbers of muscles showing supra-linear *(top)* or sub-linear *(bottom)* interactions for at least one time shift condition. *(B)* Proportions of all muscles in all stimulation electrode pairs that showed a significant difference between integrated EMG and the linear prediction for each condition. To resolve the arbitrary assignment of negative and positive time shift, all muscles belonging to one electrode pair were counted so as the majority of muscles fell to the right side of zero (cf. fig. 3.5)

We then asked whether interactions between stimulation electrodes were manifested in isometric forces measured at the wrist. We compared the average force directions and amplitudes during the latter half of the stimulation period as predicted by the linear sum of force directions and amplitudes caused by stimulation at single electrodes with those force directions and amplitudes measured during trials with different time shifts between the electrodes. Figure 3.9 shows examples for isometric force trajectories measured using different time shifts. Trajectories for single channel stimulation are shown, as is their linear combination for time shift 0 ms (linear combinations for different time shifts are virtually identical). In fig. 3.9 A, the most obvious deviation from the linear force prediction occurred at time shift 0 ms, and the difference was significant both for direction and amplitude. For other time shifts, the difference in force amplitude was not significant, and the change in direction was only different in the 10 ms time shift condition. In fig. 3.9 B, only the direction of forces was significantly different from prediction in some conditions (0, −2.5, −5 and 10 ms).

If muscles in which non-linear effects due to stimulation occurred were recorded from, it is possible to attribute the difference between expected and measured forces to those muscles using their EMG recording. In fig. 3.10 we show the integrated EMG recorded during the same sessions as the force trajectories shown in fig. 3.9. For some examined electrode pairs,

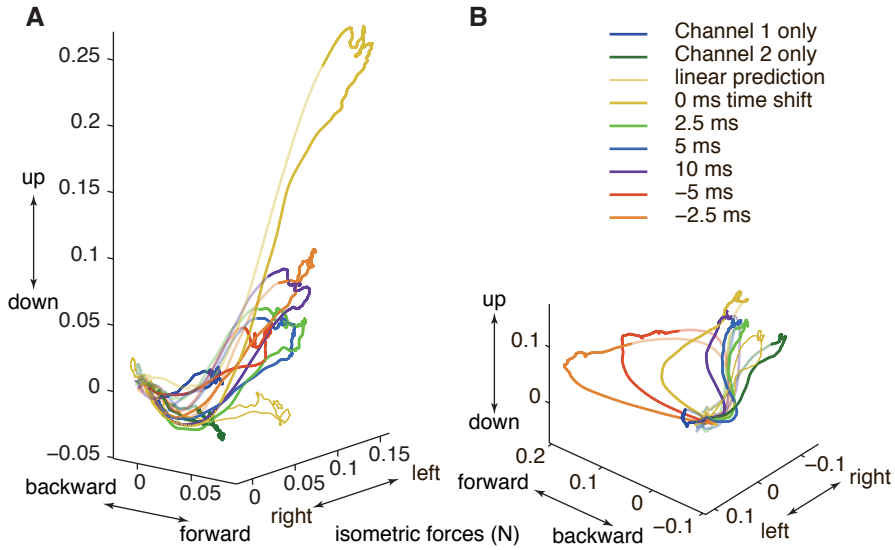

Figure 3.9: Sample isometric force trajectories measured at the wrist and averaged across trials. *(A)* example for significant difference in direction ($p < 0.02$) and amplitude between conditions ($p < 0.001$). Monkey X, recording `110620_011_9` *(B)* significant difference in direction only ($p < 0.0001$). Stimulation conditions include single channel stimulation and stimulation of both channels at different time shifts. Light part of trajectory designates force after stimulation offset. Monkey Sa, recording `058`.

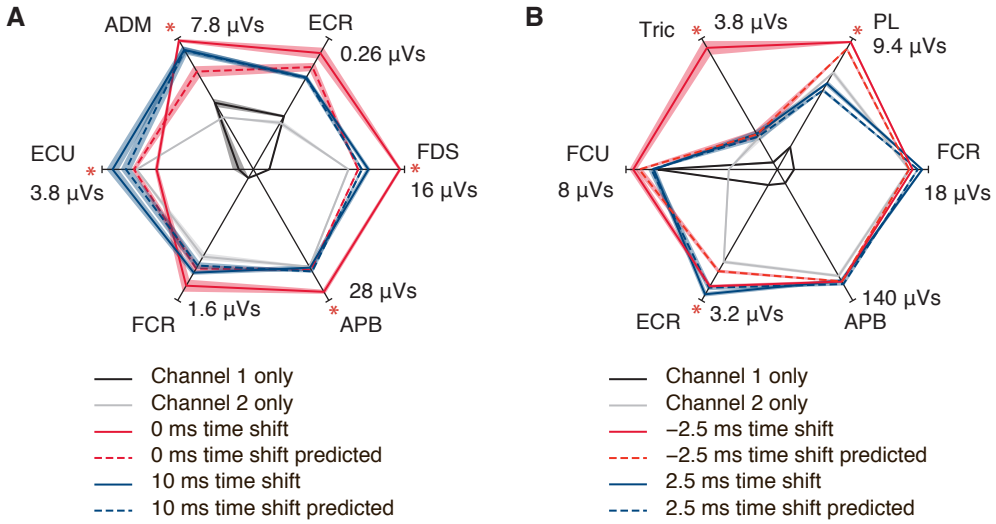

Figure 3.10: EMG activity for samples shown in fig. 3.9. Each axis represents the integrated EMG during stimulation, averaged across trials, for one muscle. Shaded areas indicate standard error of the mean. Only a subset of muscles is shown. Asterisks indicate a significant ($p < 0.0001$) difference between the measured EMG and its prediction for that muscle in condition 0 ms (for A) and −2.5 ms (for B).

supra- and sub-linear interactions in several muscles combined to the observed changes of force trajectories (cf. fig. 3.10 A), while for others, the measured force effects could be attributed mostly to one muscle (cf. fig. 3.10 B). Half of the pairs tested showed significant deviations from the linear prediction of force trajectories, in direction, amplitude, or both in at least one condition (cf. table 3.2).

Electrode pairs with:		*summation of force directions*	
		linear	non-linear
summation of absolute forces	linear	35	18
	supra-linear	2	9
	sub-linear	1	3

Table 3.2: Number of electrode pairs showing significant interaction effects on force direction and amplitude in at least one stimulation condition.

3.4 Discussion

In these experiments we have shown that paired cervical ISMS in the macaque monkey causes non-linear interactions as measured by EMG and forces measured at the wrist. Both supra- and sub-linear summation of effects occur, and these are wide-spread phenomena involving approximately half of the stimulation electrode pairs we tested.

What are the potential mechanisms for these non-linear interactions? As indicated by the time and low jitter from stimulus to onset of EMG responses most of the single electrode evoked responses is due to direct activation of motoneurons (see fig. 3.4). However, ISMS will not only excite motoneurons, given that sensory afferents are generally excited at lower stimulus intensities (Gustafsson et al. 1976, Gaunt et al. 2006). The position of the limb is known to influence the direction and strength of movements evoked by ISMS in frog, rodents and cats which is also reflected in the EMG response (Bizzi et al. 1991, Tresch et al. 1999, Lemay et al. 2004); in this study, we have not investigated this variable, however, by having an isometric setup, we avoided potential changes of interactions during long train stimulation. One potential explanation for our results is that stimulation at one site may excite proprioceptive afferents and thus provide incorrect feedback about limb position. Alternatively, excitation could spread through local networks. In both cases, this would then lead to a modulation of the EMG response due to stimulation at the second site.

We have found that sub-linear interactions occur over shorter distances than supra-linear interactions (fig. 3.5). This suggests that long-range connections activated by stimulation are

excitatory while short-range connections are inhibitory (It is interesting to note the similarity with cortical organisation). Additionally, we found that the timing between stimuli modulates the response strength (cf. fig. 3.4). On average, facilitation occurs at shorter time intervals than suppression (fig. 3.5 A). This coincides with results from repeated stimulation of the same site (cf. fig. 2.1 C), where we found in a proportion of tested sites that short stimulation intervals facilitate the EMG response, but longer intervals lead to suppression.

3.4.1 Previous Experiments

Co-stimulation experiments in acutely spinalised frogs (Bizzi et al. 1991) and chronically spinalised rats (Tresch et al. 1999) have found linear summation in almost all tested electrode pairs. In the decerebrate cat, Grill et al. (2002) found that force fields obtained by co-stimulation was best explained as 'winner-take-all'. Why did these previous studies not find significant numbers of non-linear interactions? The cited experiments were done in the lumbar cervical cord investigating hind-limb function whereas we examined the cervical cord and arm and hand functions. Additionally, primates have evolved direct CM projections and fine control of hand and arm movement (Lemon 2008). Also, in our experiments we did not sever the spinal cord from the rest of the CNS. It is therefore possible that the cortex has some modulating function on the spinal circuitry that was lacking in other experiments. However, given the short latency of interactions observed (cf. fig. 3.5), we can exclude the involvement of a cortical feedback loop in the majority of cases. In one previous study, Giszter and colleagues report non-linear interactions in bilateral stimulation of the frog lumbar cord (Giszter 2000). It is worth noting that all of our experiments were done in the ipsilateral cord. A further difference that may have facilitated the observation of non-linear interactions are the stimuli that were used. While Bizzi et al. (1991), Tresch et al. (1999), Grill et al. (2002) used only simultaneously delivered trains, we tested various inter-stimulus intervals. Most of the supra-linear effects were seen at non-zero IStIs. It is possible that simultaneously delivered stimuli could cancel or interact otherwise electrically and are thus less efficient. However, we also observed a significant number of non-linear interactions for simultaneous stimulation (figs. 3.5 and 3.8).

3.4.2 Implications for Motor Control

Force-field summation observed in frogs and rats has been viewed as evidence for a modular organisation of the motor system, with motor primitives and synergies hard-wired in the spinal cord and the cortex selecting the appropriate primitives at the time of movement execution (Bizzi et al. 2008). Our results show however that there are far-reaching interac-

tions on the spinal level. This means that any 'modules' on the spinal level would not act independently. Together with the observation that the output of the cortex to muscles is mostly linear (Baker et al. 1998) our results would suggest a linearising property of spinal circuits.

3.4.3 Non-linear Interactions May be Useful for Neural Prostheses

For a potential neural prosthesis using ISMS to restore grasp function a large movement repertoire is desirable. Electrodes that we presently implant chronically into monkeys' spinal cords have 17 electrodes (see chapter 4). While such electrode implants can activate a variety of muscles, combining electrode pairs with non-linear interactions has the potential of increasing the space of movements.

On the other hand, there are at least two cases in which non-linear interactions may not be beneficial: First, in tasks involving sequences of movements such as reaching for an object, grasping, and transporting it (Zimmermann et al. 2011b) ideally one would want to control the individual task stages without interactions. Second, since forces evoked by ISMS are often relatively weak (in the order of 0.1 N, cf. fig. 3.9), it may be necessary to combine stimulation of several electrodes having similar effects on muscles to obtain a larger net force. Of course, in such a scenario, non-linear interactions are only desirable if they yield a supra-linear activation of those muscles that are activated by the individual electrodes.

3.4.4 Variation Between Animals

There was some variation in results between animals tested, including one animal where most interactions between trains of stimuli (experiment 2) yielded sub-linear interactions independent of time shift between stimuli. This variation could have arisen from several factors, including age of the animals, different reaction to anaesthetic agents, or varying health of the spinal cord during the experiment. This variation highlights the importance of careful replication of experimental results in more than two animals.

3.5 Conclusion

In these experiments we have demonstrated that non-linear interactions arise frequently when stimulating the macaque cervical spinal cord at two sites, both with paired pulses and longer trains. These results challenge previously proposed models of independently activated synergistic modules in the spinal cord. Neural prostheses employing cISMS will

have to take these interactions into account, and they can possibly gain in range of obtainable movements.

4 Methods: Floating Microelectrode Array Spinal Cord Implants

In this chapter we describe the implantation of Floating Microelectrode Arrays into the macaque cervical spinal cord for acute and chronic stimulation. These electrode array implants will then be used in chronic neuroprosthetic experiments such as described in chapter 5.

Surgical procedures were performed jointly by Andrew Jackson and myself. Thresholds for ISMS in monkey Rv were determined by myself, and, during a period of one month, by AJ. Histological processing of tissue was performed by Shurong Li, Jennifer Tulip, and myself.

4.1 Introduction and Background

4.1.1 Motivation

ISMS has been used to investigate spinal cord physiology in acute and chronic preparations. In acute experiments, typically single microwires or other electrodes are lowered into the exposed cord (chapters 2 and 3; e.g. Riddle et al. 2009). For chronic experiments, three major requirements need to be fulfilled: (a) electrodes need to be reliably anchored to and form low impedance electrical contact with the neural tissue, (b) the spinal cord needs to be protected from the environment, and (c) stability of the vertebral column needs to be preserved. Especially in the context of potential clinical applications, long lasting implants are needed that do not pose a danger to the surrounding tissue, have a life time of years, and maintain good electrical coupling to neural populations.

Two strategies have been employed in the past for chronic preparations. Several groups use a 'chamber-based' approach to access the macaque spinal cord: A laminectomy is performed to expose the spinal cord, then a chamber is implanted over the cord, allowing access for acutely inserted electrodes and protecting the vulnerable cord (technique described in S. I. Perlmutter et al. 1998, see fig. 4.3 A). Other groups have implanted microwires or

microelectrode arrays (MEAs) into the cord for recording (Prasad et al. 2011, 2010) and stimulation (Mushahwar et al. 2000c, Yakovenko et al. 2007) in cats and rodents. While chamber implants offer the chance to insert many electrodes sequentially, they tend to last only a relatively short time (weeks to months; S. I. Perlmutter et al. 1998, Seki et al. 2009; chapter 5). A common mode of failure is for the chamber to separate from the vertebrae it was anchored to, offering a path of entry for infection and reducing stability.

Using microwire and MEA implants, on the other hand, allows the cord to be completely sealed (except for connecting wires). Microwires have not been implanted in large numbers, and the implantation procedure is challenging. As for MEAs, to our knowledge only the 'Utah' electrode array (UEA; Blackrock Microsystems) has been chronically implanted into rodent spinal cords. While UEAs afford high electrode counts and densities their electrodes are usually limited to a length of 1.5 mm and commonly all electrodes share the same length (however, staggered configurations are available, cf. Branner et al. 2001). The macaque spinal cord is larger in diameter than the rat's, and the motoneuron pools of the ventral horn reside at a depth of 3–5 mm from the dorsal surface of the cord. For this reason, standard UEAs are currently not suitable for spinal implants in macaques.

Floating microelectrode arrays are based on a ceramic die ($1.8 \times 4.2 \times 0.9\ \mathrm{mm}^3$) equipped with up to 36 platinum/iridium electrodes whose lengths can be individually specified (Musallam et al. 2007). They have been used by several groups to record chronically from cortical tissue (Newman et al. 2011, Mollazadeh et al. 2011, Townsend et al. 2011, Richardson et al. 2012). Because they offer high electrode density and can target neural populations at different levels, FMAs are a good candidate for chronic spinal implants.

When using such an array, there are numerous decisions that need to be made regarding the implant procedure. How many vertebrae should be fused in order to maintain the stability of the vertebral column and to reduce movement of the cord within the spinal canal? How should the array be held in place? How should the connector wire be routed away from the array, and where should the connector be placed? In experiments described in this chapter we aim to answer these questions.

4.1.2 Aims

The main aims of the experiments described in this chapter were to

1. Establish a configuration of FMA that is suitable for ISMS.
2. Develop an implant procedure for chronic implantation of FMAs in the macaque spinal cord.

3. Determine long-term effects of the implant and of ISMS delivered through FMAs on spinal cord tissue.

4.1.3 Experiments

In order to establish the suitability of FMAs for ISMS and to practise the implantation procedure we first used FMAs in some acute experiments whose main aim were to characterise interactions between stimulation channels (chapter 3). Next, we chronically implanted an FMA into a monkey which had not undergone behavioural training in order to test the recovery implantation procedure and long term tissue compatibility. Finally, two monkeys used for the chronic experiments (chapter 5) and another one primarily used for a different experiment received FMA implants.

In what follows I will describe the implant procedure, report results from electrode testing over time, and discuss the results.

4.2 Methods

4.2.1 Electrode Arrays

FMAs were acquired from MicroProbes, Gaithersburg, FL, USA, and made to our specifications. All arrays used in our experiments had 17 electrodes. Impedances were specified to be 50 kΩ for the 16 electrodes intended for stimulation and 10 kΩ for the reference electrode. Actual impedances varied between 40 and 90 kΩ. The array used for acute experiments and for monkey Ra consisted of nine 5 mm long and eight 3 mm long electrodes. The arrays chronically implanted into monkeys Ar, Rv, and Rp had four 3 mm long electrodes, nine 4 mm long ones, and four 5 mm long ones, with longer electrodes concentrated near the medial edge of the array (see fig. 4.7 A).

4.2.2 Acute Implants

Implant Procedure Animals were prepared as described in section 3.2.1. After laminectomy of vertebrae C4–T1 and removal of dura mater, an FMA was positioned above the cord. This was accomplished by clamping a thin metallic suction tube onto a hydraulic manipulator (MO-10, Narishige, Japan), which itself was held by a stereotactic manipulator (David Kopf Instruments, Tujunga, CA, USA). Vacuum was applied to the suction tube, holding the FMA's die in place (fig. 4.1). After the protecting layer of polyethylene glycol was washed off the array, it was lowered into the spinal cord. Care was taken to ensure that

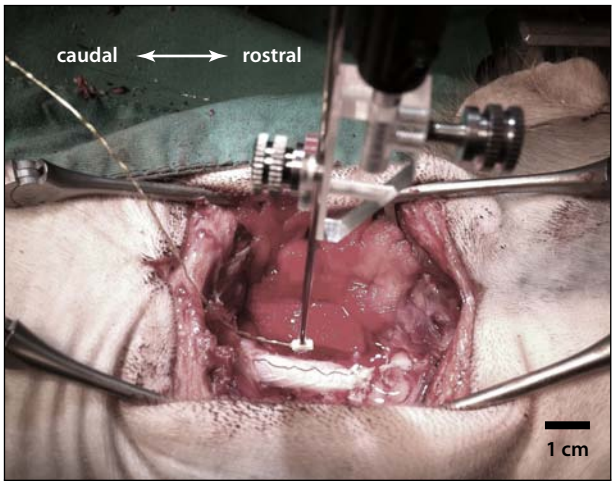

Figure 4.1: Insertion of FMA during acute experiment. Array held in place by suction tube. Wires exit caudally. Scale bar refers to plane of array. Monkey Ti. Saturation of image was adjusted.

the cord was depressed as little as possible during insertion, by maintaining slow insertion speed (~0.25 mm/min), and in some animals incision of pia and arachnoid. During the entire procedure the cord was kept moist with physiological saline solution. A bare wire attached to the array's connector serving as a stimulation return path was placed near the the surface of the cord submerged in saline solution.

Motor Threshold Test After the array had been left to settle the array was used for stimulation and motor thresholds were determined for individual electrodes. Thresholds were tested by delivering a pseudo-randomised sequence of biphasic (200 µs per phase), cathodic first, current-controlled pulses to each electrode of the array (inter-pulse interval: 0.5 s). Electrodes were tested with a sequence of pulses ranging from 5 to 50 µA in 5 µs steps, 20 repetitions.

4.2.3 Chronic Implants

First Implant – Monkey Ra The FMA was implanted without a chamber and its connecting wires were tunnelled to the head. Anaesthesia was induced with an intramuscular injection of ketamine (10 mg/kg body weight). The monkey's head was fixed into the ear bars of a stereotactic frame, allowing us to tilt the head forward in order to straighten the spine. Vertebrae C5–T1 were dissected to gain access to their lateral masses. Small screws were then inserted into the lateral masses of vertebrae C5–T1 as described by S. I. Perlmutter et al. (1998). After a bilateral laminectomy of C6 and C7 was performed, ligament covering the dura was removed, and the dura was incised along the midline. Absorbable sutures

were placed through the dura flap, two on each side, in order to later close the dura over the implant. A neuromuscular block (atracurium, initial dose 0.5 mg kg^{-1}, then 1 mg kg^{-1} h^{-1} IV) was induced and its onset was confirmed by delivering stimulus pulses to the left median nerve and observing APB EMG on the oscilloscope vanish.

The array was then implanted as described above (see page 46, fig. 4.2). The array was

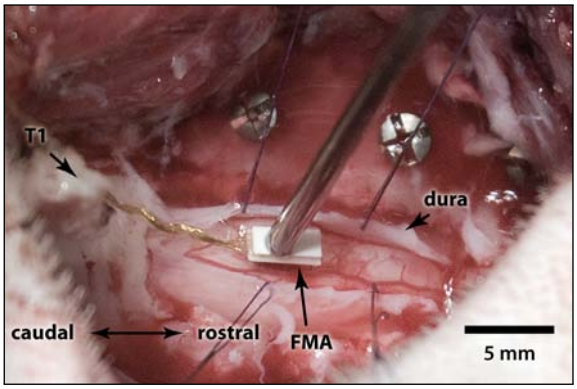

Figure 4.2: Photograph taken during insertion of an FMA. The lower cervical cord of monkey Ra is exposed. The dura has been cut open and is held by sutures, which are later used to close the incision. Screws in the lateral masses of vertebrae C5–T1 covered with dental acrylic to fuse and stabilise the column. The FMA is slowly pushed into the cord using a suction tube. Gold wires exiting the array are routed away and in this monkey lead directly to the head.

fixed to the pia mater with a drop of cyano-acrylate (Indermil) and the wires were arranged to lie flat on the pia. The ground wire (used as return path for stimulation) was tied to the dura when the dural incision was closed with the previously placed sutures. After the dura was sutured over the array, it was covered with a layer of Gelfoam. Wires were attached to the T1 process with two-part silicon (Kwik-Sil, World Precision Instruments). A thin layer of dental acrylic was applied over screws and Gelfoam-covered implant in order to fuse the vertebrae and protect the FMA. Lower muscular layers were then closed up using absorbable sutures.

A head island to place the connector was formed by resecting the scalp and periosteum in in a rectangular area (~15 × 25 mm^2) at the cranial vertex. Skull screws were placed in order to hold a head chamber commonly used in our group (see fig. 5.2 for a diagram of a similar chamber implant). The connector and connecting wire were then tunnelled subcutaneously to the head incision, and the chamber was placed over the connector. The periosteum was sutured over the wires at the margin of the incision for protection. Then two-part silastic and dental acrylic were used to cover the wires and to fixate the connector within the chamber. Finally, the head margin was tightened around the chamber with sutures and fixated with cyano-acrylate, and the back incision was closed as well.

Second Implant – Monkey Rv Because the implant in monkey Ra stopped working shortly after the implant due to broken wires (see section 4.3) we decided to pursue a more conservative approach with the next implant in monkey Rv. We essentially followed the implant technique developed by S. I. Perlmutter et al. (1998) and described on page 66, using a spinal chamber to protect the implant (fig. 4.3 B). Vertebrae C4–T1 were exposed and screws were

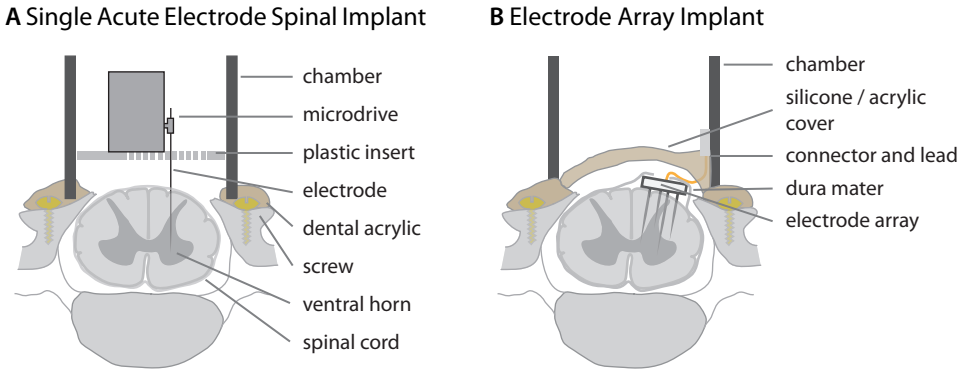

Figure 4.3: Sketch of spinal implants. *(A)* Spinal chamber commonly used for acute electrode penetrations. *(B)* Implant used for monkey Rv.

inserted into their lateral masses. A bilateral laminectomy of vertebrae C5–C7 was performed and the vertebrae were fused by application of a small amount of dental acrylic along the lateral masses. The dura was opened and the implant inserted as described above (fig. 4.4). Then the spinal chamber was placed around the implant site, fixed to the screws

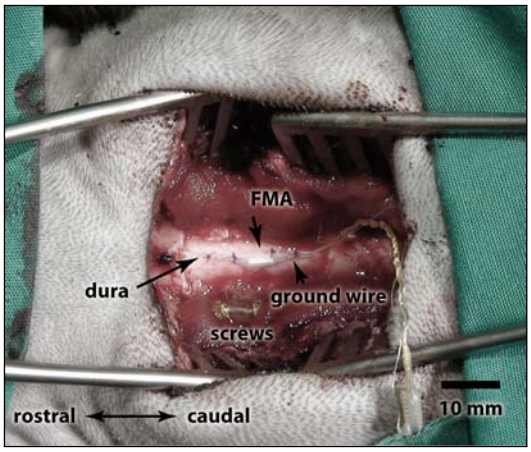

Figure 4.4: Photograph taken during the implant surgery for monkey Rv. Implant has been inserted and the dural incision is closed. See text for details.

with acrylic. The connector was attached to the inside of the chamber and the laminectomy was closed by application of more acrylic.

Third and Fourth Implants – Monkeys Ar and Rp For the next surgeries we again attempted an implant without a chamber, following essentially the procedure described for monkey Ra (page 47). To minimise the risk of broken wires we decided to use an intermediate wire bundle consisting of stranded stainless steel wires (FE6320; outer diameter 0.23 mm per wire; Advent Research Materials, Oxford, UK) commonly used in our laboratory for EMG electrodes. In monkey Ar, we applied collagenase as described by Paralikar et al. (2008) in order to facilitate penetration. We decided to not employ this this technique again due to more than expected bleeding of the spinal meninges. After the array was implanted and the dura incision sutured, the dura was covered with Kwik-Sil (monkey Ar) or Tisseel (Baxter; monkey Rp; Albala et al. 2006). In monkey Ar, the wire bundle was connected to the FMA's Omnetics connector. The connector compound was attached to the process of vertebra C4 with dental acrylic and then sealed. Kwik-Sil was applied over the wires near the connector to act as a strain relief. The wire bundle was then tunnelled to the skin margin at the head implant and terminated in a connector inside the head casing. In monkey Rp, the extension

Figure 4.5: Postmortem X-ray image of FMA implant. Lateral view of the cervical vertebral column. Arrowhead marks position of FMA between stabilising screws in lateral masses of vertebrae C5–T1. Wire from FMA are coiled for strain relief and lead to connectors fixed to T1. Stainless steel wires are tunnelled to head casing, where a connector was fixed. Object at lower left is an RFID tag.

wire bundle had been tunnelled from the head to a skin incision at the back in a previous surgery (see fig. 4.5). During the spinal implant the bundle with its connector was retrieved and connected to the FMA. The mated connectors were fixed to vertebra T1 with dental acrylic and sealed with Kwik-Sil.

Motor Threshold Test In chronically implanted animals, stimulation motor thresholds were determined at the beginning of sedation sessions (ketamine and medetomidine). Thresholds

were tested by delivering sequences of three current-controlled biphasic stimulus pulses (0.2 ms per phase, cathodic first, 300 Hz). Current was increased from zero to a maximum of 100 µA (150 µA in monkey Ar) until movements could be seen or an SCEP was reliably detected in the EMG of any of the implanted muscles.

4.2.4 Histological Processing

After perfusion with phosphate-buffered saline (PBS) and then a formalin-PBS solution, the spinal cords were extracted. Spinal cords were treated with sucrose for cryoprotection and then cut with a microtome to 50 µm slices. One set of the slices were stained with Cresyl Violet for cell bodies. Another set of slices was stained for glial fibrillary acidic protein (GFAP) in order to mark astrocytes. Slices were incubated with 150 µl 3 % normal horse serum for 1 h to prevent non-specific binding. Sectioned slices were incubated overnight with a 1:500 solution of the primary antibody for GFAP made up with PBS-triton on a rocker at 4 °C. GFAP slices underwent incubation with biotinylated antimouse for two hours. Slices were then incubated with streptavidin conjugated horseradish peroxidase (streptavidin-HRP) for one hour. After this incubation stage, five minutes washes of the slices with PBS were performed on a rocker. Next the diaminobenzidine (DAB) reaction was performed. One tablet per 5 ml of PBS of peroxide and urea hydrogen was formulated. Slices were incubated with DAB for 5 min before being transferred into PBS filled wells. Slices were mounted on gelatine-coated slides and were left to dry overnight. The slices then underwent a series of alcohol (5 min of 70 %, 95 %, 100 % and 100 %) and two 10 min Histo-Clear washes, before cover slips were mounted with Histo-Mount.

4.3 Results

4.3.1 Dataset

Stimulation thresholds were collected during the two acute experiments. Several days after the implant surgeries, thresholds were determined for the chronic animals. One animal's implant could be followed for over three months and thresholds were determined regularly. Spinal cords were recovered from all animals after perfusion and histologically examined.

4.3.2 Motor Thresholds for Stimulation

SCEPs could be evoked from 7 electrodes of the array in monkey X just after insertion, with mean (SD) thresholds at 17 (14) µA. In monkey Ti, all electrodes had a threshold be-

low 50 µA, the mean (SD) threshold being at 20 (12) µA. These thresholds are comparable to thresholds of SCEPs in other acute experiments using microwires (section 3.3.2, page 29). The slightly lower average thresholds could be explained by the fact that for FMAs, thresholds were measured just after insertion at the beginning of the experiment, whereas in other experiments, microwires are inserted at various times during an acute experiment, and thresholds measured later during the experiment are usually higher.

For chronically implanted FMAs, initial thresholds were higher (see table 4.1). Unfor-

Monkey	Number of Responsive Electrodes	Average Threshold (µA)	SD (µA)
Ra	9	77	14
Rv	17	28	22
Ar	15	88	21
Rp	13	76	30

Table 4.1: Stimulation thresholds after chronic implantation of FMAs. FMA had 17 electrodes. In monkey Rp, only 13 electrodes were tested.

tunately, due to breaking of wires (monkey Ra) and declining health for reasons unrelated to the spinal surgery (monkeys Ar and Rp), we were not able to follow the development of thresholds over a longer period. For monkey Ar, thresholds were determined again three days after the first time, and there was little change, with mean (SD) thresholds at 85 (25) µA.

4.3.3 Development of Stimulation Thresholds Over Time

Monkey Rv could be followed for over three months having a working implant. The animal was part of the cortical control of ISMS project (cf. chapter 5), involving frequent sedations as part of the experiment. At the beginning of sedation sessions stimulation thresholds of all channels of the FMA were measured. Figure 4.6 shows the development of these thresholds over time. Electrodes were only tested up to a current of 100 µA, and the proportion of electrodes which could not be excited remained low throughout. The first time the thresholds were measured was three days after surgery. Thresholds decreased on average, by 2–15 % of the first measurement, during the next two weeks. Thresholds then increased towards the end of the experiment, with a range of 112–220 % average increase from first measurement to each measured day of the last week. However, the spread of threshold changes was considerable, as at the end of the experiment six (of 17) electrodes had a threshold lower than the one first measured.

Did the position or length of electrodes have an influence on stimulation threshold? Figure 4.7 shows the threshold data from before with electrodes grouped by length (panel A)

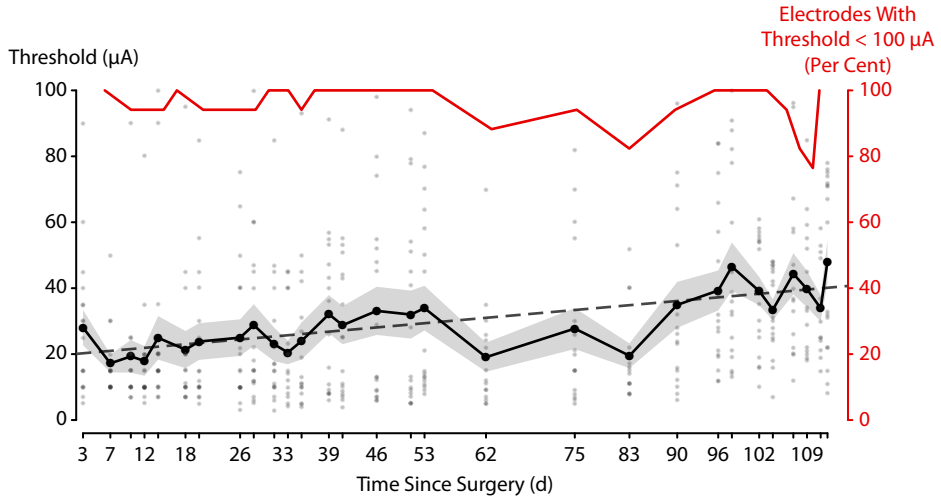

Figure 4.6: Development of motor thresholds for stimulation of an FMA implanted into monkey Rv. Thresholds were tested under sedation at the beginning of every experimental session. Dots represent measured thresholds of an electrode. Black line shows mean for each session, shaded area – SEM. Broken line is a linear fit through all measurements.

and lateral position on the array (panel B). In general, shorter and lateral electrodes had lower stimulation thresholds than longer or medial ones. All groups showed increasing stimulation thresholds, except for the group of 5 mm long electrodes, whose thresholds decreased marginally. This effect could be explained by the layer of scar tissue that formed between the array die and the spinal cord, thus pushing the array upwards. Long electrodes may have thus moved closer to neurons innervating hand and arm muscles (cf. section 4.3.6). This interpretation is supported by the fact that no holes of the shortest electrodes were visible in ventral sections of the cord (cf. fig. 4.12).

4.3.4 Electrodes on Array Stimulate Several Muscle Groups

In agreement with previous work (Moritz et al. 2007, and chapters 2 and 3), we find that electrodes distributed across even a small area such as here using FMAs will cause SCEPs in several different muscles. The array implanted in monkey Ra accidentally spanned the midline of the spinal cord (see fig. 4.11); there we found activation of both left and right wrist and finger flexors, albeit no bilateral effects from single electrode stimulation. In monkey Rv, electrodes mostly activated finger and wrist flexors and intrinsic hand muscles (see figs. 4.8 and 4.9). As previously, we observed clustering of effects for intrinsic and extrinsic hand muscles (cf. fig. 3.3), but these clusters do not seem to correspond to electrode location (cf. fig. 3.6; Moritz et al. 2007). While there seems to be a bias for distal muscles because only those muscles' EMGs were recorded, we did not observe proximal arm movements resulting

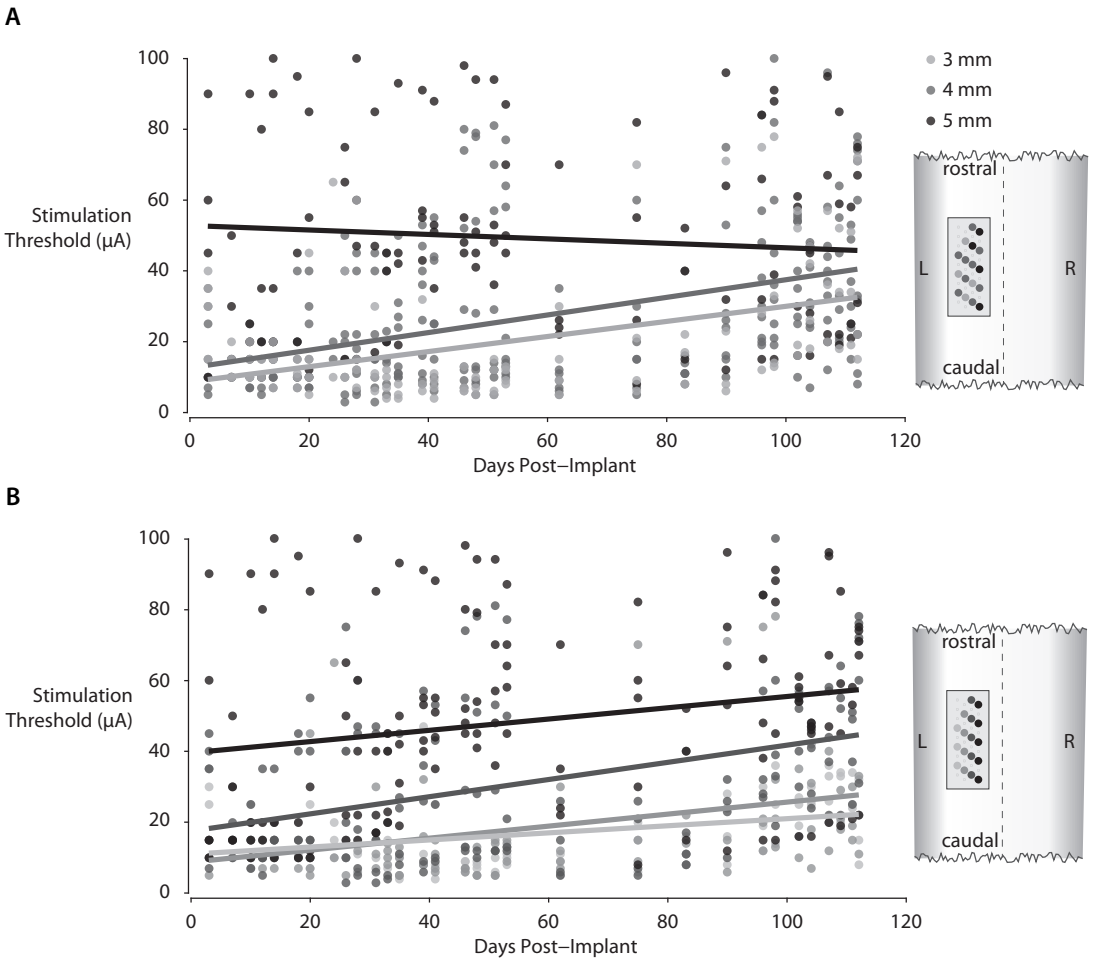

Figure 4.7: Development of motor thresholds, by length and position of electrodes. *(A)* Thresholds by length of electrode. Electrode positions on the array are marked in the drawing at right, which shows segment of the cervical spinal cord and approximate position of FMA. *(B)* Thresholds by laterality of electrode.

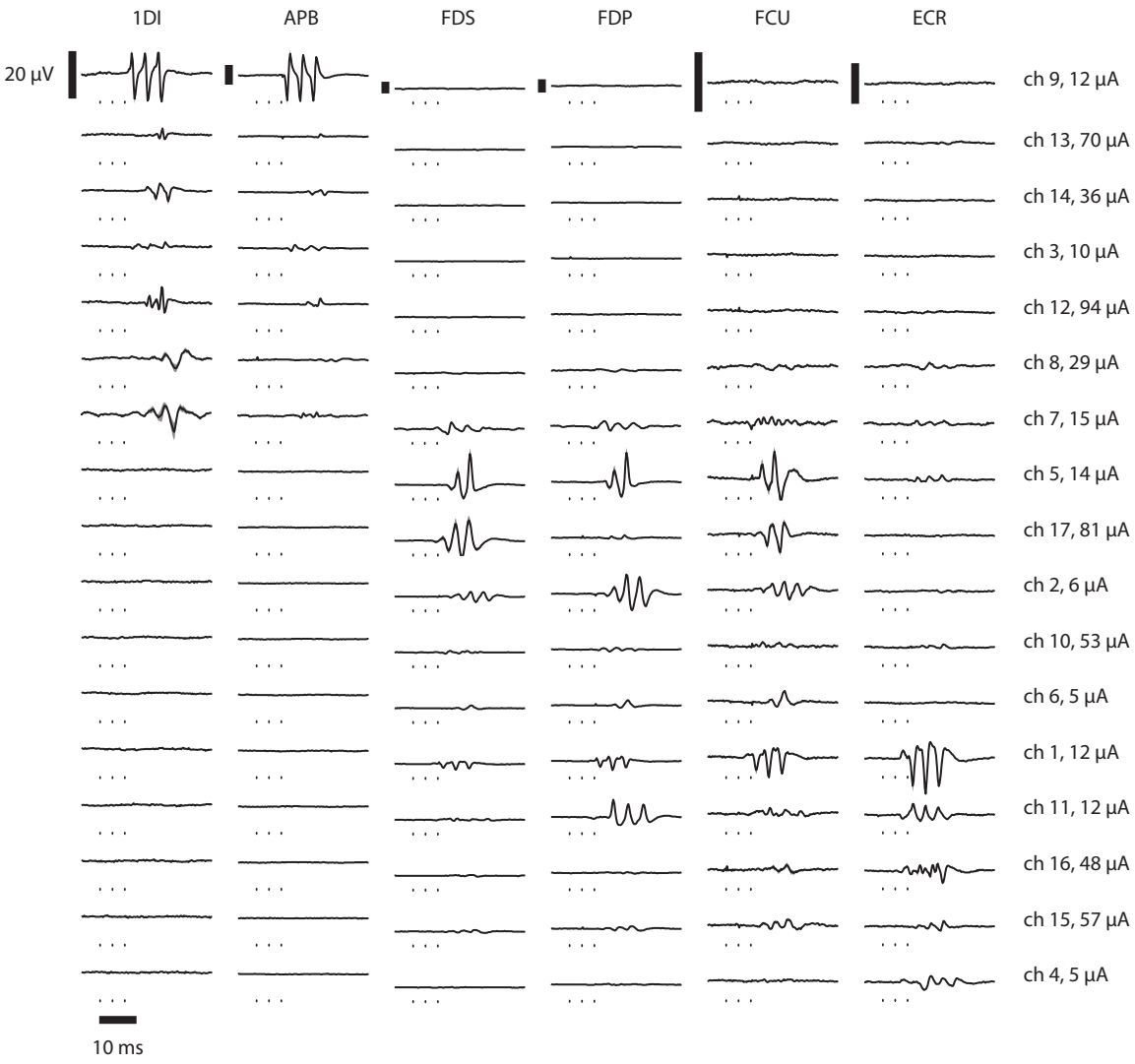

Figure 4.8: Average SCEPs from all channels of FMA. Rows represent stimulation electrodes, columns represent muscles SCEPs were recorded from. Vertical scale bars are all 20 µV. Time of stimulus pulses indicated by dots under the EMG traces. Current next to channel number is threshold for that channel. Session `Rv110717000`.

from stimulation in this monkey. In monkey Ar, whose array was implanted at C5/C6 level,

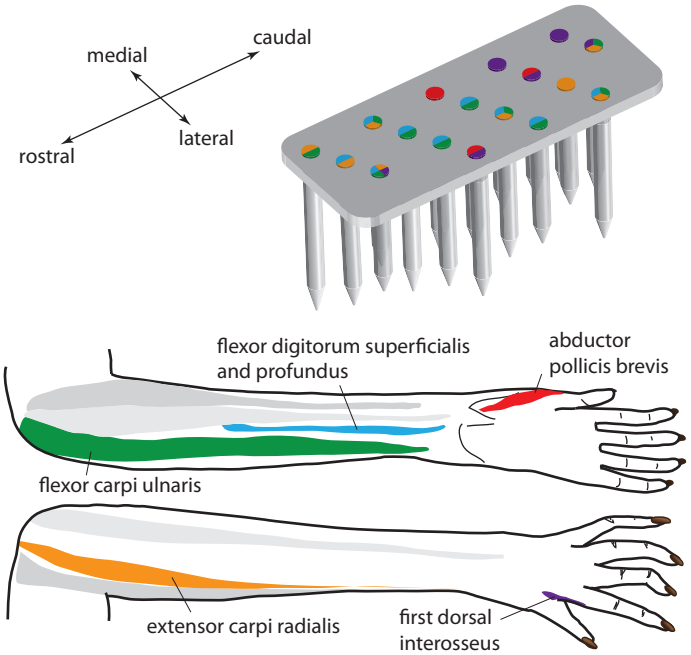

Figure 4.9: Schematic of FMA with electrode positions. Electrodes are colour-coded for muscles activated by stimulation of that electrode, at motor threshold. For reference, schematic of arm anatomy is shown at *bottom*. FDS and FDP are collated for simplicity. Session `Rv110717000`.

we found movement of the shoulder, triceps activation, elbow extension, yet also activation of ADM from several electrodes. We implanted the FMA in monkey Rp again at the C6/C7 level, and consequently, muscles activated were mostly located in the forearm and hand: stimulation of 12 electrodes caused SCEPs in FDS.

4.3.5 Recording from the Spinal Cord using the FMA

In sedation sessions with monkey Rp we also recorded from spinal FMA electrodes (fig. 4.10). It was impossible to identify the recorded neurons in this session because no EMG was recorded.However, it is encouraging that recording of neurons is possible even at low electrode impedances of ~50 kΩ.

4.3.6 Histological Examination

After perfusion of the animals we dissected the spinal cords, sliced them, and stained them either for cell bodies or a protein expressed in astrocytes (GFAP). Two monkeys had the FMA implanted for a long period of time: monkey Ra for more than 8 months, monkey Rv for 3.5 months. Figure 4.11 shows sections from monkey Ra. The GFAP stained sec-

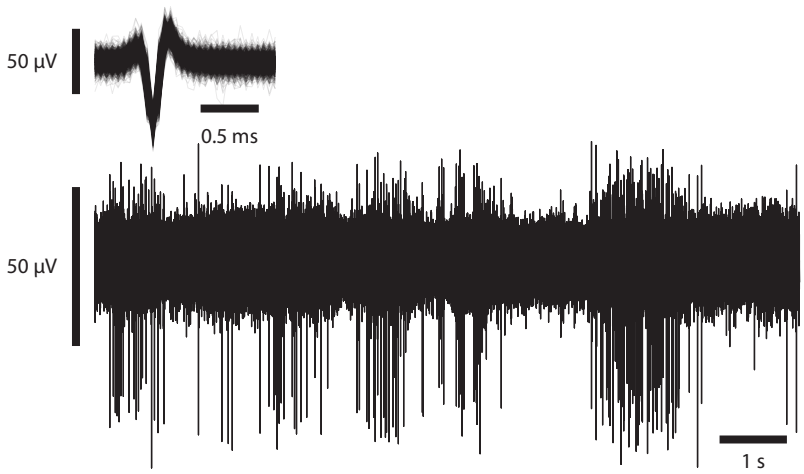

Figure 4.10: Spinal neuron recorded during a sedation session with monkey Rp. The graph shows a 10 s period of the recording of one channel, the inset shows the 1538 spike waveforms discriminated during a longer period of 130 s. Recording `Rp120329000`.

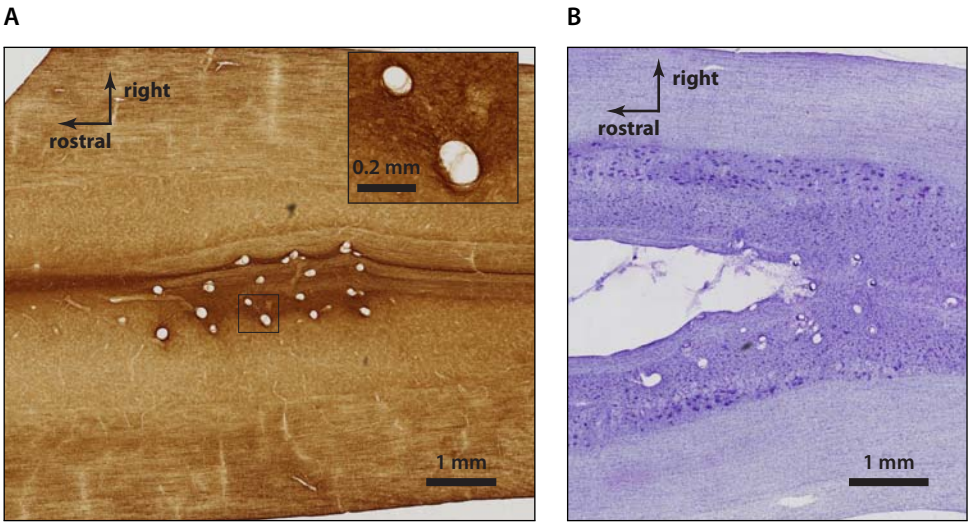

Figure 4.11: Sections of monkey Ra's cervical spinal cord around the FMA implant site, cut orthogonal to the dorsoventral axis. *(A)* GFAP stained slice, 3 mm below dorsal surface of the cord. Inset shows two electrode sites with signs of glial scarring. *(B)* Nissl-stained slice, 4 mm below the dorsal surface of the cord, near the tips of half of the electrodes. On the left side of the cord, distance between most lateral electrodes and motoneurons is ~400 µm; on the right side, this distance is ~700 µm.

tion in fig. 4.11 A shows an increased density of astrocytes around the electrodes, although electrodes are only surrounded by a very thin layer of astrocytes. This section also shows some distortion of the anatomical features of the cord. The stain for cell bodies in fig. 4.11 B shows what was suspected from stimulation experiments before: that the array was placed off-target and spanned the midline. Every other electrode of the array was 3 mm long, terminating near the plane of the section shown in fig. 4.11 B. The distance between electrodes at the left and right edges of the array and presumed motoneuron pools was approximately 400 µm and 700 µm, respectively.

Figure 4.12 shows similar sections for monkey Rv. Position of the electrodes relative to the ventral horn is shown in fig. 4.12 A. Some of the short (3 mm) electrodes did not seem to have penetrated this section. During the dissection a layer of scar tissue that had formed between the array and the dura and which was about 0.5 mm thick was discovered. This likely explains why there are no penetration traces from 3 mm-long electrodes. Figure 4.12 B

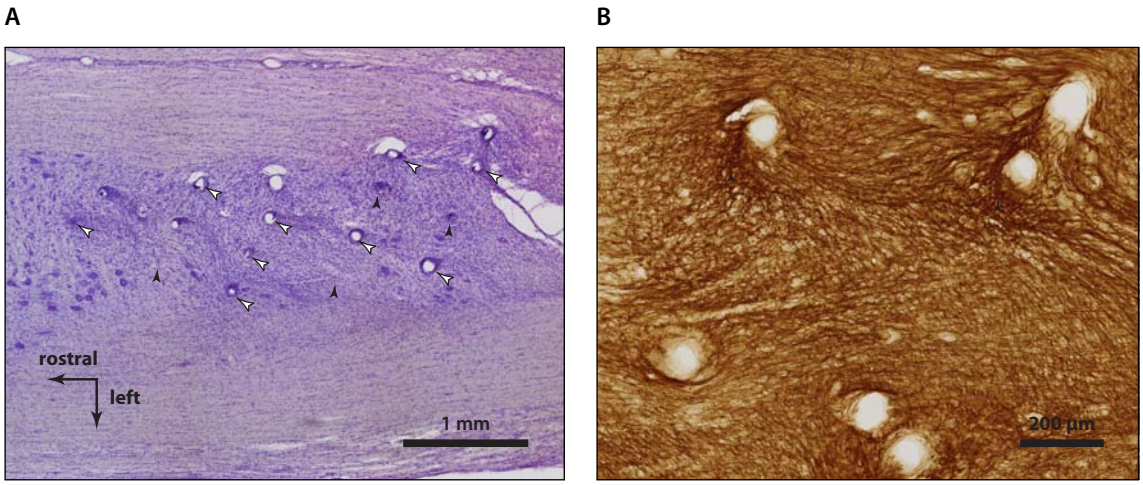

Figure 4.12: Sections of the cervical spinal cord around the FMA implant site, cut orthogonal to the dorsoventral axis (monkey Rv). *(A)* Nissl-stained slice, ~2.9 mm below dorsal surface of the cord. Electrode locations are marked for 3 and 4 mm long electrodes (black and white arrow heads, respectively), showing termination near neurons. The midline is visible near the *top*. See text for explanation. *(B)* GFAP-stained slice, 3.4 mm below the dorsal surface of the cord. Glial scar tissue has formed around some electrode (arrowheads), others are spared. Astrocytic interaction between electrodes is visible as well.

shows a section stained for astrocytes, again showing glial scarring around some electrodes and characteristic patterns connecting other electrode penetrations. Electrode shanks were free of tissue after extraction from array, suggesting that no glial sheath which might have formed around electrodes was removed during electrode extraction.

4.4 Discussion

Chronically implanted cortical microelectrode arrays have revolutionised brain research in the last two decades, allowing parallel recordings from hundreds of neurons in the awake behaving animal, and even in humans. Understanding of spinal cord function in behaving animals is lagging behind, however, for lack of a similar technique. Current preparations allowing chronic recording from and stimulation of macaque spinal cord involve chambers placed over the cord and limit the lifetime of the animal after the implant surgery to several weeks or a few months (S. I. Perlmutter et al. 1998). Alternative techniques need to be developed in order to perform long-time experiments, and especially if ISMS is ever to be used clinically. Our experiments using FMAs for spinal implants are a step towards multichannel, high density ISMS in primates.

4.4.1 FMAs for Intraspinal Microstimulation

In this series of experiments we first showed that FMAs are suitable for ISMS in acute preparations. Stimulation thresholds were found to be similar compared to ISMS with microwires (Moritz et al. 2007, section 3.3.2). Maximum forces evoked by single channel ISMS are usually weak compared to voluntary movements (chapter 2) and movements requiring high forces such as holding a cup of tea or turning a key in a lock might require stimulation of several channels at once. FMAs offer the opportunity to investigate multichannel stimulation in awake and behaving animals.

4.4.2 FMAs as Durable Implants

In our experiments, two monkeys lived with an FMA implant for a considerable length of time. The first animal had been implanted for over 8 months, and showed no signs of any complications. Stimulation thresholds on average doubled over the three months in the second animal. This development is somewhat different from the results reported by Mushahwar et al. (2000c) for microwire implants in the cat lumbosacral cord. They found thresholds to approximately double immediately after implant and then remain there over the tested period (over two months). We found a decrease first, possibly due to recovery from the implant surgery, and then an increase. Our spread of threshold changes was larger as well, with a third of electrodes having a lower threshold after more than three months than at implant. The initial decrease in thresholds resembles the results of Bamford et al. (2010), who used microwires to stimulate rat spinal cords for a period of one month.

We assume the main reason for a change of stimulation thresholds in our experiments to

be movement of the FMA out of the cord. At postmortem examination we found a thick layer of tissue between the array and the spinal cord, suggesting that over time, the FMA was lifted out of the cord from its initial position.

4.4.3 Other Chronic Implants

FMAs are a first step towards high channel count chronic stimulation electrodes. While this approach has the potential to increase the longevity of an experimental preparation, implants could still be improved. Particularly for this array, it might be beneficial to reduce thickness of the ceramic die, which sits between dura and spinal cord and through exerting pressure leads to morphological changes of the cord. Another improvement could be to use flexible electrodes, offering one way to decrease mechanical stress between tissue and electrode (Kozai et al. 2009, Lind et al. 2010, Lai et al. 2012). For example, one group tested thin flexible electrode bundles embedded in gelatine for stability during insertion and found considerable less glial scarring compared to normally used penetrating electrodes (Lind et al. 2010).

With recent advances in the application of optogenetics in macaques (Diester et al. 2011), one can also think about optic fibre arrays in the cord. As far as we know, optic stimulation of the macaque cord has not been tried yet. While behavioural effects of optic stimulation of genetically modified primate neural tissue have still to be demonstrated, arrays consisting of electrodes and optical fibres could be a useful research tool to investigate spinal cord stimulation.

4.5 Conclusion

In this chapter we have described an implant technique for a microelectrode array used to chronically stimulate the macaque cervical spinal cord. This is a step towards long-lasting chronic implants that can be useful in future basic research – to study the macaque spinal cord during free behaviour over long times – and in more applied research – such as the neural prosthesis described in the next chapter.

5 Closed Loop Intraspinal Microstimulation

In this chapter we draw on our previous results, combining cervical intraspinal microstimulation, the properties of which were investigated in chapters 2 and 3, with chronically implanted electrodes as described in chapter 4. Cortical activity is used to control stimulation and restore hand function in temporarily paralysed macaque monkeys.

The experiment was designed by Andrew Jackson and myself. AJ and I jointly performed surgical procedures. Animal training was performed by Jennifer Tulip and myself, and individual experiments were conducted by myself and AJ and/or JT. Parts of this chapter were presented in Zimmermann et al. (2011a).

5.1 Introduction

5.1.1 Motivation

Several studies have recently examined the restoration of arm and hand function lost due to paralysis using neuroprosthetic devices. Hochberg et al. (2012) report a BMI recording signals from a patient's motor cortex to control a robotic arm in real time. FES systems stimulating hand and forearm muscles have long been used clinically (Kilgore et al. 1989, Popovic et al. 2002, Peckham et al. 2002, Kilgore et al. 2008), however their control is complicated and often involves costly computation for seemingly simple movements.

Employing synergistic muscle activations as evoked by ISMS could both extend the movement repertoire of a BMI and simplify its control algorithm (chapter 2, Mushahwar et al. 2002, Moritz et al. 2007). Chronic ISMS has been demonstrated to work reliably in the cat (Mushahwar et al. 2000c), and we have developed an implant technique for chronic ISMS electrodes in the macaque (chapter 4). Furthermore, we have shown that ISMS delivered under anaesthesia evokes functional movements of the arm and hand (chapter 2). So far, however, it is unknown whether ISMS can restore functional movements and improve performance during task performance in an awake and behaving monkey.

How could the efficacy of a spinal stimulation implant be tested? In rodents or cats, preparations in which the cord is partially or completely transected are not uncommon, and are used to study recovery, therapies, or neural prostheses (Saigal et al. 2004, Guevremont et al. 2006, Bamford et al. 2010). In primates, however, because of ethical and practical concerns this kind of permanent lesion is less favoured (but see Galea et al. 1997, Schmidlin et al. 2004 for studies and Courtine et al. 2007 for a discussion). But maybe a temporary lesion could be used instead? Indeed, reversible pharmacologically induced lesions to M1 (Matsumura et al. 1991, Kermadi et al. 1997, Schieber et al. 1998, Schmidlin et al. 2008, Tsuboi et al. 2010) or local cooling (Skinner et al. 1968, Caan et al. 1976, Sasaki et al. 1984, 1987) are commonly used to investigate brain function and interaction between areas. Using either approach to simulate SCI or stroke would necessarily neglect important changes occurring after the lesion, such as plasticity and neural reorganisation. However, it offers a valuable tool to assess loss of function on a short term.

In order to control ISMS in a BMI different control signals can be used. In the 'decoding' approach (Jackson et al. 2011), brain signals are recorded during normal task performance first. A model is then built which aims to predict variables such as arm and hand position or form of grasp from neural activity. An example for this approach is Ethier and colleagues' experiment which decoded M1 activity in order to restore EMG of a grasping hand with FES (Ethier et al. 2012). The 'biofeedback' approach is an alternative way to control a BMI: here, an animal or human subject learns to control the activity of neurons in a novel way (Jackson et al. 2011). An experiment by Moritz et al. in which monkeys learned to modulate the firing rate of single neurons in order to control FES exemplifies this approach (Moritz et al. 2008).

A synthesis of these two approaches will be taken in this experiment. One could take the activity of neurons whose firing properties during normal task performance are relatively well understood – such as grasp-related neurons in PMv (Rizzolatti et al. 1988) – and use these neurons to control a BMI. Even if there is trial-by-trial variation of neural activity, the animal might be able to learn to modulate the activity to correspond to task requirements.

5.1.2 Aims

In this chapter, we describe an experiment that combines cortical recordings, a temporary motor lesion, and closed-loop control of spinal stimulation to restore functional hand movements. The main aims of the present study were to

1. Demonstrate closed-loop control of cISMS using cortical neuronal activity

2. Show that this neural prosthesis can restore motor function induced by a temporary lesion.

5.1.3 Experiments

To this end, we designed an experiment in which monkeys were trained to perform a reach and grasp task. By injecting the GABA agonist muscimol into the hand area of M1 we temporarily paralysed the hand and reduced the monkeys' performance of the task. Electrodes implanted into premotor cortices allowed us to record task-related neural activity, which we then used to control stimulation of intraspinal electrodes. With this approach, we were able to restore movement and improve motor function in several experimental sessions with two monkeys.

5.2 Materials and Methods

5.2.1 Animals and Surgical Procedures

For this experiment, two female macaque monkeys (B, Rv; see appendix B for details) were trained on a reach, grasp, and pull task (fig. 5.1).

Behavioural Training; Task Animals were initially trained to pull an object mounted onto a spring loaded lever. Different manipulanda could be attached to the lever, and they were chosen to facilitate the monkeys' task performance. Three different springs were used and adapted, according to the animal's strength[1]. Monkey Rv was trained to pull the lever against spring 3 to its full extension (8 cm). Position of the lever was measured using a linear potentiometer and digitised with a NI6323 card (National Instruments, Austin, TX, USA). A custom program (Delphi, Borland, Austin, TX, USA; later when combined with stimulation: LabView, National Instruments) running on a PC ('task computer') controlled the task and allowed experimenters to control task parameters such as hold times and gain of lever in order to adjust the difficulty of the task. The monkey received auditory feedback when the lever was at the target position, when the hold period was finished, and when the neutral position hold period was over. Trials were self-paced, and trials were not limited in time.

Implant Surgeries After the monkeys had reached stable performance at their task with at least 300 trials per day, they underwent a series of implant surgeries (see table 5.1 for

[1]Spring 1: initial force 1.645 N, spring constant: 120 N/m; spring 2: 0.845 N, 50 N/m; spring 3: 0.355 N, 20 N/m

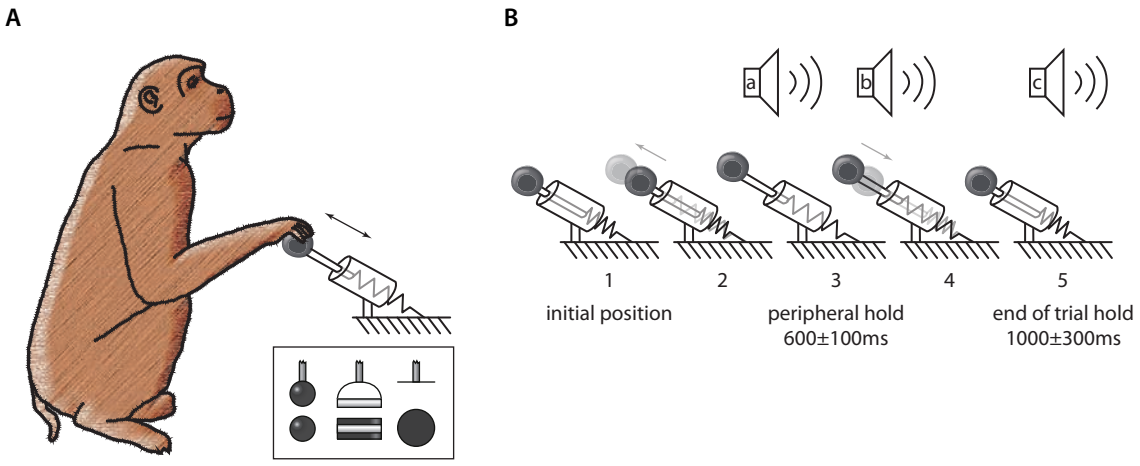

Figure 5.1: *(A)* Monkeys were trained to perform a reach-and-grasp task. Squash balls, handle bars or disks *(inset)* were mounted to a spring loaded lever. *(B)* Sequence of trial stages. *(1)* monkeys had to keep the lever in the neutral position. After this initial hold period, the monkey had to pull the lever *(2)* until a tone *(a)* indicated that the lever was at the target position, which had to be held *(3)*. After the peripheral hold period another tone *(b)* signalled to the monkey that the lever should return to the neutral position *(4)*. After holding the lever at the neutral target *(5)*, a reward tone *(c)* was played and a food reward given, and the next trial commenced.

time courses). Structural magnetic resonance imaging (MRI) scans of the head were ob-

	Monkey	
	B	Rv
Start of behavioural training	0	0
EMG implant surgery	153	143
Cortical implant surgery	175 (22)	176 (33)
Spinal implant surgery	251 (76)	248 (72)
Cortical reimplant	–	337 (89)
Perfusion	274 (23)	361 (24)

Table 5.1: Major events of closed-loop spinal cord stimulation experiments, by animal. Start of behavioural training on grasp-and-pull task was chosen as reference point. Times are given in days, numbers in brackets designate days from previous event.

tained in order to plan implant layouts (fig. 5.2; volume rendering performed using OsiriX, Rosset et al. 2004). First, an EMG implant surgery was performed (see table 5.2 for list of muscles implanted). EMG patches were tunnelled subcutaneously from an incision at the top of the cranium to the left shoulder and, depending on the target, further along the arm and forearm to the hand. During the same surgery, two chambers were fixed to the crania of monkeys B and Rv. A craniotomy was performed under the right chamber, giving

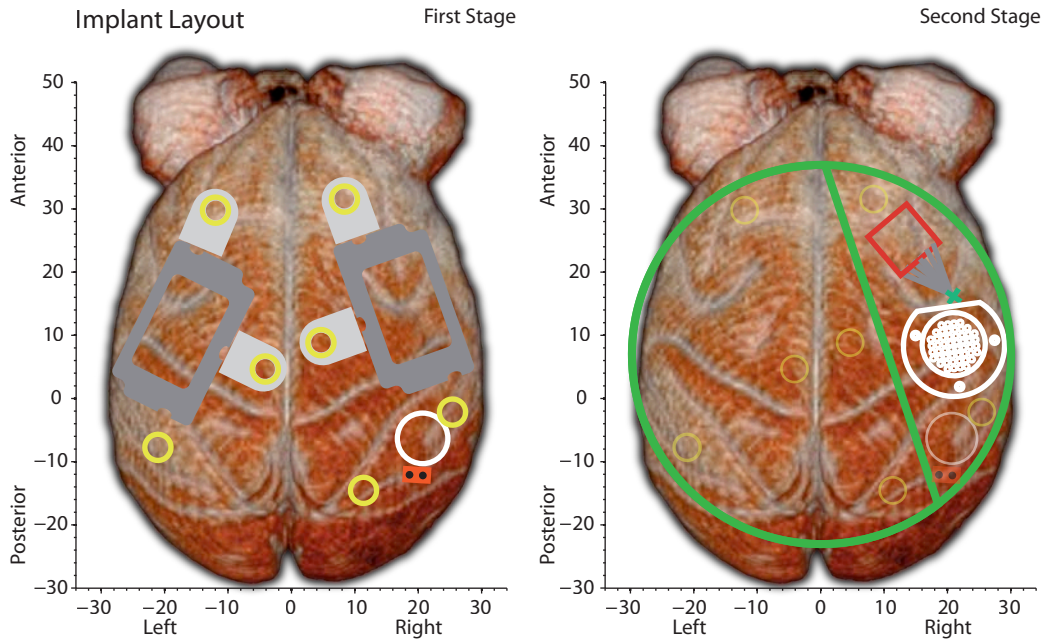

Figure 5.2: Layout of head implant for monkey B. Implants were made in two surgeries. In the first surgery *(left)*, supporting skull screws *(yellow)* were inserted into the cranium. Two chambers *(grey)* were mounted to the skull *(see text)*. Connectors for EMG implants *(white)* and ground connector *(orange)* were mounted onto the skull using dental acrylic. During the second surgery, the chambers were removed and replaced by a movable microwire implant *(red/grey)* over PMv and a chamber *(white)* over M1, and a headpiece *(green)* was added to protect the implants. A similar layout was used for monkey Rv.

Monkey	muscles with EMG implants
B	APB, 1DI, FDS, FDP, FCU, ECR
Rv	APB, 1DI, FDS, FDP, FCU, ECR

Table 5.2: List of muscles that were implanted, by animal (for definition of abbreviations, see page xv).

access to the presumed location of PMv. The left chamber was later used to fix the monkey's head during stimulation sessions in order to determine the location of PMv hand area (section 5.2.2). In a second surgery, a custom-made array of movable microwires (Jackson et al. 2007) was implanted over PMv. A small chamber was fixed over the presumed hand area of M1 and later a craniotomy was performed underneath to gain access to M1. Finally, in a third surgery, a cervical laminectomy was performed and an implant was placed to allow stimulation of the cord. The implants used to stimulate the cord differed between the animals. Monkey B's vertebrae from cervical C4 to thoracic T2 were cleared, screws were put into the lateral masses, and then the vertebrae were fused with dental acrylic. A laminectomy was performed on vertebrae C5–C7. Wires linking stimulating electrode and a connector were tunnelled to the head. Lastly, a chamber was placed over the exposed vertebrae and sealed with dental acrylic, then the incision was carefully closed with sutures (S. I. Perlmutter et al. 1998; cf. fig. 4.3 A). A plastic insert with a grid of holes onto which a micromanipulator (MO-903B, Narishige, Japan) could be fixed was fitted into the chamber. Using the manipulator, a single electrode could be lowered into the spinal cord. In monkeys Rv, an FMA was implanted chronically. A detailed account of the implant procedure was given in section 4.2.3. When no more task-related cells could be found using the original implant at the PMv site, monkey Rv received a new microwire implant into PMd.

5.2.2 Intracortical Microstimulation of PMv and M1 to Determine Arm and Hand Representation

In monkeys B and Rv, we determined areas of arm and hand representation in PMv prior to implanting the microelectrode array. For this, the monkey was sedated using ketamine and medetomidine. We then fixed its head to a table and positioned a stereotactic manipulator (David Kopf Instruments, Tujunga, CA, USA) over the PMv craniotomy. Tungsten electrodes (250 µm diameter, MicroProbes) were used to stimulate the cortex along penetration tracks. Stimulus trains consisted of 13 or 30 biphasic pulses, 200 µs per phase, cathodic first, current controlled at 1–300 µA, delivered at 300 Hz, inter-train period 2 s. Electrodes were lowered down to 8 mm at the bank of the arcuate sulcus. The contralateral hand and arm were observed for stimulation induced movements, and EMG was recorded from the implanted muscles. The implant site was chosen to be at the centre of hand-related stimulation effects (fig. 5.3).

In order to determine muscimol injection target locations (see section 5.2.4), M1 was mapped using a similar protocol. If hand or forearm movements were encountered at low thresholds (below 20–30 µA), this position was later considered as a candidate for muscimol

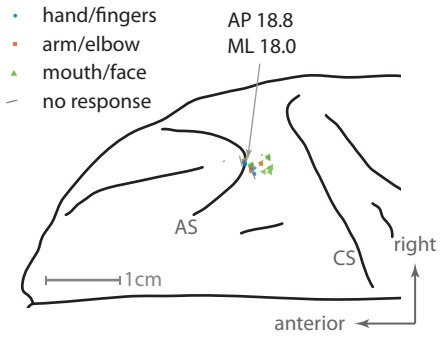

Figure 5.3: Map of stimulation effects from ICMS in monkey B. The microwire implant was targeted at head of arrow. AS – arcuate sulcus, CS – central sulcus.

injections.

5.2.3 Closed Loop Experiment Sessions

The typical time course of a closed loop experiment session consisted of two parts (fig. 5.4): First, the monkey was sedated, muscimol was injected into the hand area of M1, and either the spinal electrode was inserted (monkey B) or the stimulation thresholds and effects of the array were tested (monkey Rv). Then, the monkey recovered from sedation and performed

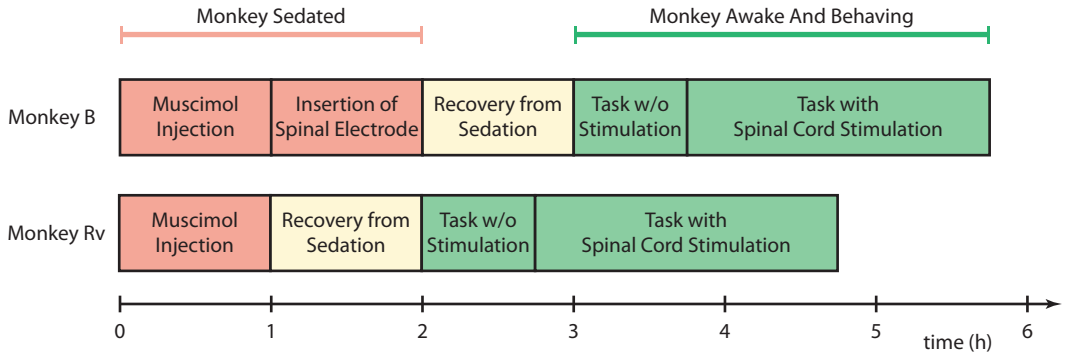

Figure 5.4: Typical time course of a closed loop experiment session. As monkey Rv had a chronic implant, no acute electrode had to be inserted into the cord before the experiment.

the grasp-and-pull task. Once it became apparent that the monkey was starting to try to perform the task, stimulation controlled by a premotor neuron was turned on. Some trials (randomly chosen, 5–30 %) were controls during which ISMS was turned off. The experimenter interacting with the animal was usually blind to the nature of the trial. Besides the effects of stimulation, the animal did not receive feedback about the nature of the trial. Since the animals were not expected to perform trials successfully during control periods at all, these periods were usually limited in length to 30 s at a time, and the experimental condition

was switched back to stimulation mode.

Experimental sessions lasted until the monkey stopped working for food rewards; the awake and behaving part of the experiment typically lasted 1–2 h. The methods employed in the individual steps are described in the following subsections.

5.2.4 Muscimol Injections into M1

Muscimol was injected at the beginning of an experimental session under ketamine/medetomidine sedation. Muscimol (Sigma-Aldrich, M1523) was dissolved in sterile saline solution (0.5 %; 5 mg in 1 ml saline). Per experimental session, muscimol was usually administered to one previously identified site. A 2.5 µl Hamilton syringe was connected to a fine (31g) needle through a Teflon tube. The needle was lowered into the cortex, to a depth of 5 mm below dura. After the needle was left to settle in the tissue for 30 s, 0.5 µl muscimol were injected slowly (0.1 µl per 30 s). The needle was slowly raised and two more injections were performed at 3.5 mm and 2 mm below the dura. After the needle was removed from the cortex, potential blockage of needle was checked by ejecting a small quantity of muscimol.

Since we found it very difficult to obtain reliable paralysis of the hand in monkey Rv, the injection protocol was adjusted for this monkey. Up to three injection tracks were run, and up to four injections were made per track. Injections were placed around the depths at which stimulation elicited hand movements.

5.2.5 Recordings of Neuronal Activity, Electromyograms, and Task

Neural signals were amplified using two 8-channel headstages and a 16-channel amplifier (MPA8I, PGA1632, MultiChannel Systems, Reutlingen, Germany). Signals were split into local field potentials (LFP) and spike channels (bandpass 1–300 Hz, 500× gain and bandpass 300–8000 Hz, 1000× gain, respectively) and recorded using a 1401 data acquisition device (Cambridge Electronic Design, Cambridge, UK) connected to a personal computer (PC). Electromyograms were filtered and amplified (100–1000 Hz bandpass, 1000× gain; A-M Systems Amplifier 1700, Sequim, WA, USA) and recorded with the neural signals. Task state and lever position were also recorded with electrophysiological signals. One spike channel was discriminated online using the 1401's template matching algorithm, and the number of the matching template was available on digital lines with low latency (approximately 2 ms). While we attempted to discriminate neurons as cleanly as possible, we did not reject multi-unit activity (as confirmed offline by spike waveform and inter-spike interval histogram (ISpIH) analyses) if its modulation was correlated with task execution. When good recordings from microwire electrodes were lost, the monkey was sedated and the wires moved.

5.2.6 Transforming Neural Signals into Stimulation Pulses

In order to transform neural signals into stimulation pulses, a custom algorithm was developed. The algorithm is described and discussed in appendix C, so only a brief account is given here. For monkeys B and Rv, we were constrained to using one channel of neural recordings due to the setup of the recording system. The digital signal that occurred whenever a spike was recognised was read by the task computer's NI6323 data acquisition card. Firing rate of a neuron at time t was estimated by counting the number of spikes in the half-second interval before t. Firing rate was transformed into a stimulus triggers in two different ways:

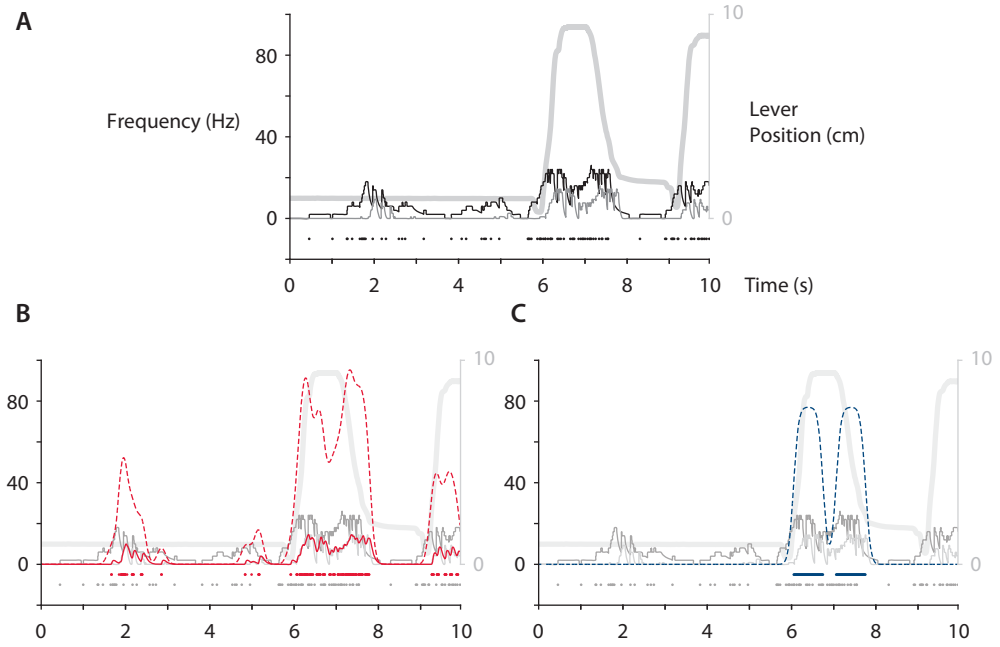

Figure 5.5: Transforming spikes into stimulus pulses. *(A)* Detected spikes (black dots) contribute to an online estimate of instantaneous firing rate (black line). This estimate is transformed by a gain, shift, and time lag (thin grey line). For reference, lever position is shown as thick grey line. *(B)* Quasi-linear mode: the transformed firing rate is used as a target function for the force response estimation algorithm (section 2.2.4). Whenever the force estimate (red line) is below the target, a stimulus (red dots) is triggered. The red broken line shows the Gauss-kernel smoothed stimulus rate. *(C)* Trigger-and-fire mode: When the firing rate estimate crossed a set threshold, stimuli (blue dots) are delivered for some time at a set rate. The blue broken line shows the Gauss-kernel smoothed stimulus rate. Spikes and lever position were recorded during a training session. Gain, lag, and threshold of spike rate estimate are chosen here for illustrative purposes.

In quasi-linear mode, the estimated firing rate was translated and scaled, and a time lag could be added (see fig. 5.5). A threshold was applied, and when the transformed firing rate crossed that threshold, this rate was used as an estimate for a desired force response. An

algorithm similar to the one described in section 2.2.4 was then used to determine online whether a stimulus needed to be delivered or not in order to match the desired force output. In trigger-and-fire mode, a threshold could be set for the firing rate; if it was crossed, a stimulus train of set duration and frequency was delivered. One (monkeys B, Rv) or sometimes two (monkey Rv) A-M Systems Model 2100 stimulators were then used to deliver stimuli. Single biphasic stimulus pulses (cathodic first, 200 µs per phase) at currents up to 300 µA were delivered on trigger. Occurrence of stimuli (given by digital pulse that triggered the stimulator) was recorded along with electrophysiological data.

In some of the sessions where we were not able to use task-related neuronal activity, we used the activity of a large motor unit recorded from 1DI in two sessions with monkey Rv[1]. In these cases, care was taken to cleanly discriminate the motor unit action potential (MUAP) in order to eliminate any potential feedback loop. Recorded MUAPs were then processed as other neural activity.

5.2.7 Data Analysis

For analysis, raw EMG data were rectified and low-pass filtered at 100 Hz. Lever position data was low-pass filtered and down-sampled to 100 Hz. Spikes were discriminated offline using Spike2's template matching algorithm and candidate channels for brain control sessions were determined: Task-relationship of discriminated spiking activity was assessed by compiling average lever position traces aligned to the times the lever position exceeded the threshold set in the task programme. Efficacy of muscimol injections was assessed by comparing EMG activity during task performance between training sessions and control periods of paralysis sessions. EMG activity was rectified and averaged over slices aligned to the times the cursor entered the target. Maxima of the averaged activity were compared between control and paralysis sessions. Impairment was rated on a scale from 0–2, where 0 means no impairment, 1 means mild impairment (EMG between 50 and 100 % of control level) and 2 means strong impairment (EMG less than 50 % of control level). In order to assess the efficacy of spinal stimulation to produce SCEPs in muscles, we compiled StTAs of EMG data.

Behavioural effects of cISMS during task performance were assessed in several ways. First, we determined the number of trials performed per minute of exposure to task. This information was extracted from the task-state information transmitted from the task computer. Because trials in the stimulation condition were not limited in duration and both monkeys tended to spend some time in this condition not attempting any trials at all, only

[1] `Rv110627004` and `Rv110714003`

periods containing stimulus pulses within 30 s were considered in calculation of the rate. In some training sessions, 'stimulation' and 'control' periods were randomly assigned as during paralysis sessions, however without stimulation being performed. In these cases, trial rates according to these conditions were used for analysis. In training sessions where no condition was assigned during recording, 'stimulation' and 'control' periods were assumed to have the same trial rate determined by all trials performed during the session. Two training recordings of monkey B did not contain the task state; for these sessions (`B100707000` and `B100708001`), the number of completed trials was reconstructed from lever position traces and recorded task parameters (lever threshold and hold time). On a session level, the difference of trial rates between stimulation and control periods was assessed by dividing the time period of each condition at points halfway between two successive trial marks. For each snippet, the time spent in this condition was taken as trial length. Then, a permutation test was performed on trial lengths, using the difference of trial rate per condition as the test statistic. The null-hypothesis that both rates have the same mean was tested at a significance level of $\alpha = 0.05$, $n_{\text{perm}} = 10^5$. We also performed a per-monkey analysis, randomising trial numbers and times pertaining to parts of recordings. Here, we tested the null-hypothesis that rates in stimulation periods are higher than in control periods ($\alpha = 0.05$, $n_{\text{perm}} = 10^5$).

Percentage of successful trials of all attempted trials was also assessed. Attempted trials here are all instances of the lever position crossing the threshold, thus giving the animal feedback that it had reached the hold period of the task; successful trials required the monkey to keep the lever above threshold for a set hold time.

In a third analysis, we divided recordings into epochs that were aligned to times where the neural firing rate used to control the stimulation crossed a certain threshold. This threshold was determined empirically, by first computing peri-event time histograms (PETHs) of neural activity aligned to times the cursor entered target. Then, we compared maximum lever position in a 3 s window after the epoch marker between stimulation and control epochs. The difference of average maxima was tested for significance again using a permutation test, the null hypothesis being that the average maximum in stimulation epochs is not larger than in control epochs ($\alpha = 0.05$, $n_{\text{perm}} = 10^4$).

Note on nomenclature: Experimental sessions are referred to by a code consisting of a shorthand for the monkey (B or Rv), and the date in `yymmdd` notation. Individual recordings during a session also carry the consecutive file number (three figures, zero-padded) assigned during recording. When it is clear what is meant from the context, no distinction is made between the words session and recording. For analysis, recordings were divided into parts whenever substantial changes of experimental parameters or the monkey's behaviour justified such a division. These parts are indicated by letters, and usually times relating to

the position of this part in the recording file are given as well. In some cases, when a whole recording was used for that analysis, the letter was omitted.

5.3 Results

The dataset for this experiment consists of six sessions with monkey B and 27 sessions with monkey Rv during which muscimol was injected into M1 and neural recordings were used to control ISMS. Data from training sessions that were recorded before the spinal implant surgeries and on days between closed loop experiments were used for comparison.

5.3.1 Cells in PMv are Systematically Modulated During Performance of Reach-Grasp-and-Pull Task

In both monkeys, we found neurons whose activity was systematically modulated during task performance. We plotted neural activity aligned to lever position (figs. 5.6 and 5.7) in order to determine whether a single neuron or multi-unit activity was related to performance of the task. For this experiment to work successfully, a neuron used for brain control of stimulation had to satisfy three conditions: (a) it had to modulate its firing frequency reliably with the task, (b) the modulation had to be strong enough to be detectable with a simple estimation algorithm on a trial-by-trial basis, and (c) the modulation had to begin before normal movement onset. During some experimental sessions, it was impossible to satisfy all three conditions. For example, in fig. 5.7 B, where the recorded neuron was clearly task related, the modulation occurred towards the end of the trial.

5.3.2 Paralysis of Hand After Muscimol Injections

In order to show an improvement of task performance due to stimulation, paralysis of the forearm and hand muscles was first induced, thus limiting the animal's ability to pull the manipulandum. Muscimol injections into M1 were used to temporarily inhibit neural activity in M1, causing hand paralysis. Number of injections, volume injected, and effects for individual experimental sessions are listed in table 5.3.

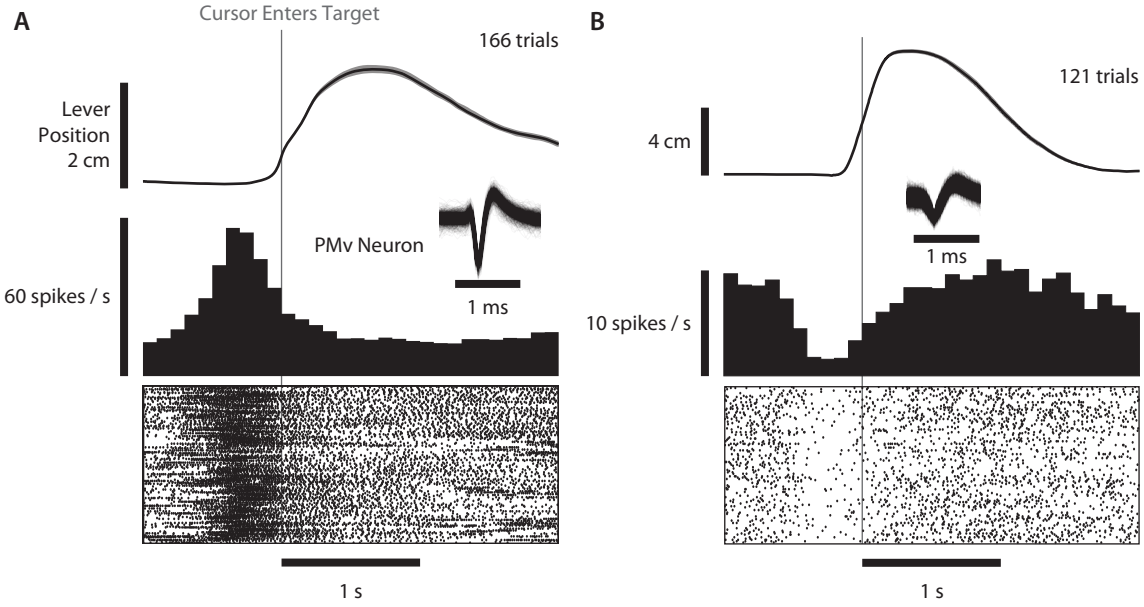

Figure 5.6: Example for task-related activity of PMv neurons, recorded during a normal training sessions. Lever position is shown at *top;* raster plot and histogram of the neuron are shown at the *middle* and *bottom*. Trials are aligned to the time the lever position entered the target zone (grey line). *(A)* Session `B100708001`, neuron channel 5. The inset shows 2500 randomly selected instances of the discriminated spike. *(B)* Neuronal activity is suppressed at start of movement. Session `B100510002`, channel 8, template 1. Inset shows 5000 waveforms. Shaded areas: SEM.

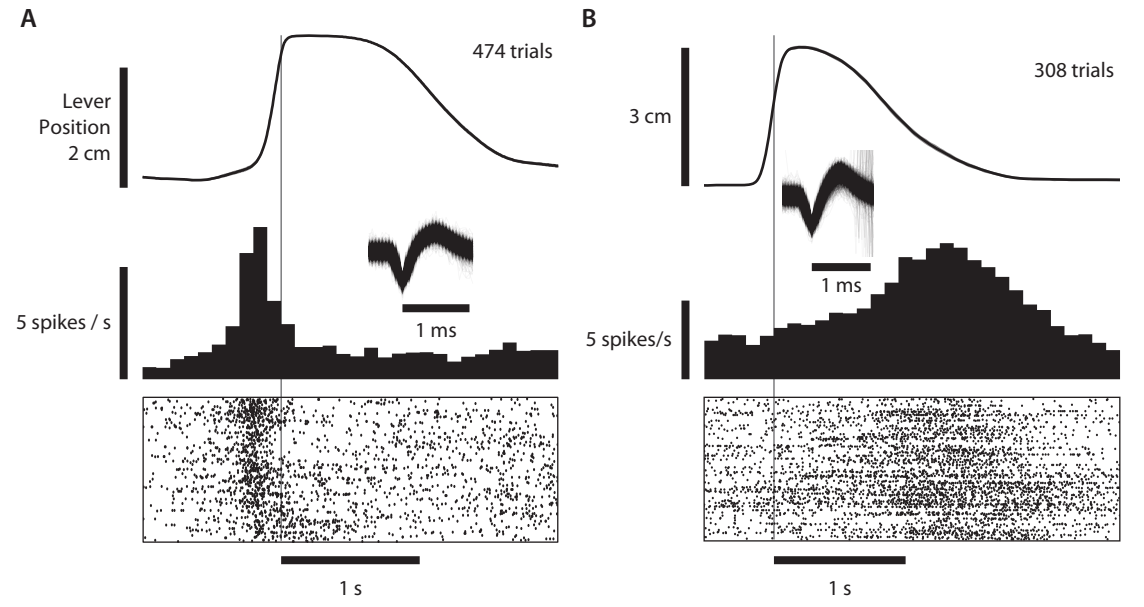

Figure 5.7: Examples for task-related spiking of PMv neurons recorded in monkey Rv. See fig. 5.6 for description. *(A)* Session `Rv110615000`, channel 2, template 4. Inset shows 4137 waveforms. *(B)* Session `Rv110603007` (paralysis session), channel 4, template 1. Inset shows 5000 of 8935 discriminated waveforms.

Table 5.3: Effects of muscimol injections into hand area of M1 on arm and hand EMGs. *Tracks* lists the number of injection tracks run in that session. *Vol.* shows the total volume of muscimol injected. Impairment levels: 2 – strong reduction of activity (more than 50 %), 1 – mild reduction (between 50 and 80 %), 0 – no effect, x – not recorded.

Session	Tracks	Injections per Track	Total Vol. (µl)	Total muscimol (µg)	Muscle Impairment
B100628	1	3	1.5	7.5	FDS, FDP, FCU, ECR: 2, APB, 1DI: 1, 0
B100706	1	3	1.5	7.5	APB, 1DI, FDS, FDP: 2, FCU, ECR: 0
B100709	1	3	1.5	7.5	APB, 1DI, FDS, FDP, FCU: 2, ECR: 0
B100711	1	3	1.5	7.5	APB, 1DI, FDS, FDP, FCU: 2, ECR: 0
B100714	1	3	1.5	7.5	APB, 1DI, FDS, FDP: 2, FCU, ECR: 0
B100715	1	3	1.5	7.5	APB, 1DI, FDS, FDP: 2, FCU, ECR: 0
Rv110603	1	3	1.5	7.5	1DI: 2, APB, FDS, ECR: 1, FDP, FCU: 0
Rv110606	1	3	1.5	7.5	1DI: 2, APB, FDS, ECR: 1, FDP, FCU: 0
Rv110608	1	3	1.5	7.5	APB, 1DI: 2, FDS, ECR: 1, FDP, FCU: 0
Rv110610	2	3	3	15	APB, 1DI, FDS: 2, FCU, ECR: 1, FDP: 0
Rv110614	3	3	4.5	22.5	APB, 1DI: 2, FDS: 1, FDP, FCU, ECR: 0
Rv110616	3	3	4.5	22.5	APB, 1DI: 2, FDS, ECR: 1, FDP, FCU: 0
Rv110622	3	3	4.5	22.5	APB, 1DI, ECR: 2, FDS: 1, FDP, FCU: 0
Rv110624	3	3	4.5	22.5	APB, 1DI: 2, FDP, FCU, FDS, ECR: 0
Rv110627	3	3	4.5	22.5	APB, 1DI: 2, ECR: 1, FDP, FDS, FCU: 0
Rv110629	3	3	4.5	22.5	APB: 2, ECR: 1, 1DI, FDP, FDS, FCU: 0
Rv110701	3	4	6	30	1DI: 2, APB: 1, ECR, FDP, FDS, FCU: 0
Rv110703	3	4	6	30	1DI: 2, APB: 1, ECR, FDS: 0, FDP, FCU: x
Rv110705	3	4	6	30	APB, 1DI: 2, ECR, FDP, FDS, FCU: 0
Rv110707	3	4	6	30	APB, 1DI: 2, ECR, FDP, FDS, FCU: 0
Rv110712	3	4	6	30	APB, 1DI, ECR: 2, FDS: 1, FDP, FCU: 0
Rv110714	3	4	6	30	ECR: 1, APB, 1DI, FDS, FDP, FCU: 0
Rv110717	3	4	6	30	1DI, ECR: 2, APB, FDS, FDP, FCU: 0
Rv110719	3	4	6	30	FDP, ECR: 1, APB, 1DI, FDS, FCU: 0
Rv110825	2	4	4	20	APB, 1DI, FDS, FCU, ECR: 2, FDP: 1
Rv110831	3	4	6	30	1DI: 2, APB, FDS, FCU: 1, FDP, ECR: 0
Rv110902	3	4	6	30	APB, ECR: 1, 1DI, FDS, FDP, FCU: 0
Rv110904	2	4	4	20	APB, 1DI, FDS: 2, FDP, FCU: 1, ECR: 0
Rv110906	1	4	2	10	1DI, FCU: 1, APB, FDS, FDP, ECR: 0
Rv110908	2	4	4	20	1DI: 2, APB: 1, FDS, FDP, FCU, ECR: 0
Rv110911	2	4	4	20	FDS, FCU: 2, APB, 1DI: 1, FDP, ECR: 0
Rv110913	2	4	4	20	APB, 1DI, FDS, FDP, FCU, ECR: 0
Rv110915	3	4	6	30	1DI: 1, APB, FDS, FDP, FCU, ECR: 0

While all muscimol injections led to strong paralysis of several hand and forearm muscles

(see for example figs. 5.8 and 5.9) and decreased task performance in monkey B, this part of the experiment was less successful in monkey Rv. Strong reduction of muscle activity re-

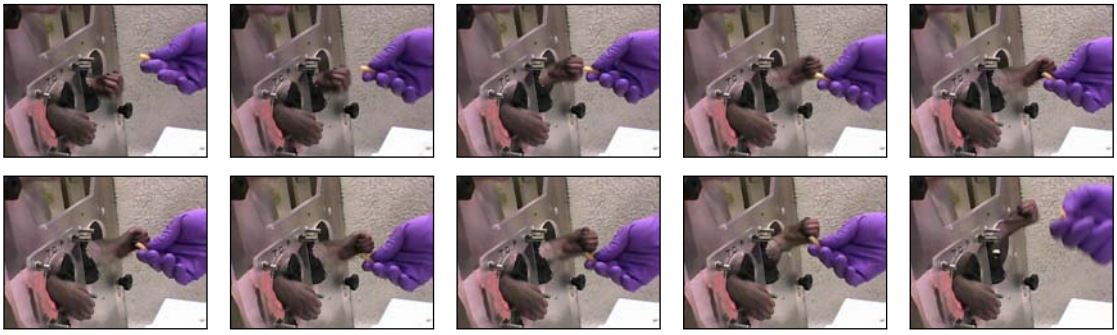

Figure 5.8: Muscimol induced paralysis of hand. Video taken at beginning of session `B100711000a`. Time between frames: 0.2 s.

mained almost exclusively confined to intrinsic hand muscles (see fig. 5.10 for an example), despite confirmation of the injection locations using ICMS, variation in the injection locations, increase in the injected volume, and change of the batch of muscimol used. However, in each monkey, task performance, as measured by trials performed per minute, was significantly worse in paralysis sessions compared to training sessions (see section 5.3.4).

5.3.3 SCEPs in Forearm and Hand Muscles

During stimulation experiments, an acutely inserted electrode (monkey B) or one or two electrodes of a chronically implanted array (monkey Rv) were used to deliver ISMS pulses to the cervical spinal cord. In all sessions we could record SCEPs in the muscles of the hand and forearm. Figure 5.11 shows SCEPs for four sessions of monkey B, fig. 5.12 shows similar data for monkey Rv. While a variety of responses was observed for different electrodes, electrodes activating finger and wrist flexors were preferred for this experiment. In monkey B, in three sessions the electrode had to be moved (after 2000–4000 s) to restore stimulation effects, and in all sessions, stimulation current was gradually increased. In monkey Rv, stimulation responses usually remained stable over the course of experimental sessions (lasting one to a few hours), demonstrating the merit of chronically implanted electrodes over acutely inserted ones. In a few cases stimulation effects decreased or vanished, we then either increased the current delivered or used a different electrode. Spinal stimulation did not seem to cause any discomfort or pain in the animals, except in one case. This session with monkey B was aborted as soon as the problem became apparent.

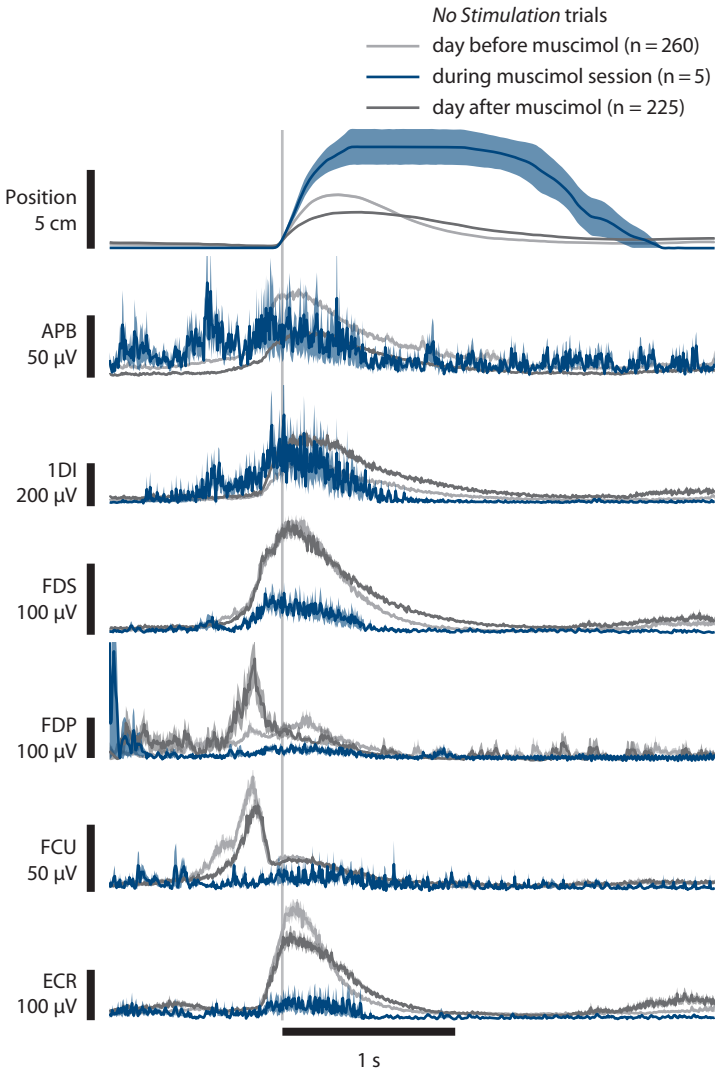

Figure 5.9: Effects of muscimol on task-related EMG (example from monkey B). Trials are aligned to threshold-crossings of lever position (0.45 cm). Traces in light grey show trials from the day before the muscimol injection, blue traces represent trials recorded shortly after muscimol injection, and dark grey traces were recorded the day after muscimol injections. Lever position is shown for reference. Maximum lever position was higher in muscimol session than during control sessions because a weaker spring was used to facilitate the monkey's task performance. Sessions `B100627001a`, `B100628001b`, `B100629001a`. Shaded areas: SEM.

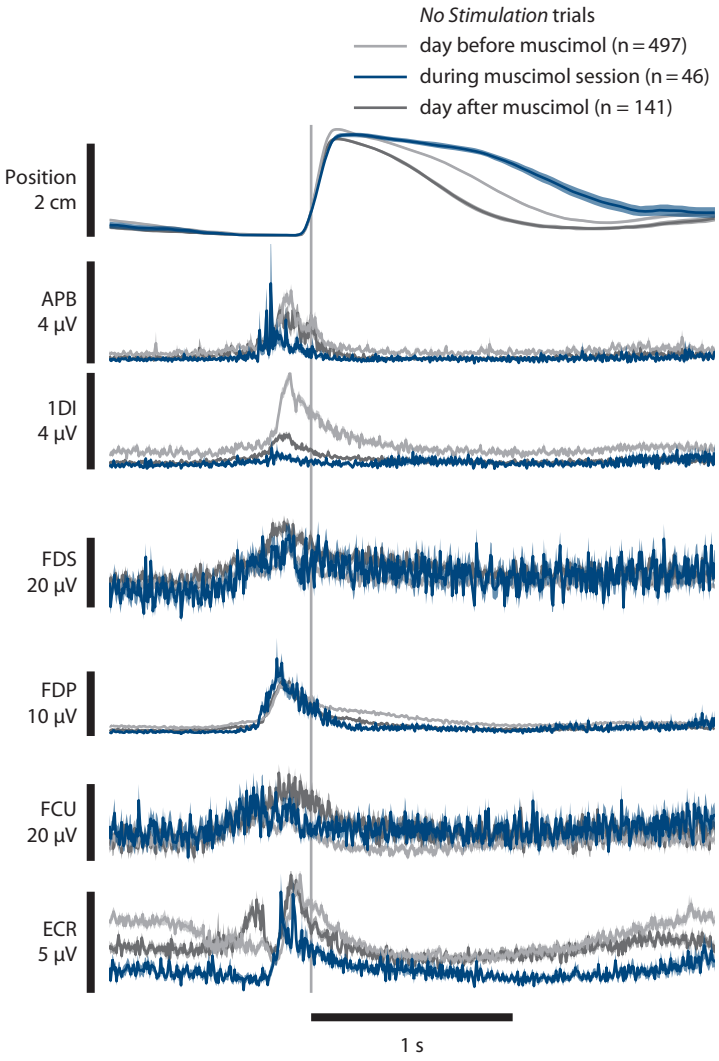

Figure 5.10: Effects of muscimol on task-related EMG (example from monkey Rv). See fig. 5.9 for description. Most pronounced effects are observed in 1DI, whose task-related activity did not completely reach pre-muscimol level one day after injections. Sessions `Rv110830001a`, `Rv110831003g`, `Rv110901000a`. Shaded areas: SEM.

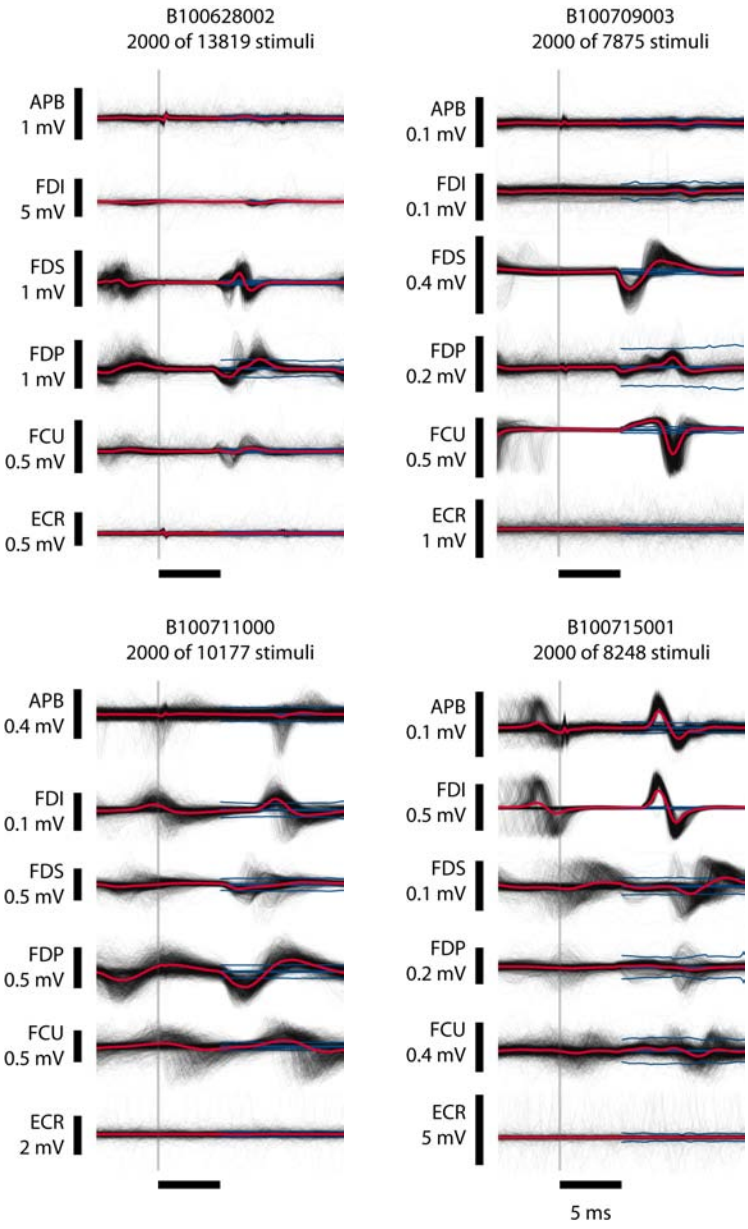

Figure 5.11: SCEP for four representative closed-loop stimulation sessions in monkey B. Semi-opaque black traces represent individual responses to one stimulus pulse (vertical grey line). Red traces are averages over all stimuli. For reference, EMG from no-stimulation, no-movement periods of session was divided in 12 ms long slices and these slices' average and ±2 SD are shown in blue. Sessions `B100628002a` (0–1250 s), stimulation current 300 µA; `B100709003b` (1800–2670 s), 40 µA; `B100711000a` (162–900 s), 30 µA; `B100715001c` (2500–3000 s), 200 µA.

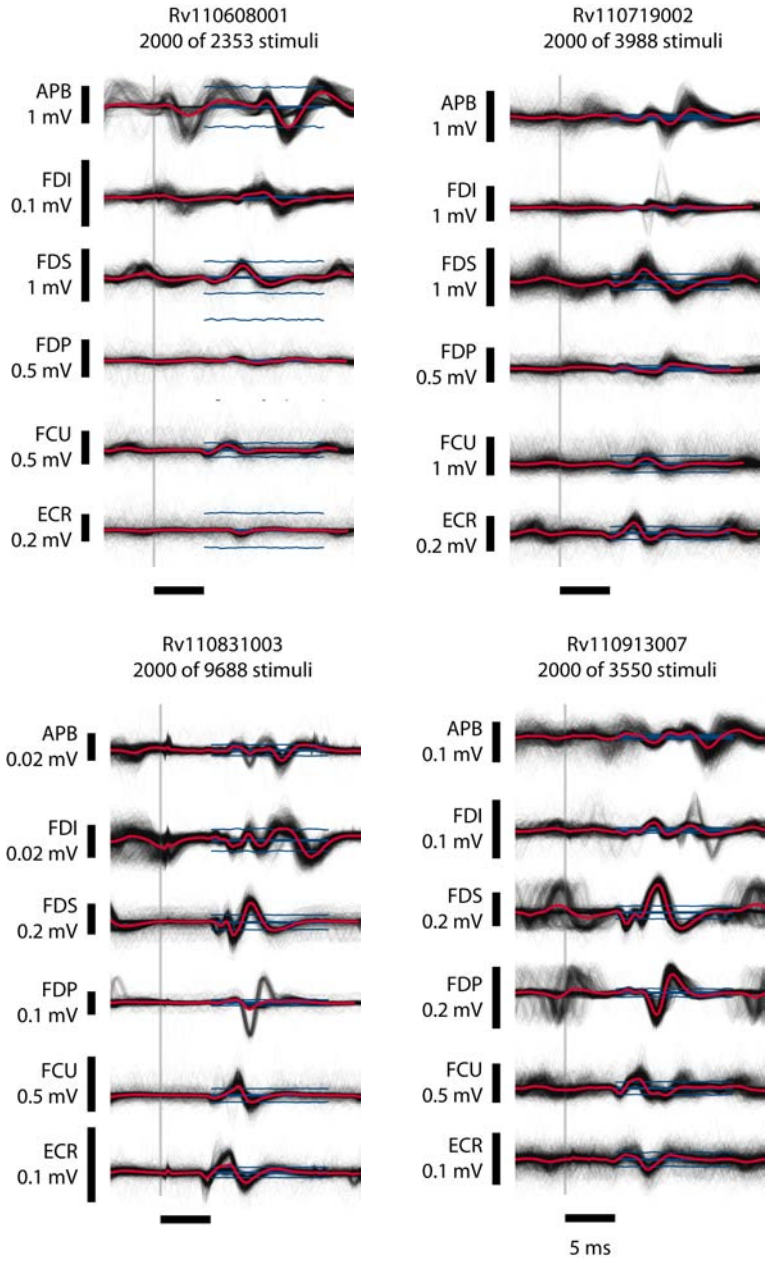

Figure 5.12: SCEP for four representative closed-loop stimulation sessions in monkey Rv. See fig. 5.11 for description. Sessions Rv110608001c (900–1255 s), electrode 7, stimulation current 60 µA; Rv110719002e (1600–3350 s), el. 6 at 50 µA; Rv110831003g (2880–4240 s), el. 10 at 70 µA; Rv110913007a (0–890 s), el. 4, 10 (at 2 ms delay), 40 µA.

5.3.4 Improving Performance and Restoring EMG Activity in the Paralysed Hand

Combining all parts of the experiment successfully was difficult to achieve. In monkey B, one paralysis session (out of six) was successful in that there was a marked increase in performed trials per minute comparing stimulation with control periods, the accuracy (number of completed trials / attempted trials) was higher during stimulation periods than during control, and the average maximum lever position was larger in stimulation epochs than in control epochs. For monkey Rv, we found in two of 27 paralysis sessions significant increases in trial rates during stimulation periods combined with higher average maximum lever positions during stimulation epochs.

We will now examine in more detail the successful sessions before we explore the grouped results. In session `B100711000` the difference in trial rates (3.1 trials/min during stimulation against 1.8 trials/min during control periods) was significant ($p < 0.034$). The difference in trial rate and other variables are shown in fig. 5.13 for a portion of recording `B100711000b`; cf. also supplementary movie. During stimulation, 62 of 76 or 92 % of initiated trials (lever

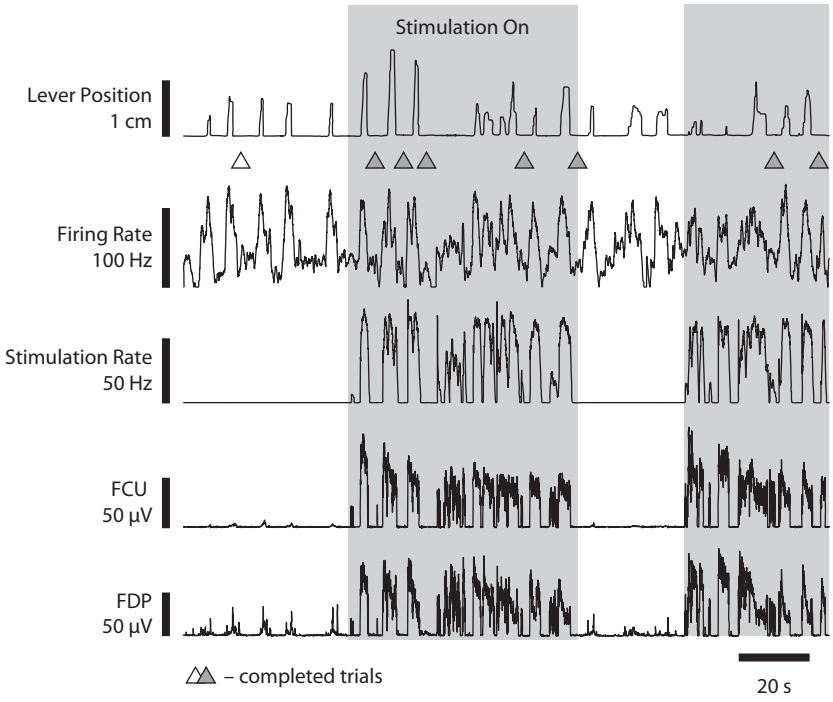

Figure 5.13: Data recorded during a portion of session `B100711000`. Lever position is shown at *(top)*. Neural firing rate below is well correlated with task. EMG on two sample muscles is abolished during no-stimulation periods. See also supplementary movie.

position crossed the threshold set in the task control program) were successful, i.e. the an-

imal was able to hold the lever above that threshold for the set hold time and received a reward at the end of the trial. This compares to 18 of 24 or 75 % successful trials without stimulation. During the training session recorded three days before the paralysis session the monkey was successful in all initiated trials, and performed at a rate of 4.0 trials per minute (163 trials). In order to see whether there was also a difference in maximum lever positions

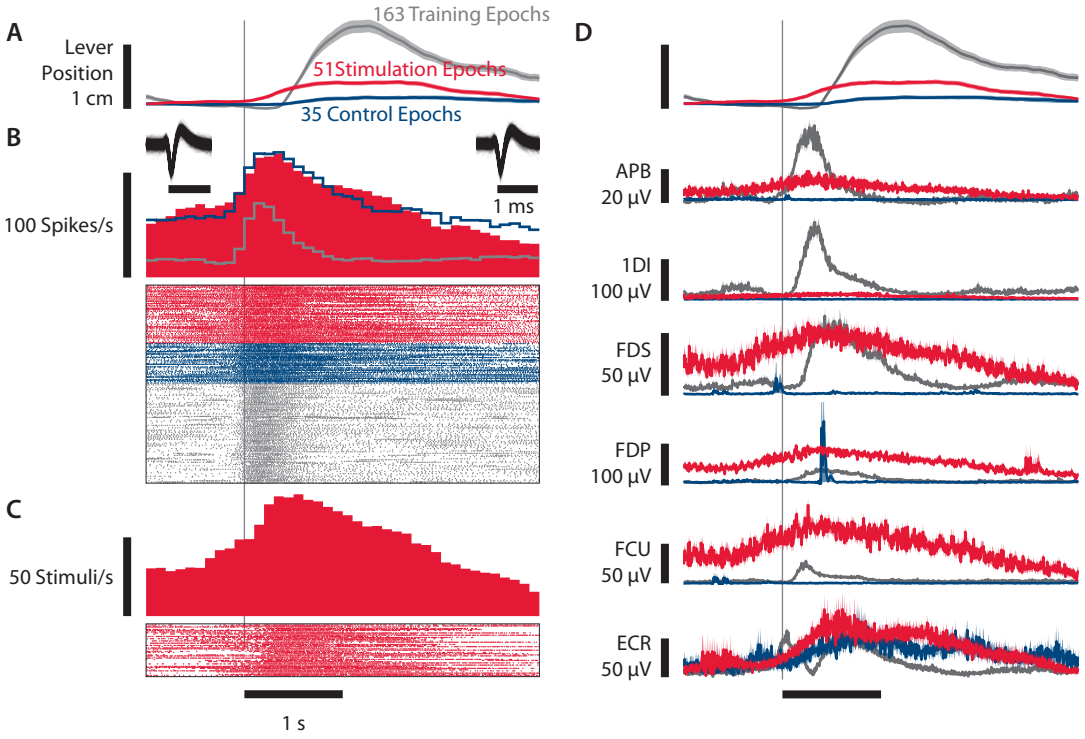

Figure 5.14: ISMS improves performance of task in monkey B. *(A)* Lever position. Epochs during which stimulation was turned on are shown in *red,* control trials (no stimulation) are shown in *blue*. Normal training session *(grey)* is shown for comparison. *(B)* Spike histograms and raster plots of neuron during stimulation, control, and training epochs. Insets show 5000 randomly selected discriminated spike waveforms each, from training *(left)* and stimulation *(right)* sessions. Note that the tail of the histogram reflects genuine changes in the firing behaviour of the cell. Only 86 training epochs are shown in raster. *(C)* Histogram and raster plot of stimulation pulses. *(D)* Lever position and rectified EMG traces. In control epochs, EMG is abolished in all recorded muscles but ECR. In stimulation epochs, EMG levels are restored or exceed normal levels in finger and wrist flexors.
Epochs are aligned to the time the neuron's smoothed firing rate exceeded 90 Hz (paralysis session) or 40 Hz (training session) for at least 0.4 s. Stimulation session `B100711000` (162–900 s), training session `B100708001` (cf. fig. 5.6, but note that the definition of epoch is different). Shaded areas: SEM.

during stimulation and control periods, data was split into epochs and aligned to times when the smoothed firing rate crossed a threshold of 90 Hz. While there was a significant differ-

ence between the mean maximum lever positions in stimulation and control trials (mean maxima during stimulation and control trials: 7 mm and 5 mm, respectively; $p < 0.0002$), the average maximum lever position during a previous training session far exceeded the stimulation condition (17 mm ±1 mm; fig. 5.14). EMG was restored in stimulation trials to levels similar to normal training sessions in finger and wrist flexors (FDS, FDP, FCU), while EMG was completely abolished during control trials (fig. 5.14 D). The muscimol injection did not seem to have an impact on the level of activity of the wrist extensor recorded (ECR), however the EMG time course was changed compared to training, presumably due to the altered movement profile.

In one of the remarkable sessions (`Rv110714003b`) with monkey Rv none of the recorded premotor neurons was well related with the task. Instead, while most of 1DI's activity was suppressed due to the muscimol block, we were able to record a single motor unit from the 1DI electrode. This motor unit, given the limited range of behaviour the monkey showed during an experimental session, was very well suited to predict task performance. Although the stimulation electrode chosen that day also caused SCEPs in 1DI, discrimination of the specific motor unit was not compromised and neither stimulus artefacts nor SCEPs were used to trigger stimulation as verified by a peri-stimulus time histogram (PStTH) (fig. 5.15 A). The animal performed 153 successful trials (of 154; 99 % completed) with stimulation enabled, at a rate of 6.3 trials per minute. This was contrasted by the relatively poorer completion of 28 control trials (of 31; 90 % completed) at 3.3 trials per minute (difference significant at $p < 0.008$). Again, we compared epochs aligned to threshold crossings of the neural control signal (here the smoothed firing rate of the 1DI motor unit) in order to compare stimulation with control performance (fig. 5.16). During stimulation epochs ($n = 178$) the average maximum lever position was 2.1 cm, whereas this average was 1.2 cm for the control epochs ($n = 43$), a significant difference (permutation test, $p \leq 0.0001$). Muscles 1DI, APB, and ECR were most strongly affected by the muscimol block (see table 5.3), and these were also the muscles most strongly affected by stimulation (fig. 5.16 D).

In another paralysis session, premotor neural activity was used to control stimulation. Spikes recorded from one electrode were discriminated using two templates, and events classified as belonging to either group were used to control stimulation (see inset in fig. 5.17 B). Of the initiated trials under stimulation, 161 of 181 (89 %) trials were successful performed at a rate of 6.8 trials per minute, whereas the 20 successful catch trials (of 22, 91 % success rate) were performed at a rate of only 4.0 trials per minute, a significant difference ($p = 0.02$).

We then compared task performance during stimulation and control epochs. Epochs were aligned to threshold crossings (11 Hz) of the firing rate used to control stimulation and di-

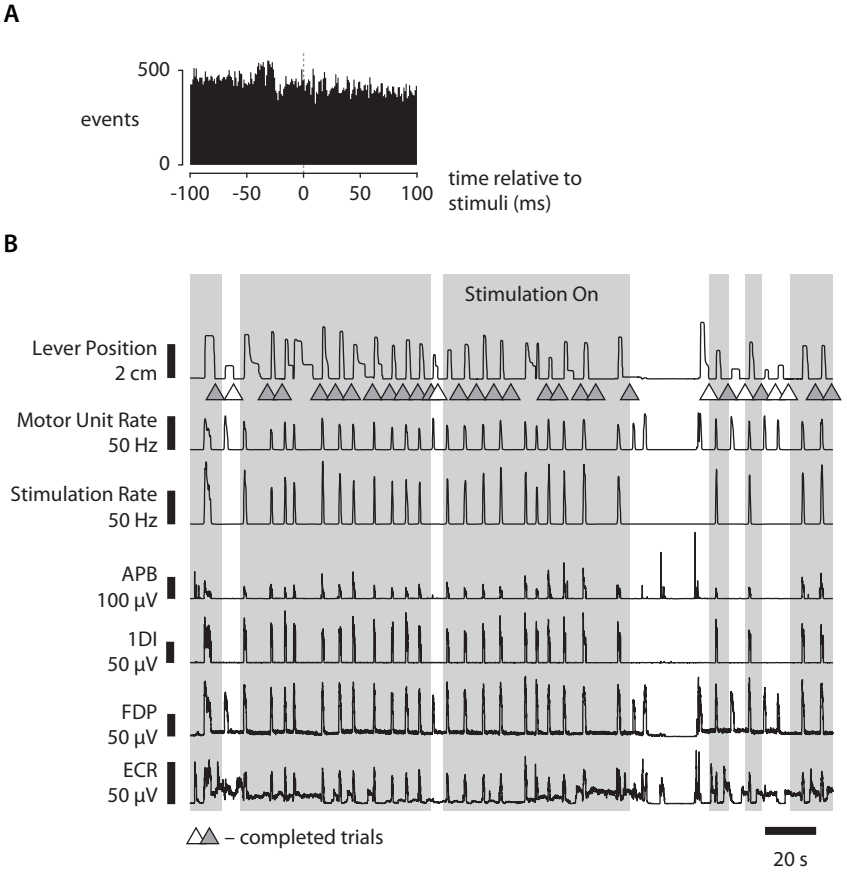

Figure 5.15: Data from a session in which stimulation was controlled by a residual motor unit of 1DI. *(A)* PStTH of discriminated 1DI MUAPs used to control stimulation. Stimuli aligned to time 0. *(B)* Trace of lever position is shown in relation to 1DI motor unit firing rate, stimulation rate, and several smoothed EMG traces during stimulation (grey background) and control periods. Note reduced EMG in APB and 1DI during control periods. Recording `Rv110714003b` (554–2711 s). PStTH shows 10428 MUAPs aligned to 12333 stimuli, bin width 1 ms.

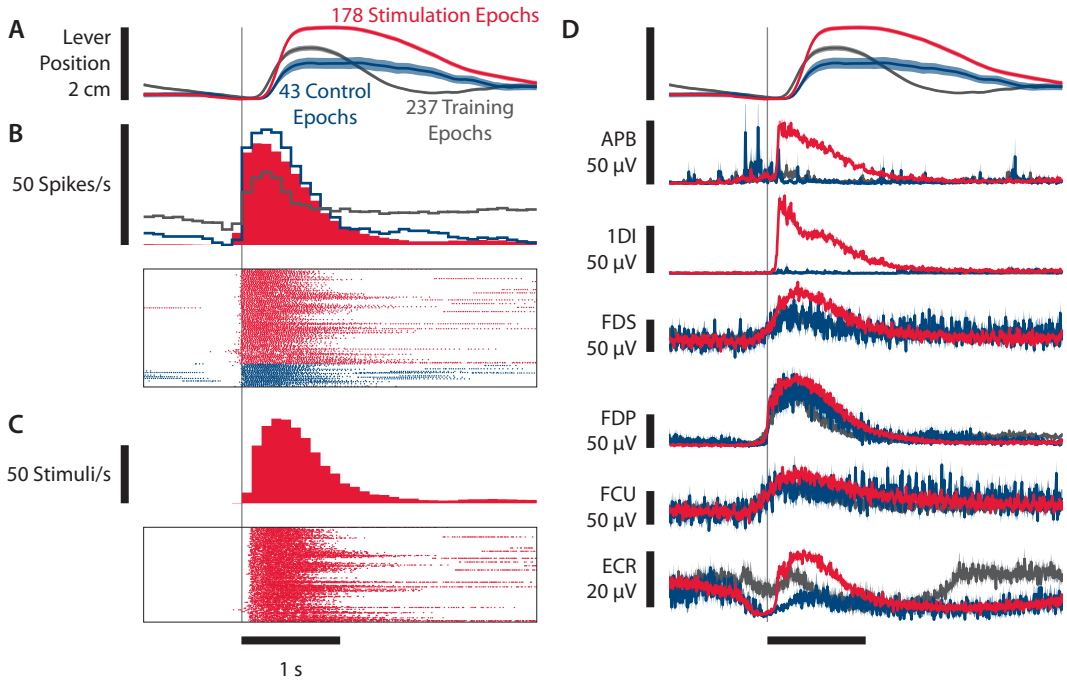

Figure 5.16: Stimulation, control, and training epochs aligned to threshold crossing of smoothed 1DI motor unit firing rate (20 Hz, in training session: 15 Hz). *(A)* Lever position. *(B)* Spike histogram and raster plots. *(C)* Stimulus pulse histogram and raster plots. *(D)* Averaged EMG traces in relation to lever position. Recording `Rv110714003b`, (554–2711 s); training session: `Rv110713000a`. Shaded areas: SEM.

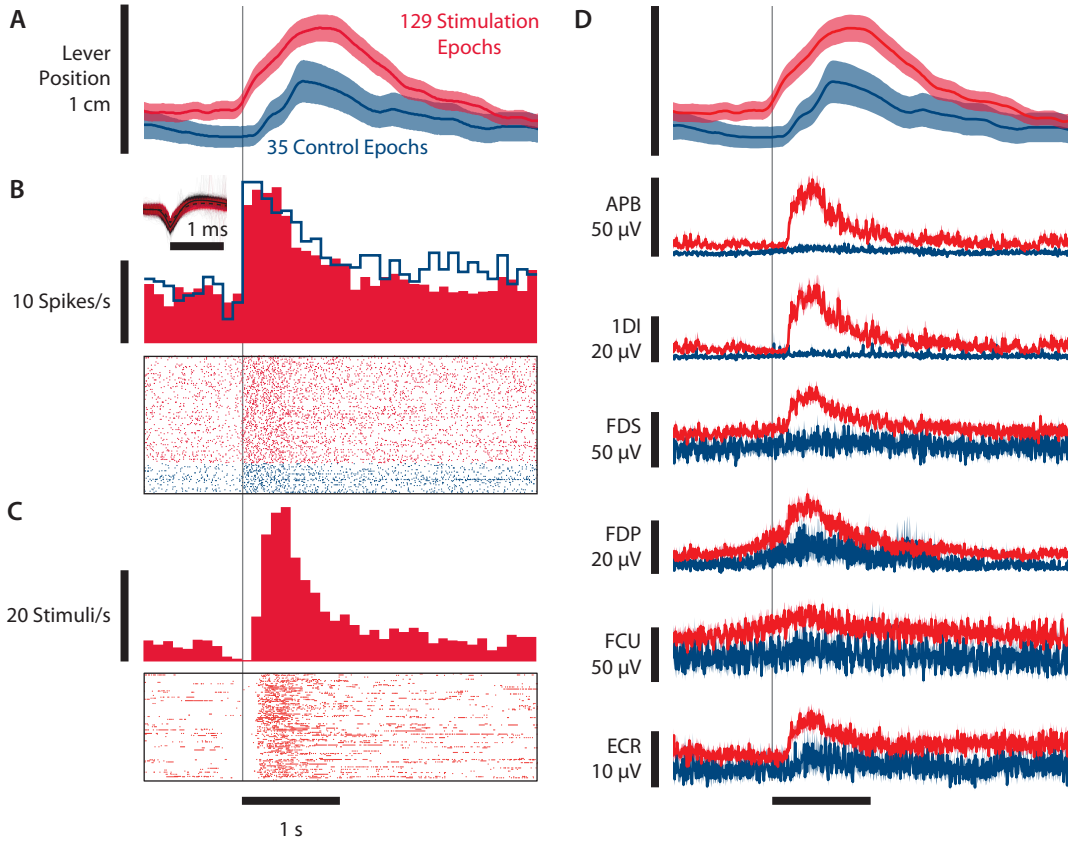

Figure 5.17: ISMS improves performance of task in monkey Rv. *(A)* Average lever position during stimulation *(red)* and control *(blue)* epochs. *(B)* Spike histograms and raster plots for stimulation and control epochs. Inset shows the 3123 spikes assigned to template 1 *(black)* and 5000 of 6360 spikes assigned to template 2; both templates were combined to control stimulation. *(C)* Raster plot and histogram of stimulation pulses delivered during stimulation epochs. *(D)* Lever position and EMG during stimulation and control epochs. EMG is elevated on average during stimulation epochs.
Epochs are aligned to the time the neuron's smoothed firing rate exceeded 11 Hz for at least 0.4 s. Session `Rv110719002e` (1600–3350 s). Comparison with training session was impossible, because the neural activity used for stimulation was only recorded during this session. Shaded areas: SEM.

vided into stimulation and control epochs. In stimulation epochs, the average maximum lever position was 13 mm, whereas during control epochs, this average was only 6 mm (significant at $p \leq 0.0001$). Compared to the data from monkey B shown above, restoration of EMG is less clear, as becomes clear in fig. 5.18, where epochs are aligned to moments when the lever crossed a (low) threshold. This plot reveals that while the monkey performs trials

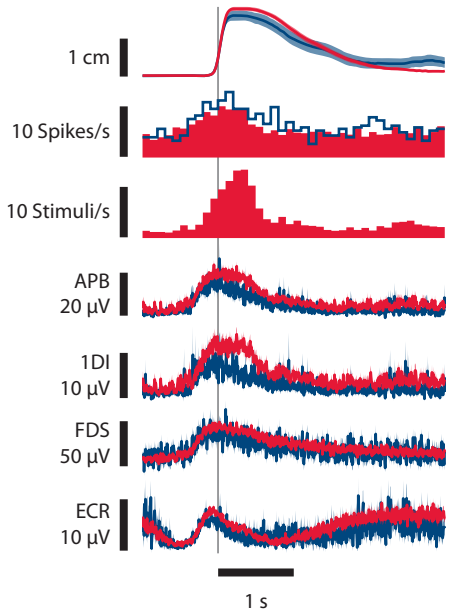

Figure 5.18: Data from the same session as fig. 5.17, but epochs are now aligned to threshold crossings (4.5 mm) of lever. 192 stimulation and 30 control epochs.

there is little difference in EMG between stimulation and control periods. Still, in both analyses maximum lever position and intrinsic hand muscle EMG are higher during stimulation than during control periods, leading us to conclude that ISMS caused an improvement here as well.

We can now look at the combined results from paralysis and training sessions after the spinal implants. Trial rates for individual paralysis and training recordings are shown in fig. 5.19. Over all paralysis recordings ($n = 6$), monkey B performed 476 trials under stimulation and 93 trials without stimulation in 297.3 and 49.6 minutes, corresponding to rates of 1.6 and 1.9 trials per minute, respectively. A permutation test randomly assigning stimulation/control condition to times and trial counts of recording sessions did not reject the null-hypothesis that the difference of average rates is zero ($n_{\text{perm}} = 10^5$, $p = 0.2$). During training recordings ($n = 7$), monkey B performed 665 trials in 215.5 minutes, at a rate of 3.1 trials per minute. The difference in average trial rate between training and paralysis sessions was significant ($p < 0.01$; comparing training trials only with control trials during paralysis sessions did not find a significant difference, at $p = 0.25$, most likely due to the low number

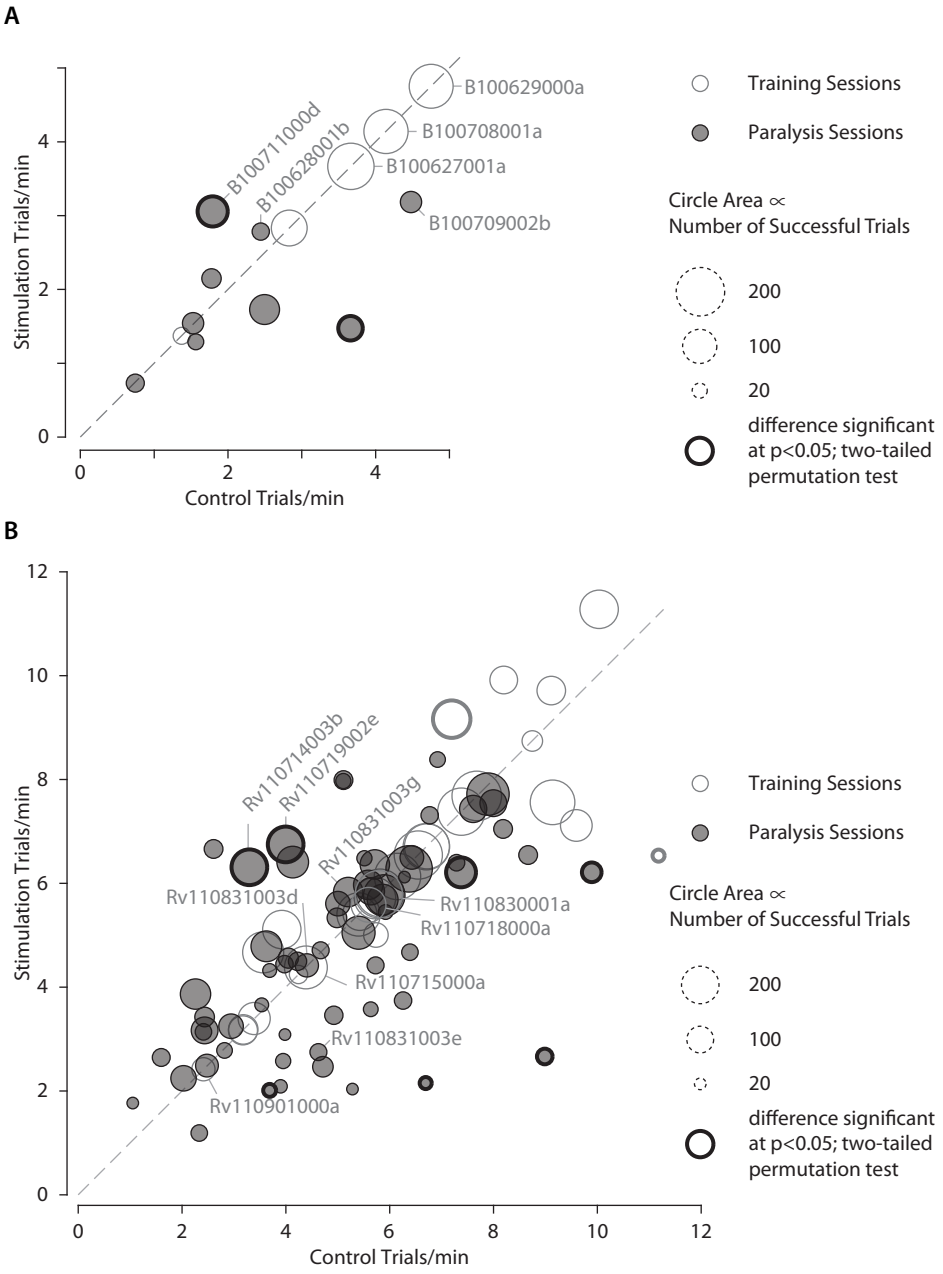

Figure 5.19: Successful trials performed per minute during stimulation and control periods. Both paralysis and normal training sessions are shown (no actual stimulation occurred in training sessions). In training sessions where no distinction was made between stimulation and control trials during recording the same value is used for both conditions. Within a session at least 3 trials had to occur in a condition for that condition to be used in this analysis. Sessions shown in other figures are labelled. Heavy borders denote sessions for whom differences in trial rate were significantly different ($\alpha < 0.05$, permutation test). *(A)* Monkey B. *(B)* Monkey Rv.

of control trials).

Monkey Rv performed 4671 successful trials in 1039.6 minutes under stimulation in paralysis recordings ($n = 27$), corresponding to 4.5 trials per minute. During control periods, monkey Rv performed significantly slower: 823 trials in 249.8 minutes, corresponding to 3.3 trials per minute ($p < 0.01$). Monkey Rv's performance in training recordings ($n = 22$) was significantly better than during control periods in paralysis sessions, at 5801 trials performed during 1000.8 minutes, yielding a rate of 5.8 trials per minute ($p = 0.01$).

Because of the various sources of variability between sessions – efficacy of muscimol injections, after-effects from sedation, cortical control, cISMS effects in monkey B – we did not necessarily expect to find significant effects combining results from all sessions. However, we could show that (a) trial rates were lower in paralysis sessions, and (b) in monkey Rv trial rates during stimulation periods were higher than during control periods in paralysis sessions.

5.3.5 Changing Dynamics of Neuron Used to Control Closed-Loop Stimulation

We were able to follow one PMv neuron whose activity was well tuned to the task over 18 days in monkey B. Since its peak activity occurred reliably before task onset, we also used it to control stimulation during paralysis sessions (cf. figs. 5.6 and 5.14). In order to see whether the identified neuron was affected by the experiment we analysed several properties of its spike trains. Figure 5.20 shows the temporal development of the neuron's ISpI distributions, its mean firing rates, and the Fano factor for each session it was recorded. Both the number of days since the neuron was first recorded and whether the session was a paralysis session were significant predictors for the mean firing rate for that session, while session length was not (table 5.4). Similarly, the Fano-factor – the ratio of variance and mean of ISpIs – decreased with increasing number of days since first recording, i.e. the ISpIs became more regular.

Variable	B	t	p
Days since first recording	9.6	3.37	0.003
Paralysis session[1]	1.7	5.92	$< 10^{-4}$
Length of session	−0.001	−0.46	0.65
Overall statistics: $F = 20.0$, $p < 10^{-5}$, $R^2 = 76.9\,\%$			

Table 5.4: Linear regression analysis of mean firing rates of neuron used for control of stimulation in sessions with monkey B.

[1] Variable is 1 for paralysis sessions, 0 otherwise.

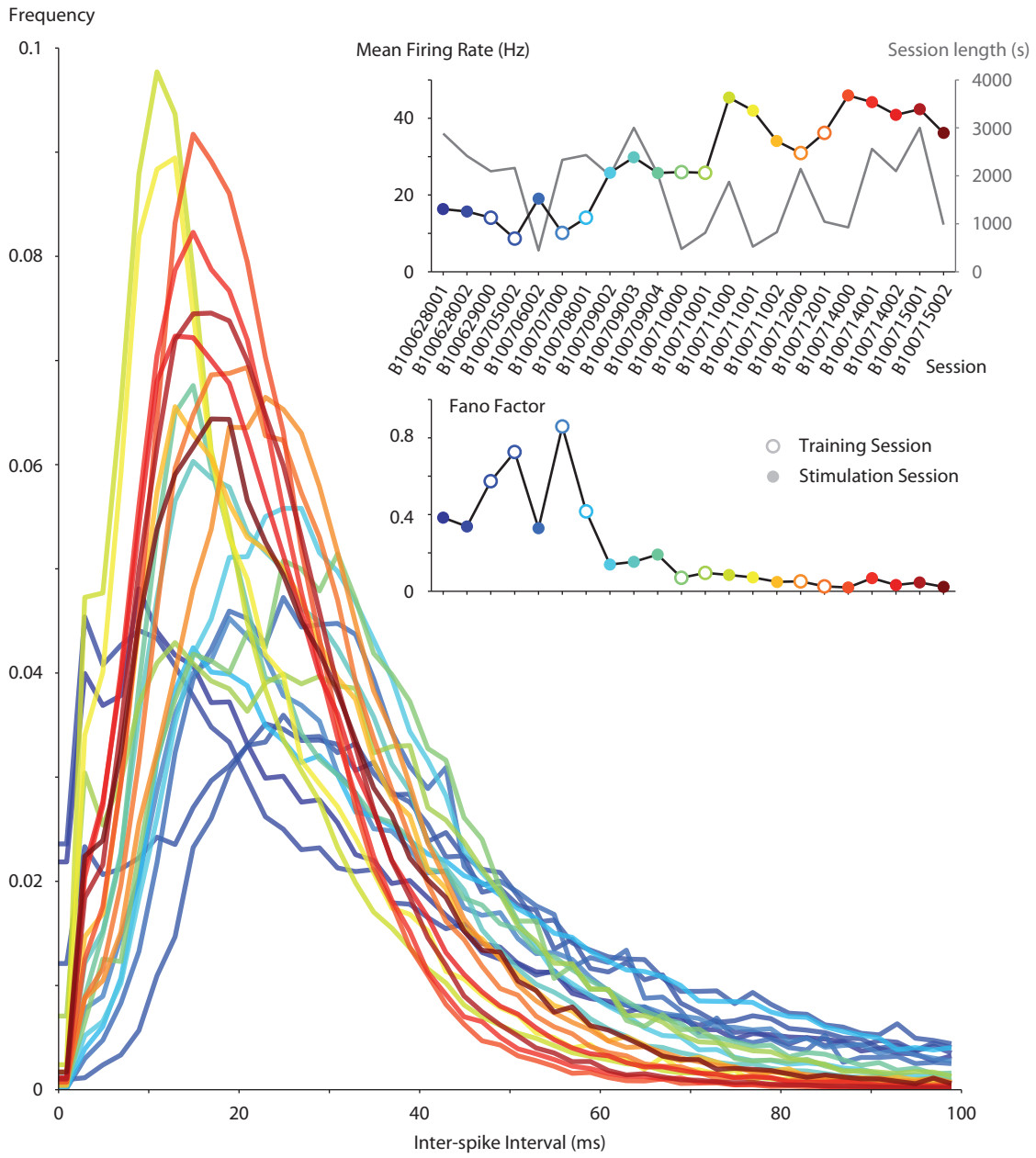

Figure 5.20: Smoothed ISpI histogram of neuron used for control of ISMS during training and stimulation sessions. Traces are colour-coded by time, the first session shown in deep blue, the last session in dark red. Upper inset shows mean firing rate of the neuron during session and session length *(grey)*. Lower inset shows Fano factor (of ISpIs) for individual sessions. Open circles – training sessions, filled circles – stimulation sessions.

5.4 Discussion

This experiment – to be successful – required several components to work together. First, there had to be a task-related neuron whose activity could be used to control ISMS. Second, stimulation of the acutely inserted electrode (in case of monkey B) or of the array (monkey Rv) had to evoke finger or wrist flexion movements. Third, the injection of muscimol into M1 had to cause a disabling yet focal paralysis of the hand. Finally, once recovered from sedation, the monkeys had to be motivated to work for food rewards and they had to persist trying to perform the task even when they failed. In what follows, we will discuss individual aspects and outcomes of this experiment.

5.4.1 Task

Impairments induced by muscimol injections and movements evoked by cISMS were hard to predict at the time of behavioural training, as were effects of the required sedation at the beginning of an experiment. Therefore, a task flexible enough to be adapted to different kinds of grasps and levels of difficulties was required. The reach, grasp and pull task employed here involves several muscle groups of the arm and hand, and features of the task such as the manipulandum or the retaining spring could be changed and adapted to accommodate for different levels of ability and motivation. Furthermore, task parameters such as displacement of the lever and hold time necessary for successful trials could be changed to adjust difficulty.

5.4.2 Induced Paralysis

While we were able to induce focal and temporary paralyses reliably in monkey B, this was not as readily achieved in monkey Rv. We started our injections with similar doses of muscimol as others before (Schieber et al. 1998, Schmidlin et al. 2008, Tsuboi et al. 2010), and increased the injected amount up to four times the initial dose in later sessions. Furthermore, we carefully mapped the exposed cortical area by ICMS and placed our injections at sites where we obtained hand movements at the lowest thresholds. Finally, we used muscimol from different batches, minimising the chance of having used an ineffective sample.

One possible explanation for our results is that our injections may have been further away from the bank of the central sulcus than we thought. In that case, it would still have been possible to obtain low threshold SCEPs by exciting passing axons during mapping, however the GABA-agonist muscimol would be less effective near axons (Martin et al. 1999). With careful histological examination of M1 slices we could potentially confirm the location of

some injections. However, it will be impossible to relate specific locations to individual sessions.

Muscimol was used in this experiment because we had previous experience with it and because it is reversible on a short time scale. Given that we now have the experience to implant chronic intraspinal electrodes, a permanent neural prosthesis using the Neurochip (Jackson et al. 2006b) could be implemented. A longer lasting impairment could then be induced either pharmacologically with e.g. tetrodotoxin (Martin et al. 1999) or by cooling (Reed et al. 1978, Sasaki et al. 1984, Imoto et al. 2006).

5.4.3 Neural Recordings and Control of Stimulation

In tradition with the operant conditioning literature, we used neural activity recorded from a single electrode to control stimulation (Moritz et al. 2008). While this strategy was very successful in monkey B, where we were able to use the action potentials of a single neuron over several days, the limitations became apparent in the experiment with monkey Rv, where finding clean, strongly modulated, and task related neurons was more difficult. Population decoding strategies employed in other studies (Velliste et al. 2008, Ganguly et al. 2009, 2011) may offer a more reliable way of controlling a BMI – as long as the population dynamics do not change. Once the network undergoes plastic changes, for example after traumatic injury (Hochberg et al. 2012) or in an experimental model such as ours, decoders may need to be retrained frequently. Indeed, we did not expect the activity of PMv neurons to remain largely unchanged in paralysis sessions compared to training sessions, given the disturbance by muscimol injections and ketamine sedation.

In two of the experimental sessions with monkey Rv (`Rv110627004`; `Rv110714003` has been described above) we used the MUAPs of a muscle (1DI) to control stimulation as a task related premotor neuron was not available. Since many SCIs are not complete (Wyndaele et al. 2006), this configuration could also be relevant in a clinical setting. Using residual muscle activity to control stimulation could induce plastic changes of spinal cord circuitry, strengthening remaining pathways and thus leading to some degree of recovery (Everaert et al. 2010).

A neuroprosthetic spinal cord stimulator will have to be able to produce a multitude of movements, which need to be independently controlled. In this study, in order to demonstrate a proof of principle, we have limited ourselves to a one-dimensional controller. While there is evidence that monkeys are capable of controlling neurons' firing rates in order to control a cursor on a screen using arbitrary filters (Ganguly et al. 2009), more experiments are needed to see whether that generalises to control of spinal stimulation using multiple

channels, especially in the light of our findings regarding non-linear interactions between stimulation channels (chapter 3).

The control algorithm we used in this study was also limited in that it did not incorporate a model of non-linear frequency responses (chapter 2). While the order of magnitude of these effects is relatively small for a large proportion of stimulation electrode – muscle pairs, it would nevertheless be beneficial for a neuroprosthetic ISMS device to incorporate our findings in order to maximise efficiency.

5.4.4 Spinal Cord Stimulation

In this experiment, we successfully used cISMS to produce grasp-related movements. While we relied on acutely inserted electrodes in sessions with monkey B, we could greatly improve the experiment by using a chronically implanted FMA in monkey Rv. Reliable responses throughout the period of the experiment (chapter 4) and many available stimulation channels show that this kind of implant can facilitate future chronic spinal stimulation experiments.

Assessing how much cISMS influenced the animals' performance of the task was not trivial. Performance in the grasp-and-pull task during paralysis and training sessions can be quantified in several ways, and no single variable captures all potentially important aspects. One way to assess performance is to compare successful trials completed per minute between paralysis and training sessions, and between stimulation and control periods during each paralysis session. If injection of muscimol caused the task to be more difficult, trial rates during paralysis sessions should on average be lower than trial rates during training sessions, a result we have observed consistently in both animals. On the other hand, if spinal stimulation improves task performance, trial rates during stimulation periods should be higher than during control periods in paralysis sessions. Again, in both monkeys such a difference in trial rates was observed in some sessions, and in monkey Rv also across all sessions. Of course, one confound here is that in paralysis sessions, monkeys had been sedated before the behavioural part of the experiment, which we would expect to decrease motivation and thus trial rates, so muscimol induced paralysis may not have been the only reason for the observed change. The increase of trial rates observed during stimulation periods observed in some individual sessions and overall in monkey Rv need not be caused by a functional restoration. Instead, animals may have perceived ISMS pulses as a cue despite all efforts to treat both experimental conditions equally and to keep the interacting experimenter blinded about the nature of the trial.

Another measure we used is the percentage of initiated trials that led to successful com-

pletions, i.e. trials that met a hold time criterion. While the monkeys were well trained and performed almost perfectly during training sessions, weakness of the hand should decrease the percentage of successful trials during paralysis sessions. Within paralysis sessions, we expected monkeys to more successful during stimulation conditions, which was indeed the case for two of the three sessions more closely examined above.

We also wanted to characterise the movement dynamics and muscle activation during task performance both with and without stimulation during paralysis sessions. If the muscimol induced paralysis is complete, we would not expect the animal to be able to perform any successful trials at all, even though she might be trying. However, the signals used to control the stimulation – premotor neuronal firing – were still present. Aligning data to epochs corresponding to a change in the control signal and grouping those epochs by stimulation and control conditions allowed us then to compare task variables such as lever position and EMG. Using this method, we could compare lever positions across conditions even if the monkey did not succeed moving the manipulandum. With this analysis method comes an important caveat, however. If the relationship between the neuron's firing and intent to perform the task is weak, and especially if a change of firing rate is not a sufficient predictor for the intended action, then falsely categorised epochs may distort the average. This is indeed a problem when comparing EMG recordings during stimulation and control periods because the neural activity directly affects these measures. Lever position however should be less affected by this distortion, as in these experiments stimulation never activated proximal muscles, which are necessary to move the manipulandum. Any change of the average lever position because of falsely included epochs (i.e. epochs where the neural firing rate reached threshold without the animal intending to perform the task) should therefore affect both stimulation and control periods equally.Of the three sessions examined in detail above only `Rv110719002e` is a likely candidate where EMG profiles are distorted by this phenomenon. While the difference between EMG activity during movement with and without stimulation seems larger than it actually was, the difference between lever position traces can be trusted.

In summary, using several measures to assess potential improvements during stimulation trials over control trials, we found that in several experimental sessions there was a behavioural improvement.

5.4.5 Development of Neural Signals

During our experiments we could only follow one neuron that was used to control spinal stimulation over several sessions. This neuron showed profound changes in its firing pattern, with both mean firing rate and regularity of ISpIs increasing over time and from training

to paralysis sessions. The change of firing behaviour improved delivery of ISMS only when the monkey tried to perform the task. Learning in BMI experiments is commonly observed (Taylor et al. 2002), albeit without changes of ISpI distributions (Ganguly et al. 2009). It is impossible to determine whether learning to control ISMS was the cause of the observed changes, given that muscimol injections affect normal PMv–M1 interactions (Shimazu et al. 2004) and the animal had been sedated just before stimulation experiments.

5.5 Conclusion

In this experiment we have – for the first time, to our knowledge – demonstrated a cortically controlled spinal cord stimulation BMI in awake monkeys. We have shown that it is possible to restore motor function with such a device. Further research will be necessary to improve spinal implants to increase the movement repertoire and provide stronger forces. Combining cISMS with peripheral FES for proximal arm movement might enable development of a neural prosthesis for SCI or stroke patients until neuroregenerative therapies become available.

6 General Discussion

6.1 Summary

Spinal cord injury and stroke remain conditions with few therapies, but recent developments in brain-machine interfaces have opened interesting avenues. Chronic recording of neural signals from intracortical electrodes is routinely done in monkeys and is becoming feasible in human patients as well, to the extent that tetraplegic patients are able to control movements of robotic arms.

In the work presented in this thesis we have aimed to further the understanding of macaque cISMS. Extending the results of Moritz et al. (2007), we established that cISMS is capable of eliciting functional hand movements, and we identified parameters that seem to be particularly suitable for sustained muscle activation (chapter 2). While we have shown that some sites in the cervical spinal cord lend themselves better to stimulation for movement, we have not identified the underlying mechanisms which might then allow prediction of optimal implant sites and electrode configurations. However, careful analysis of histological samples collected in our experiments should enhance our understanding.

Investigating interactions between stimulation sites in the macaque cervical spinal cord, we have found that a considerable proportion of electrode pairs exhibits non-linear interactions in hand and arm muscle EMG as well as forces produced at the wrist (chapter 3). These results deviate from previous experiments in other species and highlight differences in motor control. Furthermore, our results have practical implications for the design of algorithms for cISMS neuroprostheses, as these non-linear interactions have to be taken into account. Both beneficial and disadvantageous consequences are conceivable: the movement repertoire might be extended at the cost of more complicated algorithms.

In order to investigate chronic ISMS, suitable electrode implants are needed. We have started to use floating microelectrode arrays, providing a relatively high number of electrode shanks distributed over a small areas (chapter 4). We found that FMAs are well suited for chronic stimulation experiments lasting several months and that implanted arrays themselves do not seem to be detrimental to the animals' wellbeing. However, further improvements are necessary to maintain the longevity of connectors, and ultimately, flexible elec-

trodes may be the best solution for a difficult neural engineering problem. In the meantime, however, FMAs are a valuable tool to further investigate spinal cord neurophysiology in chronic experiments.

We demonstrated that brain-controlled cISMS can restore function and improve performance in a reach-and-grasp task (chapter 5). Despite the technical limitations of our experiment – we only used one channel of stimulation controlled by neural activity recorded from one electrode, and the model lesion did not always work – we established that cISMS is worth pursuing further as a neuroprosthetic technique. Aside from that, ISMS might also be a useful technique for rehabilitation, as activity-dependent plasticity induced by cortically controlled ISMS could repurpose silent but surviving pathways in patients with incomplete SCI (Jackson et al. 2006a, 2012).

6.2 Feasibility of Intraspinal Implants in Human Patients

In the last decade, electrical stimulation of the peripheral and central nervous system to restore sensory or motor function has become widely available for patient use. Cochlear implants to restore auditory perception (Pfingst 2000), deep brain stimulation for treatment of Parkinson's disease and tremor (J. S. Perlmutter et al. 2006, Lyons 2011) and epidural spinal cord stimulation for pain treatment (Simpson 1997, Compton et al. 2012, Epstein et al. 2012) are commercially available to a growing number of patients. These implants target relatively large populations of neurons, and in the case of cochlear and epidural implants do not penetrate the neural tissue. Nevertheless, cortical electrode implants relying on tight interaction with small neural populations for stimulation (Schmidt et al. 1996, Dobelle 2000) or recording (Hochberg et al. 2006, 2012) are now being tested in patients.

The spinal cord, due to its flexibility and mobility within the vertebral column, is one of the more challenging neural tissues to interface with, and development of ISMS chronic electrodes is at its early stages. Chronically implanted microwires (Mushahwar et al. 2000c) and microelectrode arrays (McCreery et al. 2004) have been used to elicit leg movements and micturition in cats. In these experiments, electrodes were implanted for several months. Similarly, our tests in macaques suggest that floating array implants can last at least for months, with little change of stimulation thresholds and little tissue damage (chapter 4). Of course, for patient use, this is not enough: Implants will have to last for years, and the risk of further tissue damage has to be minimised. Furthermore, any implant surgery should not preclude application of other therapies, such as tissue regeneration with stem cells, should they become available.

FMAs as used in our experiments are unlikely be the kind of implant that will be implanted

into human spinal cords. Instead, flexible electrodes (Rousche et al. 2001, Stieglitz et al. 2009, Sohal et al. 2012) may be better suited to the mobile environment of the spinal cord. In the meantime, however, I think ISMS should be studied in appropriate animal models with the tools at hand in order to determine whether chronic implants are practical at all.

6.3 Spinal Cord Evoked Movements

A neural prosthesis aiming to restore functional movements in patients will have to bear significant improvements over (noninvasive) muscle stimulation devices. Two major problems of muscle stimulators are fatigue and lack of specificity of stimulation. In our experiments under terminal anaesthesia (chapters 2 and 3), we have found that over the course of the experiments (up to 20 h after first stimulation) responses deteriorate and higher currents are needed to maintain comparable effects. However, this might be an effect of ongoing anaesthesia and declining health rather than of continued stimulation. In our chronic experiments (chapter 5), we found that even for long and continuous stimulation, currents had to be adjusted less to maintain the strength. From our long-term measurements of stimulation thresholds (chapter 4) it seems that the major problem for achieving stable stimulation effects with intraspinal implants is going to be movement of electrodes and possibly development of glial scar tissue.

Regarding the issue of specificity, spinal implants face problems as well. Whereas ISMS of one electrode often activates more than one muscle near threshold, the activated muscles are also often synergistic in natural grasp movements. However, it is more difficult to obtain some movements, such as wrist and finger extension, in isolation. Although this finding might be biased because in our experiments we concentrated our efforts on finding sites evoking grasping movements, Moritz et al. (2007) also report vastly more sites activating finger and wrist flexion than extension. Our chronically implanted arrays cover only small areas of the cord. It may be that more electrodes distributed over a larger area are needed to cover the less frequently encountered effects. One possible strategy might be to combine the strengths of ISMS and FES and use the former to evoke naturalistic grasp movements and the latter to target finger/wrist extensors.

6.4 Control of Spinal Implants

Control of ISMS implants appears to be the most easily solvable issue on the way to a medical device. In chapter 5 we have demonstrated a very simple yet quite reliable way to control

stimulation. As opposed to on/off control employed by some FES systems (Kilgore et al. 2008), gradation of evoked forces is possible. Different dimensions of stimulation could be controlled by the activity of individual neurons or ensembles, as has been demonstrated in the one-dimensional case (Fetz 1969, Moritz et al. 2008, Law et al. 2011). Recording of neural activity is now also possible over long times, as needed for a spinal implant (Hochberg et al. 2006, 2012).

However, non-linear interactions between stimulation channels described in chapter 3 pose a difficulty for control of a neural prosthesis. Two strategies to deal with this problem are conceivable, putting the burden either on the control logic or the user. It might be feasible to test interactions between channels after implantation and adjust the control algorithm to either use or avoid nonlinear interactions. It is yet unknown whether and how interactions between channels change over time; if they do, the system would need frequent readjustment. In a different approach, one could count on the subjects being able to learn to control interacting stimulation channels. Indeed, monkeys (Carmena et al. 2003, Velliste et al. 2008) and humans (Hochberg et al. 2012) learn to control seemingly complicated BMIs relatively easily. One might compare learning how to control a BMI with how to ride a bicycle: At first, consequences of actions are not clear, and one might over-compensate for state changes such as turning into one direction by pulling the handle bars too far in the other direction and consequently fall off the bike. Likewise, a patient may need time and practise to master the process of modulating neural activity to control a prosthesis. However, every cyclist experienced the moment when she 'got it' – when cycling became as natural as walking (which of course also had to be painfully learned at some time). One would hope that it is possible to build a prosthesis that is learnable by patients, and that unforeseen and complicated non-linearities can be avoided (in the same way as we do not build bicycles whose handle bars change their direction of action depending on the speed of cycling).

6.5 Future Directions

In addition to the follow-up experiments and obvious extensions discussed in the individual chapters, there is one technique deserving more attention. Electrical stimulation is a coarse way to excite neurons: The volume around the electrode tip is excited indiscriminately, with stimulation thresholds varying by neuron type (Gustafsson et al. 1976, Gaunt et al. 2006). This leads to both wanted and unwanted effects: while the activation of many motoneurons innervating one muscle is necessary in order to produce forceful movements and we often find co-activation of synergistic muscles, this also creates the potential of unwanted

co-activations. In order to further understand the mechanisms underlying the interactions between sites of electrical stimulation and to optimise control of neural prostheses a more selective way for stimulation of spinal neurons would be desirable.

Selective stimulation of motoneurons innervating different muscles is certainly not a new idea. As early as 1980, Kerkut suggested optical stimulation of motoneurons retrogradely labeled with dyes (Kerkut 1980). At the time this suggestion must have appeared as science fiction as it was not known whether mammalian neurons could be made photosensitive. The recent rapid development in the field of optogenetics has made these techniques available for primate research (Diester et al. 2011). Different light sensitive ion channels such as channelrhodopsin-2, halorhodopsin, and step-function opsin allow excitation, inhibition, and light pulse triggered activity changes of neurons, respectively.

Combining these photosensitive channels with selective promoter techniques, as used by Kinoshita et al. (2012), motoneurons innervating selected muscles could be activated, or spinal interneurons could be selectively silenced in order to understand the interactions brought about by multichannel ISMS. Optical stimulation of motoneurons could allow us to complement movements readily obtained with ISMS with other movements not seen as commonly, such as wrist extension or some individuated finger movements. Furthermore, it might be possible to modulate responses to ISMS with optical stimulation. Selected motoneuron populations could be brought closer to stimulation threshold, or inhibited. Likewise, by up- or downregulating interneuronal activity, the 'gain' of ISMS could be adjusted.

A Implementation of Automated Positive Reinforcement Training of Macaque Monkeys

Refinement of behavioural experiments involving non-human primates becomes an ever more important issue. Numbers of animals needed for experiments could potentially be reduced by selecting individuals performing particularly well during early training. In this chapter, I describe development and testing of a system for automated behavioural training and identification of macaque monkeys at breeding facilities and in the lab.

The experiment described here was designed by Andrew Jackson and myself. Data collection was supported by Jennifer Tulip, David Farningham, and Mellissa Nixon. Henrik Johansen and Søren Ellegaard built a coil suitable for monkeys to use with the RFID reader.

A.1 Background and Motivation

Positive reinforcement training (PRT) – the use of pleasant stimuli to reward and thereby strengthen desired behaviour – is recognised as a refinement of laboratory animal husbandry and is recommended by the UK Home Office and professional bodies (Prescott et al. 2007; and see e.g. Home Office 1989, Medical Research Council 2004). A refinement of standard operating procedures has the potential benefit of reducing stress and discomfort for the animals involved, but it may also benefit the researchers by providing better results in shorter time frames. However, PRT techniques still remain to be adopted throughout the laboratory landscape, mostly because there is a lack of staff and a lack of time to implement PRT in daily routines (Prescott et al. 2007). Especially during early stages of training the traditional approach to PRT is very time consuming, as animals need to be familiarised with technicians and learn to associate performing an action – such as touching an object – with receiving a reward. Automated positive reinforcement training (aPRT) can alleviate

time burdens on research and technical staff by allowing non-human primates (NHPs) to train unsupervised and in a self-paced manner. Furthermore, precise timing of the reward is important in a PRT paradigm, to clearly mark the desired behaviour and not inadvertently strengthen undesired behaviours. Here, an automated setup has additional benefits over human trainers, as aPRT systems can be programmed to deliver rewards always at exactly the right time and they do not get distracted by e.g. other NHPs' behaviours. APRT paradigms have been employed in rodents (e.g. Meier et al. 1998, Schaefers et al. 2011), and commercial systems allowing identification, training, and testing of animals in the home cage are available (HM-2, MBRose ApS, Faaborg, Denmark; IntelliCage, TSE Systems Inc, Chesterfield, MO, USA). Several groups have started to use aPRT with NHPs in the laboratory (e.g. Mitz et al. 2001, Wilson et al. 2005), and at least one group has implemented automated identification of animals during training (Fagot et al. 2009, 2010).

So far, however, automated training has not been taken to the breeding facilities. Employing aPRT has several potential benefits: Individual differences in docility may only become apparent once NHPs have been acquired from a breeding facility and trained for a period of time. Behavioural training of NHPs is a lengthy and labour-intensive process, especially considering how abstract some tasks in behavioural neuroscience experiments are. In extreme cases, a monkey may not respond to training attempts at all, in which case it either has to be transferred to a different project or returned to the breeding facility, if at all possible. If NHPs could undergo aPRT at the breeding facility they would be familiar with a task-reward paradigm when coming to a laboratory. Through this the time of initial training in the laboratory can be shortened and the suitability of an NHP for a given task can be established earlier. Furthermore, it should be feasible to predict a monkey's suitability for cognitive training by its performance on a similar task introduced early in life. Introducing aPRT early in life might also have the benefit of being a transferable skill: trained behaviour could be used in husbandry routine, such as moving the animals between cages or for presenting for blood, saliva, or stool sampling. Finally, introducing aPRT to breeding facilities and labs could be seen as enrichment to the animals' environment.

A.2 Design and Implementation

A.2.1 System Design

Our aPRT device – aPRTD – consists of four functional units (fig. A.1). A central Control Unit is responsible for logging all events onto an SD memory card, controlling all aspects of the task, and interacting with the technician. The RFID unit registers approaching NHPs

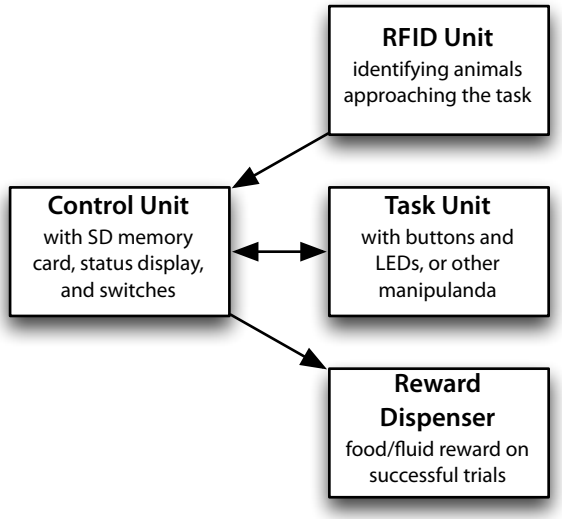

Figure A.1: Functional units of the Automated Feeder device.

and transmits its identity code to the Control Unit. The Task Unit contains manipulanda such as buttons and signalling devices such as LEDs. Finally, a reward is released through the Reward Dispenser upon successful completion of a trial. Design of our aPRT device has reached its third generation. The first generation of the device (fig. A.2) delivered solid

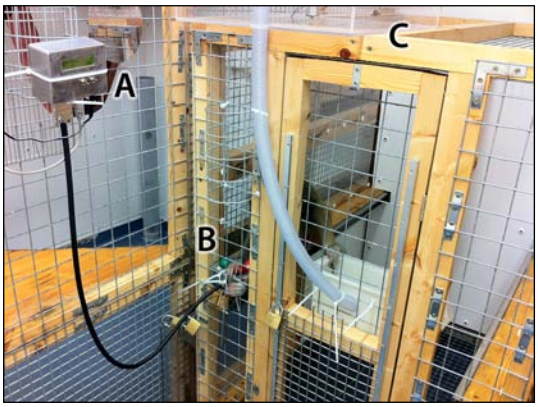

Figure A.2: First generation of Automated Feeder installed in a home cage and in use by a monkey. Control Unit *A* is fixed to an unused cage wall. A monkey interacts with the Task Unit *B*. The reward dispenser *B* is fixed out of the monkeys' reach and a tube guides released food items into a collection box.

food rewards (pellets, raisins, peanuts) by means of a rotating compartmented wheel and did not have an RFID unit fitted. Because the food capacity of such a wheel is necessarily small – our prototype had 81 compartments – the device cannot be used unsupervised for

a longer period considering that animals tend to use the device often at maximum speed (1–2 trials per 5 s). Hoppers such as used by Mitz et al. (2001) rely on the reward items to be dry and standardised in shape, such as food pellets. Similar pellets are part of most NHPs' normal diet and thus are not highly desirable and not well suited to motivate NHPs in training. Therefore, we decided to change the reward to fruit juice in the second generation. In addition to holding enough liquid (1 l) for 1000–2000 trials, the aPRTD now does not interfere with food rewards normally used in our animal training. This device was both used at Comparative Biology Centre (CBC) and Centre for Macaques (CfM).

For the third generation, a collaboration with MBRose ApS (Faaborg, Denmark), led to the development of an RFID reader gate which registers monkeys when they enter a compartment of the cage containing the aPRTD (fig. A.3). The currently used prototype setup

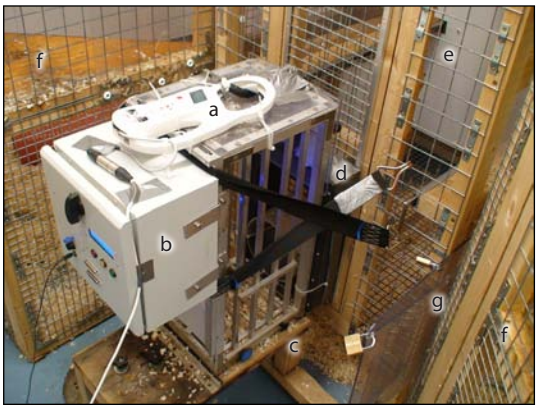

Figure A.3: Third generation of Automated Feeder installed in a home cage at CBC. RFID reader *(a)* and control box *(b)* are mounted to a mobile training cage platform *(c)*. The training cage is accessible for monkeys through a gate equipped with an RFID antenna *(d)* from a separation cage *(e)*. Access to the aPRTD can be given to groups of monkeys housed in home cages *(f)* through gates *(g)*.

is capable of operating autonomously, requiring only filling up of juice tank (usually at the end of the day).

A.2.2 Electronic Design and Software

Both electronic hardware and software were developed by the author of this thesis. Core of the Control Unit's hardware is a microcontroller (ATMega644P, Atmel Corp., San Jose, CA, USA). Peripherals include an SD card, real time clock, USB serial port for data export to computers, LEDs and buttons, a motor driver to control the liquid pump, an audio amplifier to play reward tones, and an LCD to display status information and facilitate setup.

The software was written in C/C++, using libraries provided by the Arduino[1] project. Basic operation includes monitoring buttons for presses, keeping track of the current task, logging events, playing tones, delivering rewards, updating the display, and providing a simple control interface (see fig. A.4).

A.2.3 RFID Tags

Of the four monkeys used for aPRTD training with RFID detection, only one had been tagged at the breeding facility at young age, with an RFID chip made by AVID (Norco, CA, USA). The other three monkeys were implanted with RFID tags acquired from Datamars (Bedano, Switzerland) and adhering to ISO standards for RFID of animals. Slightly different protocols mean that different reading sensitivities and accuracies might be expected.

A.2.4 Animal Training

Details about animals that underwent aPRT are listed in table B.3 on page 112. As a pilot experiment, monkeys Rp and Ri were given access to a two-button version of the task without RFID over a period of two weeks.

Monkeys Si, Sk, Te, and Un then had irregular access to a three-button model at the breeding facility. After transfer to our facilities and a brief acclimatisation period, they were given access to the task (now as a four-button version) regularly. Monkeys were implanted with RFID tags after four weeks and were subsequently identifiable when accessing the aPRTD.

During all times, monkeys received water *ad libitum*. Their regular diet consisted of pellets (MP3, Special Diets Services, Witham, Essex, UK), approximately 150 g per monkey and day. Forage mix (Lillico Forage Mix, Lillico Biotechnology, Hookwood, Surrey, UK) was additionally given on weekends and after sedations, ~125 g per monkey and day. In addition to unsupervised training on the aPRTD, monkeys Si, Sk, Te, and Un also underwent PRT using carabiners assigned to individual monkeys. Rewards for this kind of training consisted of pieces of fruit, nuts, raisins, thus not directly interfering with the fruit juice rewards dispensed by the aPRTD. Training times (mornings or afternoons) were varied between animal groups and days in order to minimise influence of time of feeding or other daily activities on task performance.

[1] The Arduino is a microcontroller platform based on Atmel's ATMega line; cf. `http://arduino.cc/`.

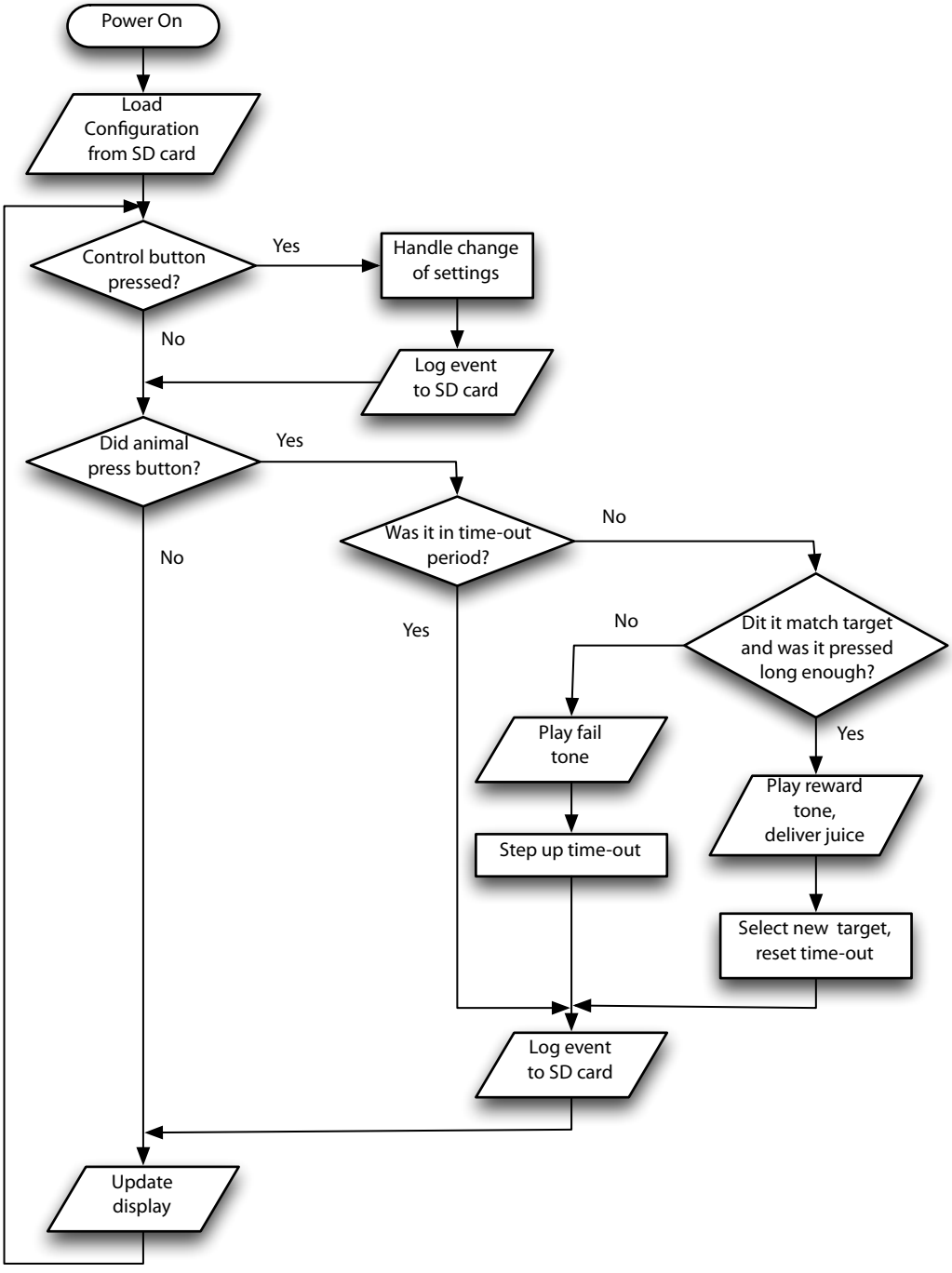

Figure A.4: Automated Feeder software flow chart.

Figure A.5: RFID tag as used to mark our animals. A hypodermic needle used to implant the tag is shown at *right*.

A.3 Preliminary Results

A.3.1 First Prototype

Data was collected from two sets of monkeys over several months both at CfM and at the CBC. A first dataset was collected over a period of 15 days using the initial prototype at CBC. Monkeys Rp and Ri were given access to the feeder on 12 days. By the end of the training period, the monkeys were pressing the correct button every time (fig. A.6). Since no RFID

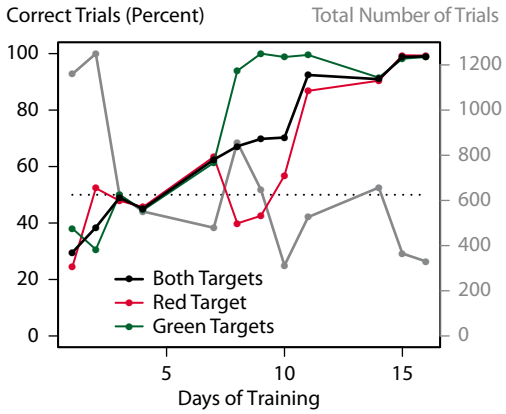

Figure A.6: Initial results of Automated Feeder training for monkeys Rp and Ri. Percentage of correct trials is shown as well as total number of button presses.

reader was available at the time, it could not be determined whether there were differences between monkeys regarding learning rate or trial numbers.

A.3.2 Second Prototype

A second group of animals (Si, Sk, Te, Un) was exposed to the second prototype, having three buttons and delivering juice rewards, at CfM. During this time, the monkeys presumably learned to discriminate between indicated target buttons well. Unfortunately, because of hardware and record-keeping issues, it could not be fully established how often these animals had access to the aPRTD during the five-month period and how individual performance developed.

A.3.3 Third Prototype

A short movie showing the aPRTD in operation is included as supplementary movie.

Learning After monkeys Si, Sk, Te, Un had been transferred from CfM to CBC, they had regular access to the third prototype of the aPRTD as shown in fig. A.3, initially without RFID, as all but one animal had not been implanted with RFID tags at the breeding facility. For more than 3 months we have been collecting data with identification (fig. A.7). Initially, monkeys performed the same task as they had been before at CfM: They were required to press the button indicated by a lit LED. After the animals were deemed competent in this task, a hold time for the button was introduced and gradually increased from 100 ms up to currently 1100 ms. While all animals learned to perform the task well initially, differences in percentages of correct trials and absolute number of button presses became apparent soon. Approximately 2 weeks after she was implanted with an RFID tag, monkey Sk started to perform fewer and fewer trials, and her rate of correct trials was lower than that of other animals as well.

Several events in the animals' environment could be seen to have had an effect on task performance. First, sedations necessary in order to implant monkeys with RFID tags[1] decreased accuracy in the task for all animals. Furthermore, noisy building work from the second half of July onwards also correlated with decreased total number of button presses for all monkeys.

Automated Animal Identification How reliably were animals detected by the RFID tag reader? Design of the RFID protocol which uses check-sums for error checking implies that mis-detection of an RFID tag can be practically excluded. However, due to reading errors, an animal passing the reading gate might not be identified at all.

[1] Monkey Si was implanted on 1 June 2012, monkeys Sk and Un on 11 June 2012.

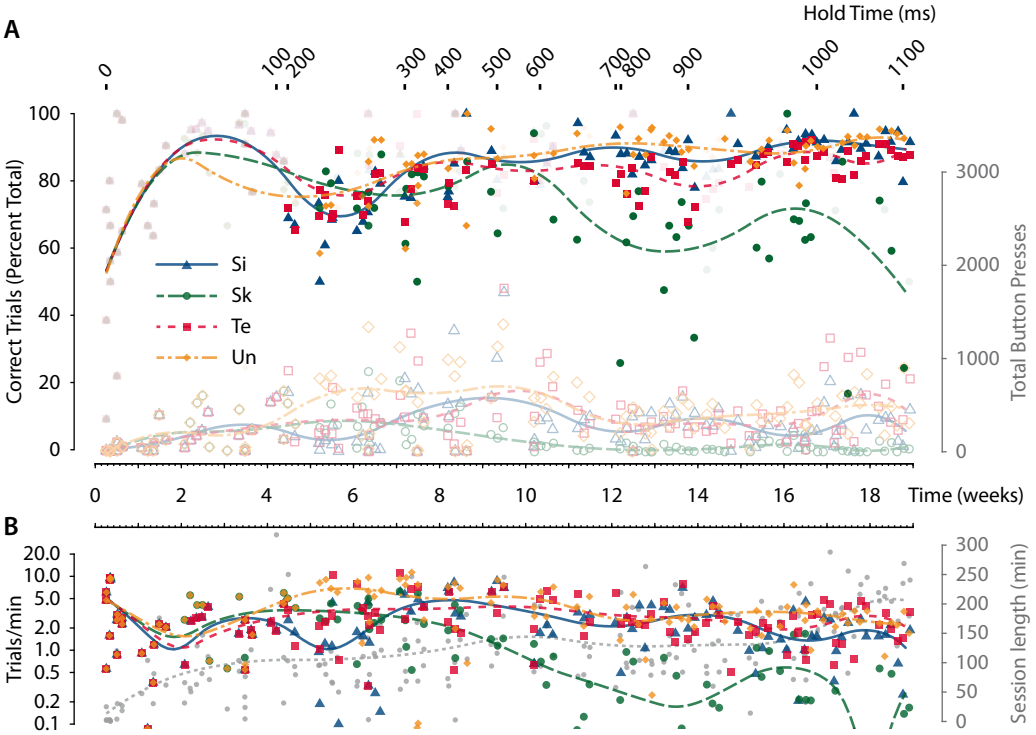

Figure A.7: Automated Feeder training with two pairs of monkeys (Si/Tk and Sk/Un). *(A)* Percentage of correct trials (pressed targeted button out of four possible, with hold time as indicated at *top*) for individual monkeys since start of training. Light lines and open symbols show total number of button presses (right axis). Light full symbols show data inferred from previous sessions when no RFID data were available. *(B)* Development of trial rates per monkey, plotted against a logarithmic scale. Grey dotted line and grey dots: session duration in minutes (right axis). Lines are splines fit with data points every two weeks.

In initial tests, we compared video recordings of animals interacting with the aPRTD with log files of the RFID reader. Recognition rate was estimated at approximately 60 %, with no difference between animals. After some experimentation with gate aperture and position of the breaking light beam triggering RFID acquisition, recognition rates are now at ~80 %.

A.4 Discussion

A.4.1 Learning

The inquisitive and explorative nature of most macaque monkeys means that they will learn to perform simple tasks such as pushing buttons without any instruction. More complicated tasks such as pushing a button indicated by an LED and keeping the button pressed for a certain hold time can be learnt as well by gradually increasing difficulty. These results are similar to those reported by Fagot et al. (2009) and Fagot et al. (2010). At this point no attempt was made to adjust task difficulty according to the individuals' learning progress in our system, however, this is planned for future iterations of our aPRTD.

Previous research has shown that temperament of monkeys correlates with success in task learning (Coleman et al. 2005). It became apparent in our training programme that individual monkeys show differences in trial rates and percentage of correct trials. At this point, animals which underwent long-term PRT have not yet been trained on the tasks required for the electrophysiological experiments they are assigned to. However, our hypothesis is that monkeys who were successful in this button-press task will acquire new tasks more easily than other monkeys. Furthermore, we hypothesise that monkeys who, despite being given food and drink *ad libitum,* choose to use the aPRTD more than other monkeys will also be more motivated during electrophysiological experiments and perform more trials.

A.4.2 Detection Accuracy

Individual monkeys were correctly detected at times of passing through the gate in approximately 8 of 10 cases. This of course leaves trials assigned to other animals than the ones who actually performed them. However, given the large amount of data collected over time, both in terms of passages through the gate and in trials performed, we expect the results to be accurate enough to allow inferences about an animal's state of learning and suitability for the task. An important caveat here are systematic differences in detection errors between animals, which could skew the results. For example, an animal whose RFID tag is only rarely detected at all could be found to be an animal not liking to work. If that same animal

is also an exceptionally good learner, performing better than its cagemates, this might make the other monkeys appear to be better learners than they are. Systematic differences can arise from different sources, e.g. the kind of RFID tag used, the orientation of the tag under the skin, or the particular way animals choose to pass the gate (slower moving animals give the RFID reader more time to read the tag). It is therefore important that identification performance is confirmed by independent means such as video recordings at certain time intervals.

A.4.3 Perspective

Further plans for this project include deploying of RFID-equipped aPRTDs to the breeding facility, and long-term monitoring of task performance of animals subject to aPRT. We already observe differences between individual monkeys regarding response to automated training in data collected over only a few months. If these differences are valid predictors for performance during actual electrophysiological experiments, early selection of monkeys suitable for behavioural neuroscience experiments is mandated, in order to maximise the quality of scientific results, minimise numbers of animals needed for experiments, and minimise project duration from training to published results.

B Overview of Animals Used for this PhD Project

All experiments were approved by the local ethics committee at Newcastle University and procedures followed the UK Animals (Scientific Procedures) Act 1986. Several macaque monkeys were used for this project. This appendix lists monkeys used for experiments described in chapters 2 to 5 and appendix A. Experiments described in chapters 2 and 3 were

Name	Experiment	Species	Age (y)	Gender	Weight (kg)
C	*Int*	MFa	12	f	2.9
R	*Int*	MFu	n/a	m	5.5
Am	*1Ch*	MMu	14.8	f	10.6
Ha	*1Ch*	MMu	13.9	f	9.3
Ma	*1Ch*	MMu	6.8	f	6.1
O	*1Ch*	MMu	15.5	f	9.2
Sa	*1Ch*, *Int*	MMu	14.6	f	10.8
Th	*1Ch*, *Int*	MMu	14.8	f	9.5
Ti	*Int*, *FMA*	MMu	6.4	f	5.6
X	*Int*, *FMA*	MMu	10.2	f	11

Table B.1: Monkeys used for acute experiments described in chapter 2 *(1Ch)*, chapter 3 *(Int)* and chapter 4 *(FMA)*. Species: MFa: *Macaca fascicularis*, crab-eating macaque; MFu: *Macaca fuscata*, Japanese macaque; MMu: *Macaca mulatta*, rhesus macaque. N/a – not available.

conducted on animals that had either retired from other research projects, or they were acquired from a breeding facility as they had reached their end of reproductive life in the breeding colony (see table B.1).

For the chronic experiments described in chapters 4 and 5, monkeys were partially shared (table B.2). The first FMA implant was performed on a monkey unresponsive to behavioural training (Ra). Monkey Ar had been trained on a different task previously and then received a spinal implant. Monkey Rv was assigned to experiments described in chapter 5.

Finally, the animals that underwent aPRT as described in appendix A were assigned to different projects and aPRT was part of their preparatory training (see table B.3).

Name	Experiment	Species	Age (y)	Gender	Weight (kg)
B	*ISMS*	MMu	4.3	f	6.4
Ra	*FMA*	MMu	3.6	f	5.4
Ar	*FMA*	MMu	7	f	10.6
Rv	*FMA & ISMS*	MMu	3.5	f	4.2
Rp	*FMA*	MMu	5.2	f	4.9

Table B.2: Monkeys used for chronic experiments. *ISMS* refers to experiments described in chapter 5, *FMA* designates monkeys who received an FMA implant as described in chapter 4. Ages and weights at time of spinal implant.

Name	Species	Age (y)	Gender	Weight (kg)
Ri	MMu	3.8	f	5.3
Rp	MMu	3.8	f	5.5
Si	MMu	3.8	f	5.4
Sk	MMu	3.8	f	5.8
Te	MMu	3.3	f	5
Un	MMu	2.3	f	3.4

Table B.3: Animals exposed to aPRT described in appendix A. Age and weight refer to the time when the animals were first exposed to the aPRTD device. N/a – not available.

C Description of Algorithm and its Implementation used for Online Closed Loop Stimulation

The closed loop experiment (chapter 5) was controlled by two computers. One recorded all neural signals, the other one controlled the task and spinal cord stimulation. The task computer received its input (lever position, spike times indicated by digital pulses) through a National Instruments data acquisition card. In order to achieve near-real time performance, it was decided to programme the task and stimulation control in LabView (National Instruments), a visual programming environment.

The programme had to perform three tasks:

1. control the behavioural part of the experiment (cf. fig. C.1)
2. record neural activity and estimate a desired muscle activity or force (cf. fig. C.2)
3. use this estimate to deliver stimulus pulses in order to match the estimate (cf. fig. C.3).

The LabView programme has reached a complexity that makes it impractical to be reproduced here in total. On the other hand, the graphical structure of LabView does not lend itself to easy conversion to a textual representation. Instead, we give simplified flow diagrams for the three tasks here. A complete representation of the LabView programme is part of the accompanying CD.

C.1 Spike Rate Estimation

A fast and easy to implement method to estimate the firing rate of a single neuron was desired. Cunningham et al. (2009) tested implementations of various algorithms, including kernel smoothing and probabilistic methods. The choice of algorithm had little influence on the correlation of a reach movement with predicted movements decoded from estimated firing rates. For this reason, we chose to implement a box-car kernel smoothing algorithm

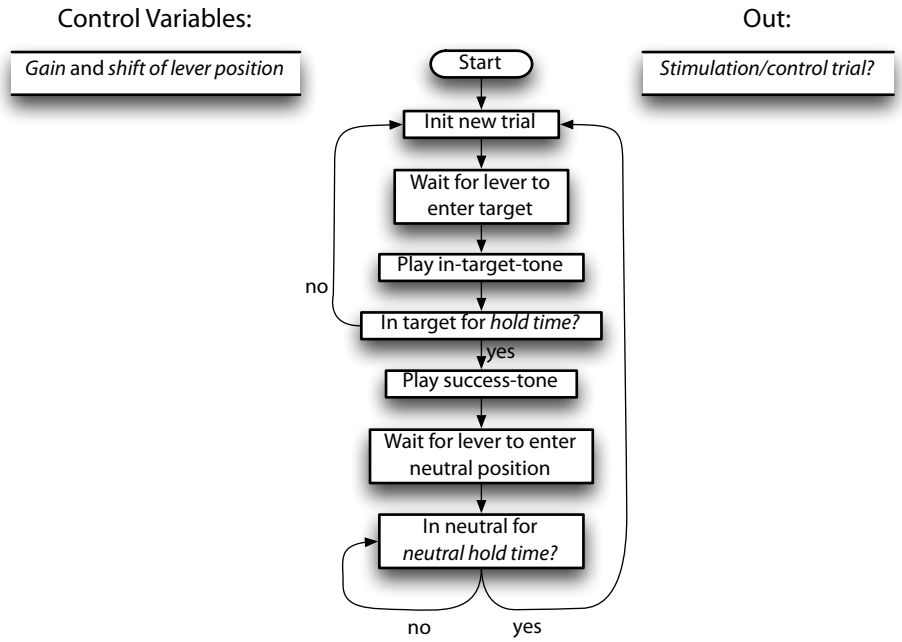

Figure C.1: Simplified flow diagram for control of behavioural task.

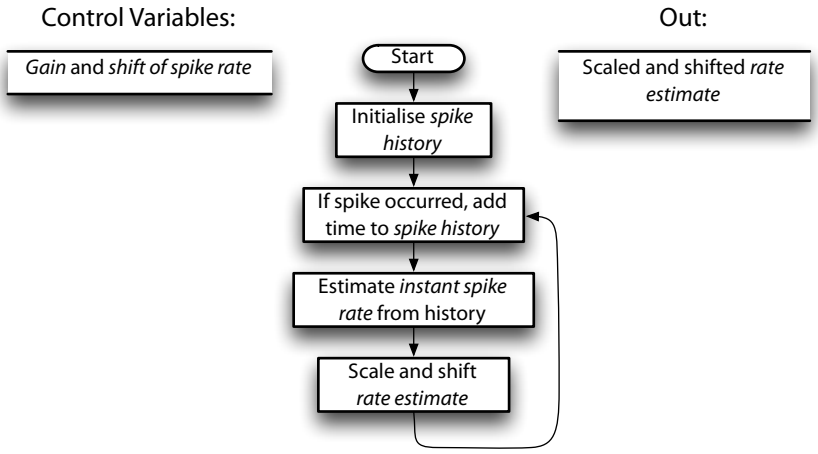

Figure C.2: Simplified flow diagram for estimation of neural firing rate and its transformation.

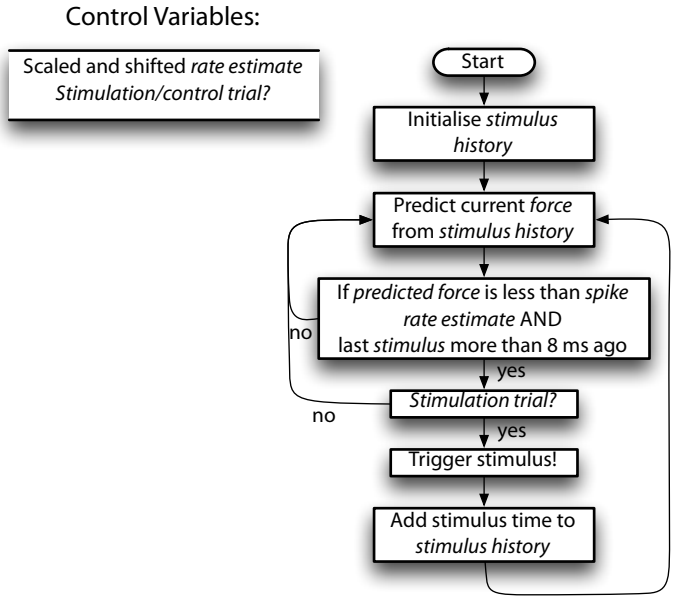

Figure C.3: Simplified flow diagram for control of ISMS.

(Nawrot et al. 1999). The width of the kernel T_w was chosen to be $T_w = 0.5\,\mathrm{s}$, and additional smoothing for the transition from high to low firing rates was added to determine the instantaneous firing rate $r(t)$:

$$r(t) = \begin{cases} \frac{N_w(t)}{T_w} & \text{if } T_w/N_w(t) > t - s_{N(t)} \\ \frac{1}{t - s_{N(t)}} & \text{else,} \end{cases} \tag{C.1}$$

where $s_{1,\ldots,N(t)}$ is the sequence of spikes up to time t, $N_w(t) = \#\{s_i | t - s_i < T_w\}$ is the number of spikes in the the window before t.

C.2 Generation of Stimulation Pulses

Many premotor neurons exhibit a modulation of activity before and during reaching and grasping movements. While this modulation often lasts as long as the movement, sometimes a shorter change in firing rate is observed (section 5.3.1). In the former case, a scaled and shifted firing rate estimate $\hat{r}(t)$ was used as a target function for muscle activation (section 2.2.4, fig. C.2):

$$\hat{r}(t) = a \cdot r(t - \delta) + b,$$

where δ is a delay. When the change of firing rate was not long enough for the desired stimulation, we triggered stimulus pulses at a given frequency and for a set duration when the instantaneous firing rate crossed a threshold.

We now describe the former method in more detail. The force f evoked by one stimulus pulse at time t is assumed to follow the response of a critically damped second order system (repeating eq. (2.1); Milner-Brown et al. 1973):

$$f(t) = \begin{cases} \frac{t}{\tau} \exp\left(1 - \frac{t}{\tau}\right) & t \geq 0 \\ 0 & \text{otherwise,} \end{cases}$$

where τ is the time of the maximum and here assumed to be 50 ms. Let $t_{1,\ldots,M(t)}$ be the sequence of times of stimuli delivered before t. Not considering the modulation of force responses by previous stimuli (see eq. 2.2), the force $F(t)$ at time t evoked by the stimulus train equals

$$F(t) = \sum_{i=1}^{M(t)} f(t - t_i).$$

If $F(t) < \hat{r}(t)$ and $t - t_{M(t)} \geq 8$ ms then a stimulus is delivered at this time. Both $f(t)$ and $F(t)$ are on an arbitrary scale; parameters a and b have to be chosen so that during resting conditions, $\hat{r}(t)$ is zero and thus no stimuli are delivered; equally, the stimulation rate should not saturate, either, which happens when $\hat{r}(t)$ is too large.

Bibliography

Albala, David M. and Jeffrey H. Lawson (2006). 'Recent clinical and investigational applications of fibrin sealant in selected surgical specialties'. In: *Journal of the American College of Surgeons* 202.4, pp. 685–97 (cit. on p. 50).

Aoyagi, Yoichiro, Vivian K. Mushahwar, Richard B. Stein and Arthur Prochazka (2004). 'Movements elicited by electrical stimulation of muscles, nerves, intermediate spinal cord, and spinal roots in anesthetized and decerebrate cats'. In: *IEEE Transactions on Neural Systems and Rehabilitation Engineering* 12.1, pp. 1–11 (cit. on pp. 7, 21).

Baker, Stuart N. and Roger N. Lemon (1995). 'Non-linear summation of responses in averages of rectified EMG'. In: *Journal of Neuroscience Methods* 59.2, pp. 175–81 (cit. on p. 25).

Baker, Stuart N., E. Olivier and Roger N. Lemon (1998). 'An investigation of the intrinsic circuitry of the motor cortex of the monkey using intra-cortical microstimulation'. In: *Experimental Brain Research* 123.4, pp. 397–411 (cit. on pp. 22, 25, 42).

Bamford, Jeremy A., C. T. Putman and Vivian K. Mushahwar (2005). 'Intraspinal microstimulation preferentially recruits fatigue-resistant muscle fibres and generates gradual force in rat'. In: *The Journal of Physiology* 569.3, pp. 873–84 (cit. on pp. 8, 12, 21).

Bamford, Jeremy A., Kathryn G. Todd and Vivian K. Mushahwar (2010). 'The effects of intraspinal microstimulation on spinal cord tissue in the rat'. In: *Biomaterials* 31.21, pp. 5552–63 (cit. on pp. 59, 62).

Barbeau, Hugues, David A. McCrea, Michael J. O'Donovan, Serge Rossignol, Warren M. Grill and Michel A. Lemay (1999). 'Tapping into spinal circuits to restore motor function'. In: *Brain Research Reviews* 30.1, pp. 27–51 (cit. on pp. 6, 7).

Barthélemy, Dorothy, Hugues Leblond, Janyne Provencher and Serge Rossignol (2006). 'Nonlocomotor and locomotor hindlimb responses evoked by electrical microstimulation of the lumbar cord in spinalized cats'. In: *Journal of Neurophysiology* 96.6, pp. 3273–92 (cit. on p. 8).

Birbaumer, Niels, N. Ghanayim, T. Hinterberger, I. Iversen, B. Kotchoubey, A. Kübler, J. Perelmouter, E. Taub and H. Flor (1999). 'A spelling device for the paralysed'. In: *Nature* 398.6725, pp. 297–298 (cit. on p. 5).

Bizzi, Emilio, Ferdinando A. Mussa-Ivaldi and Simon F. Giszter (1991). 'Computations underlying the execution of movement: a biological perspective'. In: *Science* 253.5017, pp. 287–91 (cit. on pp. 7, 40, 41).

Bizzi, Emilio, Simon F. Giszter, Eric P. Loeb, Ferdinando A. Mussa-Ivaldi and Philippe Saltiel (1995). 'Modular organization of motor behavior in the frog's spinal cord'. In: *Trends in Neurosciences* 18.10, pp. 442–446 (cit. on pp. 8, 11).

Bizzi, Emilio, Matthew C. Tresch, Philippe Saltiel and Andrea d'Avella (2000). 'New perspectives on spinal motor systems'. In: *Nature Reviews Neuroscience* 1.2, pp. 101–8 (cit. on p. 8).

Bizzi, Emilio, Vincent C. K. Cheung, Andrea d'Avella, Philippe Saltiel and Matthew C. Tresch (2008). 'Combining modules for movement'. In: *Brain Research Reviews* 57.1, pp. 125–33 (cit. on pp. 8, 41).

Boulenguez, Pascale and Laurent Vinay (2009). 'Strategies to restore motor functions after spinal cord injury'. In: *Current Opinion in Neurobiology* 19.6, pp. 587–600 (cit. on p. 6).

Branner, Almut, Richard B. Stein and Richard A. Normann (2001). 'Selective stimulation of cat sciatic nerve using an array of varying-length microelectrodes'. In: *Journal of Neurophysiology* 85.4, pp. 1585–94 (cit. on p. 45).

Caan, A. W. and J. F. Stein (1976). 'The effect of cooling the motor cortex of a rhesus monkey upon visually controlled movement and associated motor potentials [proceedings]'. In: *The Journal of Physiology* 263.1, 142P–144P (cit. on p. 62).

Carmena, Jose M., Mikhail A. Lebedev, Roy E. Crist, Joseph E. O'Doherty, David M. Santucci, Dragan F. Dimitrov, Parag G. Patil, Craig S. Henriquez and Miguel A. L. Nicolelis (2003). 'Learning to control a brain-machine interface for reaching and grasping by primates'. In: *PLoS Biology* 1.2, E42 (cit. on p. 98).

Chapin, John K. and Karen A. Moxon, eds. (2000). *Neural prostheses for restoration of sensory and motor function*. Methods and New Frontiers in Neuroscience. Boca Raton: CRC Press.

Coleman, Kristine, Leigh Ann Tully and Jennifer L. McMillan (2005). 'Temperament correlates with training success in adult rhesus macaques'. In: *Am J Primatol* 65.1, pp. 63–71 (cit. on p. 109).

Compton, Aaron K., Binit Shah and Salim M. Hayek (2012). 'Spinal cord stimulation: a review'. In: *Current Pain and Headache Reports* 16.1, pp. 35–42 (cit. on pp. 9, 96).

Courtine, Grégoire, Mary Bartlett Bunge, James W. Fawcett, Robert G. Grossman, Jon H. Kaas, Roger N. Lemon, Irin Maier, John Martin, Randolph J. Nudo, Almudena Ramon-Cueto, Eric M. Rouiller, Lisa Schnell, Martin E. Schwab and Thierry Wannier (2007).

'Can experiments in nonhuman primates expedite the translation of treatments for spinal cord injury in humans?' In: *Nature Medicine* 13.5, pp. 561–566 (cit. on p. 62).

Cunningham, John P., Vikash Gilja, Stephen I. Ryu and Krishna V. Shenoy (2009). 'Methods for estimating neural firing rates, and their application to brain-machine interfaces'. In: *Neural Networks* 22.9, pp. 1235–46 (cit. on p. 113).

Davare, Marco, Alexander Kraskov, John C. Rothwell and Roger N. Lemon (2011). 'Interactions between areas of the cortical grasping network'. In: *Current Opinion in Neurobiology* 21.4, pp. 565–70 (cit. on p. 5).

d'Avella, Andrea, Philippe Saltiel and Emilio Bizzi (2003). 'Combinations of muscle synergies in the construction of a natural motor behavior'. In: *Nature Neuroscience* 6.3, pp. 300–8 (cit. on p. 8).

Decker, M. J., Lisa Griffin, L. D. Abraham and L. Brandt (2010). 'Alternating stimulation of synergistic muscles during functional electrical stimulation cycling improves endurance in persons with spinal cord injury'. In: *Journal of Electromyography and Kinesiology* 20.6, pp. 1163–9 (cit. on p. 7).

Diester, Ilka, Matthew T. Kaufman, Murtaza Mogri, Ramin Pashaie, Werapong Goo, Ofer Yizhar, Charu Ramakrishnan, Karl Deisseroth and Krishna V. Shenoy (2011). 'An optogenetic toolbox designed for primates'. In: *Nature Neuroscience* 14.3, pp. 387–97 (cit. on pp. 60, 99).

Dimitrijevic, Milan R., Yury P. Gerasimenko and M. M. Pinter (1998). 'Evidence for a spinal central pattern generator in humans'. In: *Annals of the New York Academy of Sciences* 860, pp. 360–76 (cit. on p. 9).

Dobelle, William H. (2000). 'Artificial vision for the blind by connecting a television camera to the visual cortex'. In: *ASAIO J* 46.1, pp. 3–9 (cit. on p. 96).

Dum, Richard P. and Peter L. Strick (1991). 'The origin of corticospinal projections from the premotor areas in the frontal lobe'. In: *Journal of Neuroscience* 11.3, pp. 667–89 (cit. on p. 2).

— (2002). 'Motor areas in the frontal lobe of the primate'. In: *Physiology & Behavior* 77.4–5, pp. 677–82 (cit. on p. 2).

— (2005). 'Motor Areas in the Frontal Lobe: The Anatomical Substrate for the Central Control of Movement'. In: Riehle, Alexa and Eilon Vaadia. *Motor cortex in voluntary movements: a distributed system for distributed functions*. Frontiers in neuroscience. Boca Raton: CRC Press. Chap. 1, pp. 2–50 (cit. on p. 2).

Eken, T., H. Hultborn and O. Kiehn (1989). 'Possible functions of transmitter-controlled plateau potentials in alpha motoneurones'. In: *Progress in Brain Research* 80, pp. 257–67 (cit. on p. 20).

Epstein, Lawrence J. and Marco Palmieri (2012). 'Managing chronic pain with spinal cord stimulation'. In: *Mount Sinai Journal of Medicine* 79.1, pp. 123–32 (cit. on pp. 9, 96).

Ethier, Christian, Laurent Brizzi, Warren G. Darling and Charles Capaday (2006). 'Linear summation of cat motor cortex outputs'. In: *Journal of Neuroscience* 26.20, pp. 5574–81 (cit. on p. 22).

Ethier, Christian, Emily R. Oby, M. J. Bauman and Lee E. Miller (2012). 'Restoration of grasp following paralysis through brain-controlled stimulation of muscles'. In: *Nature* 485, pp. 368–371 (cit. on pp. 1, 6, 62).

Evarts, Edward V. (1968). 'Relation of pyramidal tract activity to force exerted during voluntary movement'. In: *Journal of Neurophysiology* 31.1, pp. 14–27 (cit. on pp. 3, 4).

Everaert, Dirk G., Aiko K. Thompson, Su Ling Chong and Richard B. Stein (2010). 'Does functional electrical stimulation for foot drop strengthen corticospinal connections?' In: *Neurorehabilitation and Neural Repair* 24.2, pp. 168–77 (cit. on p. 91).

Fagot, Joël and Dany Paleressompoulle (2009). 'Automatic testing of cognitive performance in baboons maintained in social groups'. In: *Behavior Research Methods* 41.2, pp. 396–404 (cit. on pp. 101, 109).

Fagot, Joël and Elodie Bonté (2010). 'Automated testing of cognitive performance in monkeys: use of a battery of computerized test systems by a troop of semi-free-ranging baboons (Papio papio)'. In: *Behavior Research Methods* 42.2, pp. 507–16 (cit. on pp. 101, 109).

Ferrier, David (1874). 'Experiments on the Brain of Monkeys.–No. I'. In: *Proceedings of the Royal Society London* 23, pp. 409–430 (cit. on p. 3).

Fetz, Eberhard E. (1969). 'Operant conditioning of cortical unit activity'. In: *Science* 163.3870, pp. 955–8 (cit. on pp. 6, 98).

Fetz, Eberhard E., Paul D. Cheney and D. C. German (1976). 'Corticomotoneuronal connections of precentral cells detected by postspike averages of EMG activity in behaving monkeys'. In: *Brain Research* 114.3, pp. 505–10 (cit. on p. 3).

Fetz, Eberhard E. and Bengt Gustafsson (1983). 'Relation between shapes of post-synaptic potentials and changes in firing probability of cat motoneurones'. In: *The Journal of Physiology* 341, pp. 387–410 (cit. on p. 29).

Fisher, Nicholas I., Toby Lewis and Brian J. J. Embleton (1987). *Statistical analysis of spherical data*. Cambridge: Cambridge University Press (cit. on p. 27).

Fluet, Marie-Christine, Markus A. Baumann and Hansjörg Scherberger (2010). 'Context-specific grasp movement representation in macaque ventral premotor cortex'. In: *Journal of Neuroscience* 30.45, pp. 15175–84 (cit. on p. 4).

Fritsch, Gustav and Eduard Hitzig (1870). 'Ueber die elektrische Erregbarkeit des Grosshirns'. German. In: *Archiv für Anatomie, Physiologie, und Wissenschaftliche Medicin* 37, pp. 300–332 (cit. on p. 3).

Galea, Mary P. and Ian Darian-Smith (1997). 'Manual dexterity and corticospinal connectivity following unilateral section of the cervical spinal cord in the macaque monkey'. In: *The Journal of Comparative Neurology* 381.3, pp. 307–19 (cit. on p. 62).

Gallese, Vittorio, Luciano Fadiga, Leonardo Fogassi and Giacomo Rizzolatti (1996). 'Action recognition in the premotor cortex'. In: *Brain* 119.2, pp. 593–609 (cit. on p. 4).

Ganguly, Karunesh and Jose M. Carmena (2009). 'Emergence of a stable cortical map for neuroprosthetic control'. In: *PLoS Biology* 7.7, e1000153 (cit. on pp. 91, 94).

Ganguly, Karunesh, Dragan F. Dimitrov, Jonathan D. Wallis and Jose M. Carmena (2011). 'Reversible large-scale modification of cortical networks during neuroprosthetic control'. In: *Nature Neuroscience* 14.5, pp. 662–7 (cit. on p. 91).

Gaunt, R. A., Arthur Prochazka, Vivian K. Mushahwar, Lisa Guevremont and P. H. Ellaway (2006). 'Intraspinal microstimulation excites multisegmental sensory afferents at lower stimulus levels than local alpha-motoneuron responses'. In: *Journal of Neurophysiology* 96.6, pp. 2995–3005 (cit. on pp. 21, 40, 98).

Georgopoulos, Apostolos P., John F. Kalaska, Roberto Caminiti and Joe T. Massey (1982). 'On the relations between the direction of two-dimensional arm movements and cell discharge in primate motor cortex'. In: *Journal of Neuroscience* 2.11, pp. 1527–37 (cit. on p. 3).

Georgopoulos, Apostolos P., Roberto Caminiti, John F. Kalaska and Joe T. Massey (1983). 'Spatial coding of movement: A hypothesis concerning the coding of movement direction by motor cortical populations'. In: *Neural Coding of Motor Performance*. Ed. by J. Massion, J. Paillard, W. Schultz and M. Wiesendanger. Vol. 7. Experimental Brain Research Supplements. Springer, pp. 327–336 (cit. on p. 3).

Georgopoulos, Apostolos P., Andrew B. Schwartz and Ronald E. Kettner (1986). 'Neuronal population coding of movement direction'. In: *Science* 233.4771, pp. 1416–9 (cit. on p. 3).

Georgopoulos, Apostolos P., Ronald E. Kettner and Andrew B. Schwartz (1988). 'Primate motor cortex and free arm movements to visual targets in three-dimensional space. II. Coding of the direction of movement by a neuronal population'. In: *Journal of Neuroscience* 8.8, pp. 2928–37 (cit. on p. 3).

Giszter, Simon F., Ferdinando A. Mussa-Ivaldi and Emilio Bizzi (1993). 'Convergent force fields organized in the frog's spinal cord'. In: *Journal of Neuroscience* 13.2, 467–91 (cit. on p. 7).

Giszter, Simon F., Warren M. Grill, Michel A. Lemay, Vivian K. Mushahwar and Arthur Prochazka (2000a). 'Intraspinal microstimulation: Techniques, perspectives and prospects for FES'. In: *Neural prostheses for restoration of sensory and motor function*. Ed. by John K. Chapin and Karen A. Moxon. Methods and New Frontiers in Neuroscience. Boca Raton: CRC Press. Chap. 4, pp. 101–138 (cit. on p. 7).

Giszter, Simon F., Eric Loeb, Ferdinando A. Mussa-Ivaldi and Emilio Bizzi (2000b). 'Repeatable spatial maps of a few force and joint torque patterns elicited by microstimulation applied throughout the lumbar spinal cord of the spinal frog'. In: *Human Movement Science* 19.4, pp. 597–626 (cit. on p. 11).

Giszter, Simon F. (2000). 'Spinal recruitment of primitives in frog and rat: Basic observations and implications for intraspinal FES'. In: *Neural prostheses for restoration of sensory and motor function*. Ed. by John K. Chapin and Karen A. Moxon. Methods and New Frontiers in Neuroscience. Boca Raton: CRC Press. Chap. 4.2, pp. 104–116 (cit. on p. 41).

— (2008). 'Spinal cord injury: present and future therapeutic devices and prostheses'. In: *Neurotherapeutics* 5.1, pp. 147–62 (cit. on p. 6).

Godschalk, Moshe, Roger N. Lemon, Henricus G. J. M. Kuypers and H. K. Ronday (1984). 'Cortical afferents and efferents of monkey postarcuate area: an anatomical and electrophysiological study'. In: *Experimental Brain Research* 56.3, pp. 410–24 (cit. on p. 5).

Grafton, Scott T. (2010). 'The cognitive neuroscience of prehension: recent developments'. In: *Experimental Brain Research* 204.4, pp. 475–91 (cit. on p. 3).

Grill, Warren M. (2000). 'Electrical activation of spinal neural circuits: application to motor-system neural prostheses'. In: *Neuromodulation: Technology at the Neural Interface* 3.2, pp. 97–106 (cit. on p. 7).

Grill, Warren M. and Michel A. Lemay (2002). 'Hindlimb motor responses evoked by dual-electrode intraspinal microstimulation in the cat'. In: *7th Annual Conference of the International Functional Electrical Stimulation Society*. International Functional Electrical Stimulation Society (cit. on pp. 8, 11, 41).

Grill, Warren M., Sharon E. Norman and Ravi V. Bellamkonda (2009). 'Implanted neural interfaces: biochallenges and engineered solutions'. In: *Annual Review of Biomedical Engineering* 11, pp. 1–24 (cit. on p. 6).

Grünbaum, Albert S. F. and Charles Scott Sherrington (1901). 'Observations on the Physiology of the Cerebral Cortex of Some of the Higher Apes. (Preliminary Communication.)' In: *Proceedings of the Royal Society London* 69.451-458, pp. 206–209 (cit. on pp. 2, 3).

Guevremont, Lisa, Costantino G. Renzi, Jonathan A. Norton, Jan Kowalczewski, Rajiv Saigal and Vivian K. Mushahwar (2006). 'Locomotor-related networks in the lumbosacral en-

largement of the adult spinal cat: activation through intraspinal microstimulation'. In: *IEEE Transactions on Neural Systems and Rehabilitation Engineering* 14.3, pp. 266–72 (cit. on pp. 8, 62).

Gustafsson, Bengt and Elżbieta Jankowska (1976). 'Direct and indirect activation of nerve cells by electrical pulses applied extracellularly'. In: *The Journal of Physiology* 258.1, pp. 33–61 (cit. on pp. 21, 40, 98).

Harkema, Susan, Yury Gerasimenko, Jonathan Hodes, Joel Burdick, Claudia Angeli, Yangsheng Chen, Christie Ferreira, Andrea Willhite, Enrico Rejc, Robert G. Grossman and V. Reggie Edgerton (2011). 'Effect of epidural stimulation of the lumbosacral spinal cord on voluntary movement, standing, and assisted stepping after motor complete paraplegia: A case study'. In: *Lancet* 377.9781, pp. 1938–1947 (cit. on p. 9).

He, San-Qiang, Richard P. Dum and Peter L. Strick (1993). 'Topographic organization of corticospinal projections from the frontal lobe: motor areas on the lateral surface of the hemisphere'. In: *Journal of Neuroscience* 13.3, pp. 952–80 (cit. on pp. 2, 5).

Histed, Mark H., Vincent Bonin and R. Clay Reid (2009). 'Direct activation of sparse, distributed populations of cortical neurons by electrical microstimulation'. In: *Neuron* 63.4, pp. 508–22 (cit. on p. 21).

Hochberg, Leigh R., Mijail D. Serruya, Gerhard M. Friehs, Jon A. Mukand, Maryam Saleh, Abraham H. Caplan, Almut Branner, David Chen, Richard D. Penn and John P. Donoghue (2006). 'Neuronal ensemble control of prosthetic devices by a human with tetraplegia'. In: *Nature* 442.7099, pp. 164–71 (cit. on pp. 96, 98).

Hochberg, Leigh R., Daniel Bacher, Beata Jarosiewicz, Nicolas Y. Masse, John D. Simeral, Joern Vogel, Sami Haddadin, Jie Liu, Sydney S. Cash, Patrick van der Smagt and John P. Donoghue (17th2012). 'Reach and grasp by people with tetraplegia using a neurally controlled robotic arm'. In: *Nature* 485.7398, pp. 372–375 (cit. on pp. 1, 5, 61, 91, 96, 98).

Home Office (1989). *Code of Practice for the Housing and Care of Animals Used in Scientific Procedures*. London: HMSO. URL: `http://www.official-documents.gov.uk/document/hc8889/hc01/0107/0107.pdf` (cit. on p. 100).

Imoto, Hirochika, Masami Fujii, Jouji Uchiyama, Hirosuke Fujisawa, Kimihiko Nakano, Ichiro Kunitsugu, Sadahiro Nomura, Takashi Saito and Michiyasu Suzuki (2006). 'Use of a Peltier chip with a newly devised local brain-cooling system for neocortical seizures in the rat. Technical note'. In: *Journal of Neurosurgery* 104.1, pp. 150–6 (cit. on p. 91).

Jabre, Joe F., James Rainville, Byron Salzsieder, Johannes Smuts and Janet Limke (1995). 'Correlates of motor unit size, recruitment threshold, and H-reflex jitter'. In: *Muscle & Nerve* 18.11, pp. 1300–5 (cit. on p. 29).

Jackson, Andrew, Jaideep Mavoori and Eberhard E. Fetz (2006a). 'Long-term motor cortex plasticity induced by an electronic neural implant'. In: *Nature* 444.7115, pp. 56–60 (cit. on p. 96).

Jackson, Andrew, Chet T. Moritz, Jaideep Mavoori, Timothy H. Lucas and Eberhard E. Fetz (2006b). 'The Neurochip BCI: towards a neural prosthesis for upper limb function'. In: *IEEE Transactions on Neural Systems and Rehabilitation Engineering* 14.2, pp. 187–90 (cit. on pp. 20, 91).

Jackson, Andrew and Eberhard E. Fetz (2007). 'Compact movable microwire array for long-term chronic unit recording in cerebral cortex of primates'. In: *Journal of Neurophysiology* 98.5, pp. 3109–18 (cit. on p. 66).

— (2011). 'Interfacing with the computational brain'. In: *IEEE Transactions on Neural Systems and Rehabilitation Engineering* 19.5, pp. 534–41 (cit. on p. 62).

Jackson, Andrew and Jonas B. Zimmermann (2012). 'Neural interfaces for the brain and spinal cord – restoring motor function'. In: *Nature Reviews Neurology* (cit. on pp. 6, 96).

Jeannerod, Marc, M. A. Arbib, Giacomo Rizzolatti and H. Sakata (1995). 'Grasping objects: the cortical mechanisms of visuomotor transformation'. In: *Trends in Neurosciences* 18.7, pp. 314–20 (cit. on p. 4).

Jenny, A. B. and J. Inukai (1983). 'Principles of motor organization of the monkey cervical spinal cord'. In: *Journal of Neuroscience* 3.3, pp. 567–75 (cit. on p. 9).

Johnson, Lise A. and Andrew J. Fuglevand (2009). 'Evaluation of probabilistic methods to predict muscle activity: implications for neuroprosthetics'. In: *Journal of Neural Engineering* 6.5, p. 55008 (cit. on p. 6).

Kakei, Shinji, Donna S. Hoffman and Peter L. Strick (1999). 'Muscle and movement representations in the primary motor cortex'. In: *Science* 285.5436, pp. 2136–9 (cit. on p. 3).

— (2001). 'Direction of action is represented in the ventral premotor cortex'. In: *Nature Neuroscience* 4.10, pp. 1020–5 (cit. on p. 4).

Kalaska, John F., Stephen H. Scott, Paul Cisek and L. E. Sergio (1997). 'Cortical control of reaching movements'. In: *Current Opinion in Neurobiology* 7.6, pp. 849–59 (cit. on p. 2).

Keith, Michael W., Kevin L. Kilgore, P. Hunter Peckham, Kathryn Stroh Wuolle, Graham Creasey and Michel A. Lemay (1996). 'Tendon transfers and functional electrical stimulation for restoration of hand function in spinal cord injury'. In: *The Journal of Hand Surgery* 21.1, pp. 89–99 (cit. on p. 7).

Keith, Michael W. (2001). 'Neuroprostheses for the upper extremity'. In: *Microsurgery* 21.6, pp. 256–63 (cit. on p. 11).

Kerkut, G. A. (1980). 'Can fibre optic systems drive lower motoneurones?' In: *Progress in Neurobiology* 14.1, pp. 1–23 (cit. on p. 99).

Kermadi, I., Yu Liu, A. Tempini and Eric M. Rouiller (1997). 'Effects of reversible inactivation of the supplementary motor area (SMA) on unimanual grasp and bimanual pull and grasp performance in monkeys'. In: *Somatosensory & Motor Research* 14.4, pp. 268–80 (cit. on p. 62).

Kilgore, Kevin L., P. Hunter Peckham, Geoffrey B. Thrope, Michael W. Keith and Karen A. Gallaher-Stone (1989). 'Synthesis of hand grasp using functional neuromuscular stimulation'. In: *IEEE Transactions on Biomedical Engineering* 36.7, pp. 761–70 (cit. on p. 61).

Kilgore, Kevin L., Harry A. Hoyen, Anne M. Bryden, Ronald L. Hart, Michael W. Keith and P. Hunter Peckham (2008). 'An implanted upper-extremity neuroprosthesis using myoelectric control'. In: *The Journal of Hand Surgery* 33.4, pp. 539–50 (cit. on pp. 6, 61, 98).

Kinoshita, Masaharu, Ryosuke Matsui, Shigeki Kato, Taku Hasegawa, Hironori Kasahara, Kaoru Isa, Akiya Watakabe, Tetsuo Yamamori, Yukio Nishimura, Bror Alstermark, Dai Watanabe, Kazuto Kobayashi and Tadashi Isa (2012). 'Genetic dissection of the circuit for hand dexterity in primates'. In: *Nature* 487.7406, pp. 235–8 (cit. on p. 99).

Knutson, Jayme S., Gregory G. Naples, P. Hunter Peckham and Michael W. Keith (2002). 'Electrode fracture rates and occurrences of infection and granuloma associated with percutaneous intramuscular electrodes in upper-limb functional electrical stimulation applications'. In: *Journal of Rehabilitation Research and Development* 39.6, pp. 671–83 (cit. on p. 7).

Kozai, Takashi D. Yoshida and Daryl R. Kipke (2009). 'Insertion shuttle with carboxyl terminated self-assembled monolayer coatings for implanting flexible polymer neural probes in the brain'. In: *Journal of Neuroscience Methods* 184.2, pp. 199–205 (cit. on p. 60).

Kurata, Kiyoshi (1993). 'Premotor cortex of monkeys: set- and movement-related activity reflecting amplitude and direction of wrist movements'. In: *Journal of Neurophysiology* 69.1, pp. 187–200 (cit. on p. 4).

Lai, Hsin-Yi, Lun-De Liao, Chin-Teng Lin, Jui-Hsiang Hsu, Xin He, You-Yin Chen, Jyh-Yeong Chang, Hui-Fen Chen, Siny Tsang and Yen-Yu I. Shih (2012). 'Design, simulation and experimental validation of a novel flexible neural probe for deep brain stimulation and multichannel recording'. In: *Journal of Neural Engineering* 9.3, p. 036001 (cit. on p. 60).

Law, Andrew J. and Marc H. Schieber (2011). 'Effect of redundant ensemble encoding on brain-computer interface control'. In: *Society for Neuroscience Annual Meeting 2011*. 280.15/OO16. Society for Neuroscience. Washington, DC (cit. on p. 98).

Lemay, Michel A. and Warren M. Grill (1999). 'Endpoint forces evoked by microstimulation of the cat spinal cord'. In: *Proceedings of The First Joint EMES/EMBS Conference*. Vol. 1. IEEE, p. 481 (cit. on p. 7).

— (2004). 'Modularity of motor output evoked by intraspinal microstimulation in cats'. In: *Journal of Neurophysiology* 91.1, pp. 502–14 (cit. on pp. 8, 40).

Lemay, Michel A., Dane Grasse and Warren M. Grill (2009). 'Hindlimb endpoint forces predict movement direction evoked by intraspinal microstimulation in cats'. In: *IEEE Transactions on Neural Systems and Rehabilitation Engineering* 17.4, pp. 379–89 (cit. on p. 8).

Lemon, Roger N. (1993). 'The G. L. Brown Prize Lecture. Cortical control of the primate hand'. In: *Experimental physiology* 78.3, pp. 263–301 (cit. on p. 2).

— (2008). 'Descending pathways in motor control'. In: *Annual Review of Neuroscience* 31, pp. 195–218 (cit. on pp. 2, 9, 12, 41).

Lind, Gustav, Cecilia Eriksson Linsmeier, Jonas Thelin and Jens Schouenborg (2010). 'Gelatine-embedded electrodes–a novel biocompatible vehicle allowing implantation of highly flexible microelectrodes'. In: *Journal of Neural Engineering* 7.4, p. 046005 (cit. on p. 60).

Lyons, Mark K. (2011). 'Deep brain stimulation: current and future clinical applications'. In: *Mayo Clinic Proceedings* 86.7, pp. 662–72 (cit. on p. 96).

Maher, Mary Grey, Arthur Mourtzinos, Nasim Zabihi, U. Zehra Laiwalla, Shlomo Raz and Larissa V. Rodríguez (2007). 'Bilateral caudal epidural neuromodulation for refractory urinary retention: a salvage procedure'. In: *Journal of Urology* 177.6, 2237–40, discussion (cit. on p. 9).

Martin, John H. and C. Ghez (1999). 'Pharmacological inactivation in the analysis of the central control of movement'. In: *Journal of Neuroscience Methods* 86.2, pp. 145–59 (cit. on pp. 90, 91).

Matsumura, Michikazu, Toshiyuki Sawaguchi, Takao Oishi, Koichiro Ueki and Kisou Kubota (1991). 'Behavioral deficits induced by local injection of bicuculline and muscimol into the primate motor and premotor cortex'. In: *Journal of Neurophysiology* 65.6, pp. 1542–53 (cit. on p. 62).

McCreery, Douglas B., Victor Pikov, Albert Lossinsky, Leo Bullara and William F. Agnew (2004). 'Arrays for chronic functional microstimulation of the lumbosacral spinal cord'. In: *IEEE Transactions on Neural Systems and Rehabilitation Engineering* 12.2, pp. 195–207 (cit. on p. 96).

Medical Research Council (2004). *Best practice in the accommodation and care of primates used in scientific procedures*. London: Medical Research Council. URL: `http://www.mrc.ac.uk/Utilities/Documentrecord/index.htm?d=MRC002395` (cit. on p. 100).

Meier, Martin, Ralf Reinermann, Jochen Warlich and Gerhard Manteuffel (1998). 'An automated training device for pattern discrimination learning of group-housed gerbils'. In: *Physiology & Behavior* 63.4, pp. 497–8 (cit. on p. 101).

Milner-Brown, H. S., Richard B. Stein and R. Yemm (1973). 'Changes in firing rate of human motor units during linearly changing voluntary contractions'. In: *The Journal of Physiology* 230.2, pp. 371–90 (cit. on pp. 14, 116).

Mitz, Andrew R., Steven A. Boring, Steven P. Wise and Mikhail A. Lebedev (2001). 'A novel food-delivery device for neurophysiological and neuropsychological studies in monkeys'. In: *Journal of Neuroscience Methods* 109.2, pp. 129–35 (cit. on pp. 101, 103).

Mollazadeh, Mohsen, Vikram Aggarwal, Adam G. Davidson, Andrew J. Law, Nitish V. Thakor and Marc H. Schieber (2011). 'Spatiotemporal variation of multiple neurophysiological signals in the primary motor cortex during dexterous reach-to-grasp movements'. In: *Journal of Neuroscience* 31.43, pp. 15531–43 (cit. on p. 45).

Moritz, Chet T., Timothy H. Lucas, Steve I. Perlmutter and Eberhard E. Fetz (2007). 'Forelimb movements and muscle responses evoked by microstimulation of cervical spinal cord in sedated monkeys'. In: *Journal of Neurophysiology* 97.1, pp. 110–120 (cit. on pp. 9, 12, 13, 29, 34, 53, 59, 61, 95, 97).

Moritz, Chet T., Steve I. Perlmutter and Eberhard E. Fetz (2008). 'Direct control of paralysed muscles by cortical neurons'. In: *Nature* 456.7222, pp. 639–42 (cit. on pp. 6, 62, 91, 98).

Muakkassa, Kamel F. and Peter L. Strick (1979). 'Frontal lobe inputs to primate motor cortex: evidence for four somatotopically organized 'premotor' areas'. In: *Brain Research* 177.1, pp. 176–82 (cit. on p. 5).

Musallam, Sam, Martin J. Bak, Philip R. Troyk and Richard A. Andersen (2007). 'A floating metal microelectrode array for chronic implantation'. In: *Journal of Neuroscience Methods* 160.1, pp. 122–7 (cit. on p. 45).

Mushahwar, Vivian K. and Kenneth W. Horch (1997). 'Proposed specifications for a lumbar spinal cord electrode array for control of lower extremities in paraplegia'. In: *IEEE transactions on rehabilitation engineering* 5.3, pp. 237–43 (cit. on p. 7).

— (1998). 'Selective activation and graded recruitment of functional muscle groups through spinal cord stimulation'. In: *Annals of the New York Academy of Sciences* 860, pp. 531–5 (cit. on p. 8).

— (2000a). 'Muscle recruitment through electrical stimulation of the lumbo-sacral spinal cord'. In: *IEEE transactions on rehabilitation engineering* 8.1, pp. 22–9 (cit. on p. 21).

— (2000b). 'Selective activation of muscle groups in the feline hindlimb through electrical microstimulation of the ventral lumbo-sacral spinal cord'. In: *IEEE transactions on rehabilitation engineering* 8.1, pp. 11–21 (cit. on p. 8).

Mushahwar, Vivian K., David F. Collins and Arthur Prochazka (2000c). 'Spinal cord microstimulation generates functional limb movements in chronically implanted cats'. In: *Experimental Neurology* 163.2, pp. 422–9 (cit. on pp. 7, 8, 11, 45, 59, 61, 96).

Mushahwar, Vivian K., Deborah M. Gillard, Michel J. A. Gauthier and Arthur Prochazka (2002). 'Intraspinal micro stimulation generates locomotor-like and feedback-controlled movements'. In: *IEEE Transactions on Neural Systems and Rehabilitation Engineering* 10.1, pp. 68–81 (cit. on pp. 8, 61).

Mussa-Ivaldi, Ferdinando A., Simon F. Giszter and Emilio Bizzi (1994). 'Linear combinations of primitives in vertebrate motor control'. In: *Proceedings of the National Academy of Sciences of the United States of America* 91.16, pp. 7534–8 (cit. on pp. 8, 12).

Nandoe Tewarie, Rishi S., Andres Hurtado, Ronald H. Bartels, Andre Grotenhuis and Martin Oudega (2009). 'Stem cell-based therapies for spinal cord injury'. In: *Journal of Spinal Cord Medicine* 32.2, pp. 105–14 (cit. on p. 6).

Nathan, R. H. (1997). 'Handmaster NMS1 - Present Technology & the next Generation'. In: *2nd Annual Conference of the International Functional Electrical Stimulation Society*. Ed. by Dejan Popovic. Simon Fraser University, Burnaby, British Columbia, Canada (cit. on p. 6).

Nawrot, Martin, Ad Aertsen and Stefan Rotter (1999). 'Single-trial estimation of neuronal firing rates: from single-neuron spike trains to population activity'. In: *Journal of Neuroscience Methods* 94.1, pp. 81–92 (cit. on p. 115).

Nazarpour, Kianoush, Christian Ethier, Liam Paninski, James M. Rebesco, R. Chris Miall and Lee E. Miller (2012). 'EMG prediction from motor cortical recordings via a nonnegative point-process filter'. In: *IEEE Transactions on Biomedical Engineering* 59.7, pp. 1829–38 (cit. on p. 6).

Newman, Geoffrey I., Vikram Aggarwal, Marc H. Schieber and Nitish V. Thakor (2011). 'Identifying neuron communities during a reach and grasp task using an unsupervised clustering analysis'. In: *Conference proceedings: Annual International Conference of the IEEE Engineering in Medicine and Biology Society* 2011, pp. 6401–4 (cit. on p. 45).

Paralikar, Kunal J. and Ryan S. Clement (2008). 'Collagenase-aided intracortical microelectrode array insertion: effects on insertion force and recording performance'. In: *IEEE Transactions on Biomedical Engineering* 55.9, pp. 2258–67 (cit. on p. 50).

Peckham, P. Hunter, Kevin L. Kilgore, Michael W. Keith, Anne M. Bryden, Niloy Bhadra and Fred W. Montague (2002). 'An advanced neuroprosthesis for restoration of hand and upper arm control using an implantable controller'. In: *The Journal of Hand Surgery* 27.2, pp. 265–76 (cit. on pp. 6, 61).

Penfield, Wilder and Edwin Boldrey (1937). 'Somatic motor and sensory representation in the cerebral cortex of man as studied by electrical stimulation'. In: *Brain* 60.4, p. 389 (cit. on pp. 2, 3).

Perlmutter, Joel S. and Jonathan W. Mink (2006). 'Deep brain stimulation'. In: *Annual Review of Neuroscience* 29, pp. 229–57 (cit. on p. 96).

Perlmutter, Steve I., Marc A. Maier and Eberhard E. Fetz (1998). 'Activity of spinal interneurons and their effects on forearm muscles during voluntary wrist movements in the monkey'. In: *Journal of Neurophysiology* 80.5, pp. 2475–94 (cit. on pp. 12, 44, 45, 47, 49, 59, 66).

Pesaran, Bijan, Matthew J. Nelson and Richard A. Andersen (2006). 'Dorsal premotor neurons encode the relative position of the hand, eye, and goal during reach planning'. In: *Neuron* 51.1, pp. 125–34 (cit. on p. 4).

Pfingst, Bryan E. (2000). 'Auditory Prostheses'. In: *Neural prostheses for restoration of sensory and motor function*. Ed. by John K. Chapin and Karen A. Moxon. Methods and New Frontiers in Neuroscience. Boca Raton: CRC Press. Chap. 1, pp. 3–44 (cit. on p. 96).

Pohlmeyer, Eric A., Emily R. Oby, Eric J. Perreault, Sara A. Solla, Kevin L. Kilgore, Robert F. Kirsch and Lee E. Miller (2009). 'Toward the restoration of hand use to a paralyzed monkey: brain-controlled functional electrical stimulation of forearm muscles'. In: *PLOS ONE* 4.6, e5924 (cit. on p. 6).

Popović, Lana Z. and Nebojša M. Malešević (2009). 'Muscle fatigue of quadriceps in paraplegics: comparison between single vs. multi-pad electrode surface stimulation'. In: *Conference proceedings: Annual International Conference of the IEEE Engineering in Medicine and Biology Society* 2009, pp. 6785–8 (cit. on p. 7).

Popovic, Milos R., Dejan B. Popovic and Thierry Keller (2002). 'Neuroprostheses for grasping'. In: *Neurological Research* 24.5, pp. 443–52 (cit. on pp. 11, 61).

Prasad, Abhishek and Mesut Sahin (2010). 'Characterization of neural activity recorded from the descending tracts of the rat spinal cord'. In: *Frontiers in Neuroscience* 4, p. 21 (cit. on p. 45).

— (2011). 'Chronic recordings from the rat spinal cord descending tracts with microwires'. In: *Conference proceedings: Annual International Conference of the IEEE Engineering in Medicine and Biology Society* 2011, pp. 2993–6 (cit. on p. 45).

Prescott, Mark J. and Hannah M. Buchanan-Smith (2007). 'Training laboratory-housed nonhuman primates, part 1: a UK survey'. In: *Animal Welfare* 16.1, pp. 21–36 (cit. on p. 100).

Prochazka, Arthur (1993). 'Comparison of natural and artificial control of movement'. In: *IEEE transactions on rehabilitation engineering* 1.1, pp. 7–17 (cit. on pp. 7, 11).

Raos, Vassilis, Maria-Alessandra Umiltá, Akira Murata, Leonardo Fogassi and Vittorio Gallese (2006). 'Functional properties of grasping-related neurons in the ventral premotor area F5 of the macaque monkey'. In: *Journal of Neurophysiology* 95.2, pp. 709–29 (cit. on p. 4).

Rathelot, Jean-Alban and Peter L. Strick (2006). 'Muscle representation in the macaque motor cortex: an anatomical perspective'. In: *Proceedings of the National Academy of Sciences of the United States of America* 103.21, pp. 8257–62 (cit. on p. 2).

— (2009). 'Subdivisions of primary motor cortex based on cortico-motoneuronal cells'. In: *Proceedings of the National Academy of Sciences of the United States of America* 106.3, pp. 918–23 (cit. on p. 3).

Reed, Dwain J. and Alan D. Miller (1978). 'Thermoelectric Peltier device for local cortical cooling'. In: *Physiology & Behavior* 20.2, pp. 209–11 (cit. on p. 91).

Richardson, Andrew G., Tommaso Borghi and Emilio Bizzi (2012). 'Activity of the same motor cortex neurons during repeated experience with perturbed movement dynamics'. In: *Journal of Neurophysiology* 107.11, pp. 3144–54 (cit. on p. 45).

Riddle, C. Nicholas, Steve A. Edgley and Stuart N. Baker (2009). 'Direct and indirect connections with upper limb motoneurons from the primate reticulospinal tract'. In: *Journal of Neuroscience* 29.15, pp. 4993–9 (cit. on p. 44).

Rizzolatti, Giacomo, R. Camarda, Leonardo Fogassi, M. Gentilucci, G. Luppino and M. Matelli (1988). 'Functional organization of inferior area 6 in the macaque monkey. II. Area F5 and the control of distal movements'. In: *Experimental Brain Research* 71.3, pp. 491–507 (cit. on pp. 4, 5, 62).

Rizzolatti, Giacomo, Luciano Fadiga, Vittorio Gallese and Leonardo Fogassi (1996). 'Premotor cortex and the recognition of motor actions'. In: *Cognitive Brain Research* 3.2, pp. 131–41 (cit. on p. 4).

Rosset, Antoine, Luca Spadola and Osman Ratib (2004). 'OsiriX: an open-source software for navigating in multidimensional DICOM images'. In: *Journal of Digital Imaging* 17.3, pp. 205–16 (cit. on p. 64).

Rousche, Patrick J., David S. Pellinen, David P. Pivin Jr, Justin C. Williams, Rio J. Vetter and Daryl R. Kipke (2001). 'Flexible polyimide-based intracortical electrode arrays with bioactive capability'. In: *IEEE Transactions on Biomedical Engineering* 48.3, pp. 361–71 (cit. on p. 97).

Rupp, R. and H. J. Gerner (2007). 'Neuroprosthetics of the upper extremity–clinical application in spinal cord injury and challenges for the future'. In: *Acta Neurochirurgica. Supplementum* 97.Pt 1, pp. 419–26 (cit. on p. 7).

Sahni, Vibhu and John A. Kessler (2010). 'Stem cell therapies for spinal cord injury'. In: *Nature Reviews Neurology* 6.7, pp. 363–72 (cit. on p. 6).

Saigal, Rajiv, Costantino G. Renzi and Vivian K. Mushahwar (2004). 'Intraspinal microstimulation generates functional movements after spinal-cord injury'. In: *IEEE Transactions on Neural Systems and Rehabilitation Engineering* 12.4, pp. 430–40 (cit. on pp. 8, 62).

Sasaki, Kazuo and Hisae Gemba (1984). 'Compensatory motor function of the somatosensory cortex for the motor cortex temporarily impaired by cooling in the monkey'. In: *Experimental Brain Research* 55.1, pp. 60–8 (cit. on pp. 62, 91).

— (1987). 'Plasticity of cortical function related to voluntary movement motor learning and compensation following brain dysfunction'. In: *Acta Neurochirurgica. Supplementum* 41, pp. 18–28 (cit. on p. 62).

Schaefers, Andrea T. U. and York Winter (2011). 'Rapid task acquisition of spatial-delayed alternation in an automated T-maze by mice'. In: *Behavioural Brain Research* 225.1, pp. 56–62 (cit. on p. 101).

Schieber, Marc H. and Andrew V. Poliakov (1998). 'Partial inactivation of the primary motor cortex hand area: effects on individuated finger movements'. In: *Journal of Neuroscience* 18.21, pp. 9038–54 (cit. on pp. 62, 90).

Schmidlin, Eric, Thierry Wannier, Jocelyne Bloch and Eric M. Rouiller (2004). 'Progressive plastic changes in the hand representation of the primary motor cortex parallel incomplete recovery from a unilateral section of the corticospinal tract at cervical level in monkeys'. In: *Brain Research* 1017.1-2, pp. 172–83 (cit. on p. 62).

Schmidlin, Eric, Thomas Brochier, Marc A. Maier, Peter A. Kirkwood and Roger N. Lemon (2008). 'Pronounced reduction of digit motor responses evoked from macaque ventral premotor cortex after reversible inactivation of the primary motor cortex hand area'. In: *Journal of Neuroscience* 28.22, pp. 5772–83 (cit. on pp. 5, 62, 90).

Schmidt, E. M., M. J. Bak, F. T. Hambrecht, C. V. Kufta, D. K. O'Rourke and P. Vallabhanath (1996). 'Feasibility of a visual prosthesis for the blind based on intracortical microstimulation of the visual cortex'. In: *Brain* 119 (Pt 2), pp. 507–22 (cit. on p. 96).

Schouenborg, Jens (2008). 'Action-based sensory encoding in spinal sensorimotor circuits'. In: *Brain Research Reviews* 57.1, pp. 111–7 (cit. on p. 12).

Schwartz, Andrew B., Ronald E. Kettner and Apostolos P. Georgopoulos (1988). 'Primate motor cortex and free arm movements to visual targets in three-dimensional space. I. Relations between single cell discharge and direction of movement'. In: *Journal of Neuroscience* 8.8, pp. 2913–27 (cit. on p. 3).

Seki, Kazuhiko, Steve I. Perlmutter and Eberhard E. Fetz (2009). 'Task-dependent modulation of primary afferent depolarization in cervical spinal cord of monkeys performing an instructed delay task'. In: *Journal of Neurophysiology* 102.1, pp. 85–99 (cit. on p. 45).

Shimazu, Hideki, Marc A. Maier, Gabriella Cerri, Peter A. Kirkwood and Roger N. Lemon (2004). 'Macaque ventral premotor cortex exerts powerful facilitation of motor cortex outputs to upper limb motoneurons'. In: *Journal of Neuroscience* 24.5, pp. 1200–11 (cit. on p. 94).

Simpson, B. A. (1997). 'Spinal cord stimulation'. In: *British Journal of Neurosurgery* 11.1, pp. 5–11 (cit. on pp. 9, 96).

Skinner, James E. and Donald B. Lindsley (1968). 'Reversible cryogenic blockade of neural function in the brain of unrestrained animals'. In: *Science* 161.3841, pp. 595–7 (cit. on p. 62).

Sohal, Harbaljit, Andrew Jackson, K. Vassilevski, Gavin Clowry, Anthony O'Neill and Stuart N. Baker (2012). 'The sinusoidal electrode: Towards increasing chronic recording longevity through decreased micromotion related trauma'. In: *Society for Neuroscience Annual Meeting 2012*. 277.17/NN16. Society for Neuroscience. New Orleans, LA, USA (cit. on p. 97).

Stieglitz, Thomas, Birthe Rubehn, Christian Henle, Sebastian Kisban, Stanislaw Herwik, Patrick Ruther and Martin Schuettler (2009). 'Brain–computer interfaces: an overview of the hardware to record neural signals from the cortex'. In: *Neurotherapy: Progress in Restorative Neuroscience and Neurology*. Ed. by Joost Verhaagen, Elly M. Hol, Inge Huitenga, Jan Wijnholds, Arthur B. Bergen, Gerald J. Boer and Dick F. Swaab. Vol. 175. Progress in Brain Research. Elsevier, pp. 297–315 (cit. on p. 97).

Tai, Changfeng, August M. Booth, Charles J. Robinson, William C. de Groat and James R. Roppolo (2003). 'Multi-joint movement of the cat hindlimb evoked by microstimulation of the lumbosacral spinal cord'. In: *Experimental Neurology* 183.2, pp. 620–7 (cit. on p. 8).

Taylor, Dawn M., Stephen I. Helms Tillery and Andrew B. Schwartz (2002). 'Direct cortical control of 3D neuroprosthetic devices.' In: *Science* 296.5574, pp. 1829–32 (cit. on p. 94).

Townsend, Benjamin R., Erk Subasi and Hansjörg Scherberger (2011). 'Grasp movement decoding from premotor and parietal cortex'. In: *Journal of Neuroscience* 31.40, pp. 14386–98 (cit. on pp. 4, 45).

Travis, Ann Marie (1955). 'Neurological deficiencies after ablation of the precentral motor area in Macaca mulatta'. In: *Brain* 78.2, pp. 155–73 (cit. on p. 3).

Tresch, Matthew C. and Emilio Bizzi (1999). 'Responses to spinal microstimulation in the chronically spinalized rat and their relationship to spinal systems activated by low thresh-

old cutaneous stimulation'. In: *Experimental Brain Research* 129.3, pp. 401–16 (cit. on pp. 7, 8, 11, 40, 41).

Tsuboi, Fumiharu, Yukio Nishimura, Kimika Yoshino-Saito and Tadashi Isa (2010). 'Neuronal mechanism of mirror movements caused by dysfunction of the motor cortex'. In: *European Journal of Neuroscience* 32.8, pp. 1397–406 (cit. on pp. 62, 90).

Vargas-Irwin, Carlos E., Gregory Shakhnarovich, Payman Yadollahpour, John M. K. Mislow, Michael J. Black and John P. Donoghue (2010). 'Decoding complete reach and grasp actions from local primary motor cortex populations'. In: *Journal of Neuroscience* 30.29, pp. 9659–69 (cit. on p. 5).

Velliste, Meel, Sagi Perel, M. Chance Spalding, Andrew S. Whitford and Andrew B. Schwartz (2008). 'Cortical control of a prosthetic arm for self-feeding'. In: *Nature* 453.7198, pp. 1098–101 (cit. on pp. 5, 91, 98).

Westerveld, Ard J., Alfred C. Schouten, Peter H. Veltink and Herman van der Kooij (2012). 'Selectivity and resolution of surface electrical stimulation for grasp and release'. In: *IEEE Transactions on Neural Systems and Rehabilitation Engineering* 20.1, pp. 94–101 (cit. on p. 7).

Wilson, Fraser A. W., Byoung-Hoon Kim, Jae-Wook Ryou and Yuan-Ye Ma (2005). 'An automated food delivery system for behavioral and neurophysiological studies of learning and memory in freely moving monkeys'. In: *Behavior Research Methods* 37.2, pp. 368–72 (cit. on p. 101).

Wise, Steven P., Driss Boussaoud, Paul B. Johnson and Roberto Caminiti (1997). 'Premotor and parietal cortex: corticocortical connectivity and combinatorial computations'. In: *Annual Review of Neuroscience* 20, pp. 25–42 (cit. on p. 4).

Woolsey, C. N., P. H. Settlage, D. R. Meyer, W. Sencer, P. T. Hamuy and A. M. Travis (1952). 'Patterns of localization in precentral and "supplementary" motor areas and their relation to the concept of a premotor area'. In: *Research Publications: Association for Research in Nervous and Mental Disease* 30, p. 238 (cit. on p. 3).

Wyndaele, Michel and Jean-Jacques Wyndaele (2006). 'Incidence, prevalence and epidemiology of spinal cord injury: what learns a worldwide literature survey?' In: *Spinal Cord* 44.9, pp. 523–9 (cit. on pp. 1, 91).

Yakovenko, Sergiy, Jan Kowalczewski and Arthur Prochazka (2007). 'Intraspinal stimulation caudal to spinal cord transections in rats. Testing the propriospinal hypothesis'. In: *Journal of Neurophysiology* 97.3, pp. 2570–4 (cit. on p. 45).

Zimmermann, Jonas B. (2009). 'Restoring Function to the Spinal Cord and Retina Using Electrical Stimulation'. MA thesis. Newcastle upon Tyne, United Kingdom: Institute of Neuroscience, Medical School, Newcastle University (cit. on p. 11).

Zimmermann, Jonas B. and Andrew Jackson (2010). 'Investigating microstimulation of the macaque cervical spinal cord to elicit functional upper limb movements'. In: *BCI Meeting 2010*. Monterey, CA (cit. on p. 11).

— (2011a). 'Closed-loop cortical control of intraspinal microstimulation restores hand function in the macaque monkey'. In: *41st Society for Neuroscience Annual Meeting*. 142.80/E23. Society for Neuroscience. Washington, DC (cit. on p. 61).

Zimmermann, Jonas B., Kazuhiko Seki and Andrew Jackson (2011b). 'Reanimating the arm and hand with intraspinal microstimulation'. In: *Journal of Neural Engineering* 8.5 (cit. on pp. 9, 11, 42).

Zimmermann, Jonas B. and Andrew Jackson (2012). 'Nonlinear summation of evoked forces and EMG using intraspinal microstimulation trains in the macaque monkey'. In: *Neural Control of Movement 22nd Annual Meeting*. 2-D-83. Venice, Italy (cit. on p. 22).